RADIOLOGY AND ONCOLOGY

December 2002
Vol. 36 No. 4
Ljubljana

ISSN 1318-2099

SIEMENS

SiemensMedical.com/oncology

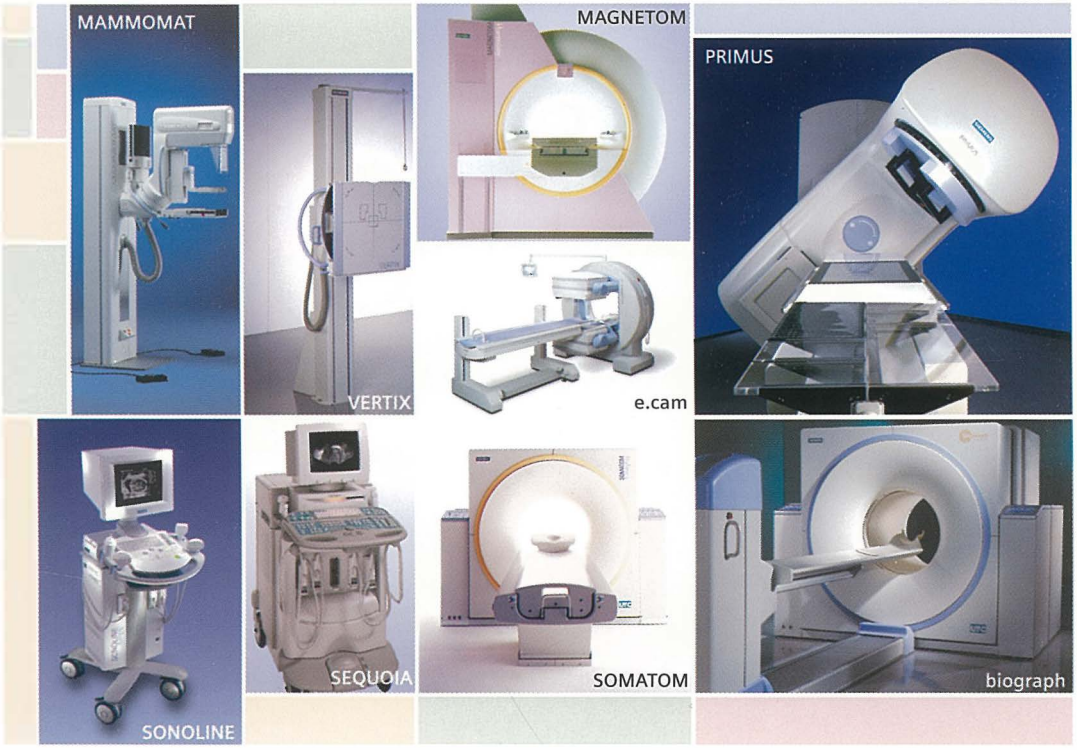

SEEK-FIND-ACT-FOLLOW - the Continuum of Oncology Care™

Siemens oncology portfolio comprises comprehensive workflow solutions integrating the full spectrum of care from screening/early detection and diagnosis through therapy and follow-up. All from one provider — with over 100 years history of innovation in medical technology.

Siemens proven clinical methods can help you to achieve more successful outcomes. How? Through industry-leading technology, increased productivity measures for maximized utilization potential, and patient-friendly design and features.

Every day in the United States alone, 29,000 cancer patients receive radiation therapy delivered by Siemens linear accelerators. As clinical protocols transition to include IMRT and IGRT, Siemens seamlessly integrates the diagnostic and treatment modalities. That's what we call Best Practice Oncology Care.

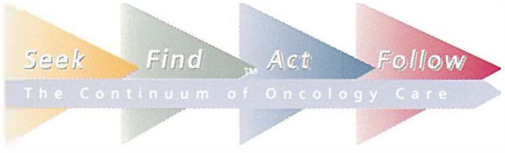

Siemens medical
Solutions that help

RADIOLOGY AND ONCOLOGY

Editorial office
Radiology and Oncology
Institute of Oncology
Zaloška 2
SI-1000 Ljubljana
Slovenia
Phone: +386 1 4320 068
Phone/Fax: +386 1 4337 410
E-mail: gsersa@onko-i.si

December 2002
Vol. 36 No. 4
Pages 265-347
ISSN 1318-2099
UDC 616-006
CODEN: RONCEM

Aims and scope
Radiology and Oncology is a journal devoted to publication of original contributions in diagnostic and interventional radiology, computerized tomography, ultrasound, magnetic resonance, nuclear medicine, radiotherapy, clinical and experimental oncology, radiobiology, radiophysics and radiation protection.

Publisher
Association of Radiology and Oncology

Affiliated with
Slovenian Medical Association – Slovenian Association of Radiology, Nuclear Medicine Society,
Slovenian Society for Radiotherapy and Oncology, and Slovenian Cancer Society
Croatian Medical Association – Croatian Society of Radiology
Societas Radiologorum Hungarorum
Friuli-Venezia Giulia regional groups of S.I.R.M.
(Italian Society of Medical Radiology)

Reader for English
Mojca Čakš

Key words
Eva Klemenčič

Secretaries
Milica Harisch
Mira Klemenčič

Design
Monika Fink-Serša

Printed by
Imprint d.o.o., Ljubljana, Slovenia

Published quarterly in 700 copies

Bank account number 02010-0090006751
Foreign currency account number
010-7100-900067/4
NLB d.d., Podružnica Ljubljana Center, Ljubljana
S.W.I.F.T. Code LJBASI2X

Subscription fee for institutions $ 100 (16000 SIT), individuals $ 50 (5000 SIT)

The publication of this journal is subsidized by the Ministry of Education, Science and Sport of the Republic of Slovenia.

Indexed and abstracted by:
BIOMEDICINA SLOVENICA
CHEMICAL ABSTRACTS
EMBASE / Excerpta Medica
Sci Base

This journal is printed on acid- free paper

Radiology and Oncology is available on the internet at: http://www.onko-i.si/radiolog/rno.html

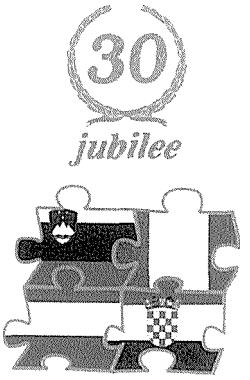

XXX. Jubilee Annual Meeting of the Radiologists of the Alpe Adria Region

26-27 October 2001
Portorož, Slovenia

Guest Editor
Prof. Vladimir Jevtić, PhD, MD

Foreword

I have the honour to be the guest editor of this anniversary issue of Radiology & Oncology dedicated to the 30th Jubilee Meeting of the Radiologists of the Alpe Adria Region. From the first official meeting held in Dobrna in 1968 more than thirty years ago, radiologists from the university radiological departments of Trieste, Padua, Verona, Graz, Ljubljana and Zagreb have been meeting in one of the neighbouring countries to share their research and scientific experiences. The enriching success of our meetings has shown the vision of the founders of the Alpe Adria Radiological Group Prof. Dr. Emo Bianchi from Monfalcone, Prof. Dr. Guerrino Lenarduzzi from Padua, Prof. Dr. Stanko Hernja and Prof. Dr. Ludvik Tabor from Ljubljana. The meetings have survived all the political differences and changes which have occurred in the last three decades proving the deep historical and cultural connection between the four European nations and the enduring friendship which has developed throughout all these years. At the very beginning the meetings were rare and precious opportunity for the radiologists from - at that time - the »Eastern« Countries to get informed about modern radiological technologies from the more developed »western« participants of the group. But even now when technological differences are not so great the great wish to share research experiences, which have always been the main driving force behind our group, will ensure a brilliant future of the Alpe Adria Radiological Meetings.

This issue of Radiology & Oncology reflects the current status of different fields of diagnostic and interventional radiology at the university departments of four neighbouring countries which is at the level of the world's most modern radiology. So far, there has been no official record of the history of the Alpe Adria Radiological group. Therefore, I am grateful for the contribution of Prof. Dr. Ludovico Dalla Palma »Past, present and future«, which was presented at the opening ceremony of our 30th Jubilee meeting.

Guest Editor
Prof. Vladimir Jevtić, PhD, MD

RADIOLOGY AND ONCOLOGY

Ljubljana, Slovenia
December 2002
Vol. 36 No. 4

ISSN 1318-2099
UDC 616-006
CODEN: RONCEM

CONTENTS

Radiology and Oncology is covered in *Biomedicina Slovenica, Chemical Abstracts, EMBASE / Excerpta Medica, and Sci Base*

Radiol Oncol 2002; 36(4): 275-80.

Radiologic-pathologic correlation of the mammographic findings retrospectively detected in inflammatory breast cancer: usefulness in clinical practice

Francesca Caumo, Erminia Manfrin, Franco Bonetti, Lucia Pinali, Carlo Procacci

Department of Radiology, University of Verona, Italy

Background. *The aim of this study was to describe the clinical, mammographical and pathological characteristics of inflammatory carcinoma.*

Patients and methods. *Clinical, mammographical and histological sections of twenty-two women (age range 28-60 years) were reviewed. The examinations had been performed over a period of four years.*

Results. *The clinical findings were: erythema, edema, thickening of the skin and breast heat in ten patients; palpable mass in nine patients; nipple discharge in one patient; absent in two patients. Pathological findings were: tumor emboli in the dermal lymphatics in eight patients; tumor emboli in the vessels in ten patients; tumor emboli both in the dermal lymphatics and in the vessels in four patients. The radiologic findings were: skin thickening, trabecular thickening and blurring of structure in ten patients (common presentation); mass in nine patients; malignant-type calcifications in two patients (uncommon presentation); absent in one patient. The follow-up examination (eighteen months) detected that only one patient with common presentation of inflammatory carcinoma had no local or systemic recurrence against eight patients with uncommon presentation.*

Conclusions. *The clinical and mammographical aspects, which suggest the presence of an inflammatory carcinoma, occur only in 45.4% of the patients. The radiological aspect seems to correlate with the different prognosis of the tumour, resulting in a better prognosis in those with an uncommon aspect.*

Key words: breast neoplasms - radiography - pathology; inflammation, inflammatory carcinoma

Received 18 June 2002
Accepted 2 July 2002

Correspondence to: Francesca Caumo, M.D., Department of Radiology, University of Verona, Policlinico G.B. Rossi, Piazzale L.A. Scuro, 10, 37 134 Verona, Italy; Phone: +39 (0)45 582 445; Fax: +39 (0)45 827 7808 ; E-mail: francesca.caumo@mail.azosp.vr.it

Introduction

Inflammatory carcinoma (IC) represents 1% of all breast cancer. The diagnosis of IC depends on clinical (erythema, edema and breast heat without any pain) and/or histological findings (any subtype of breast carcinoma with tumor emboli in the dermal lymphatics or/and tumor emboli in the vessels).

The purposes of our work were: (a) to evaluate the clinical and radiological aspects of

this pathology; (b) to determine the correlation between radiological and pathological findings; (c) to identify any usefulness of this correlation in clinical practice.

Patients and methods

From 1997 to 2000, 22 women aged from 28 to 60 years were treated for IC. We reviewed the clinical history, mammograms and histological sections of these patients. All the patients were examined to evaluate their response to therapy.

Results

The clinical findings were: erythema, edema (peau d'orange), thickening of the skin and breast heat in ten patients (45.4%); palpable mass in nine patients (40.9%); nipple discharge in one patient (4.5%) and two patients showed no clinical signs (9.2%).

In eight patients (36.3%) histological sections showed tumor emboli in the dermal lymphatics (Figure 1); in ten patients (45.4%) there were tumor emboli in the vessels, and four patients (18.3%) had tumor emboli in both **the** dermal lymphatics and in the vessels.

In ten patients (45.4%), the mammograms revealed the typical aspect of IC: skin thickening, trabecular thickening and blurring of structure caused by edema (Figure 2). These findings can be defined as »common presentation« of inflammatory breast carcinoma. In twelve patients (54.5%), IC had an uncommon mammographic aspect: a mass with or without malignant-type calcifications in nine patients (40.9%) (Figure 3); malignant-type calcifications in two patients (9.2%) (Figure 4), and no radiological findings in one patient (4.5%).

In the histological sections of patients with common presentations, emboli in the dermal lymphatics, emboli in the vessels, emboli in both the vessels and **the** dermal lymphatics were found in six, two and two cases, respectively (Figure 5a). In the histological sections of patients with uncommon presentations, the same findings were found in two, eight and two cases respectively (Figure 5b).

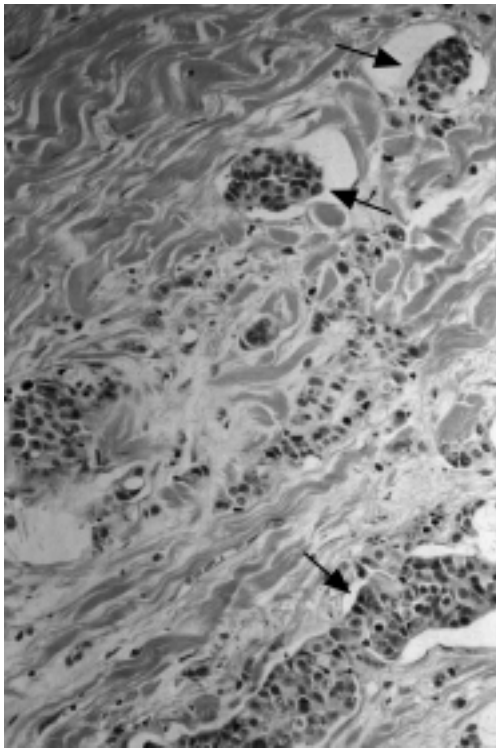

Figure 1. Inflammatory carcinoma. Microscopically, the primary tumor is an infiltrated, poorly differentiated ductal carcinoma with clusters of carcinoma cells in dilated lymphatic channels in the derma (arrows).

All patients were treated with a multimodality therapy that consisted of chemotherapy and then mastectomy followed by chemotherapy or radiotherapy. The survival rate, without local or systemic recurrence in the patients with common presentation of IC, was 10% after a follow-up period of 18 months. In the patients with uncommon presentation after an average follow-up period of 28 months, the survival rate was 66.6%.

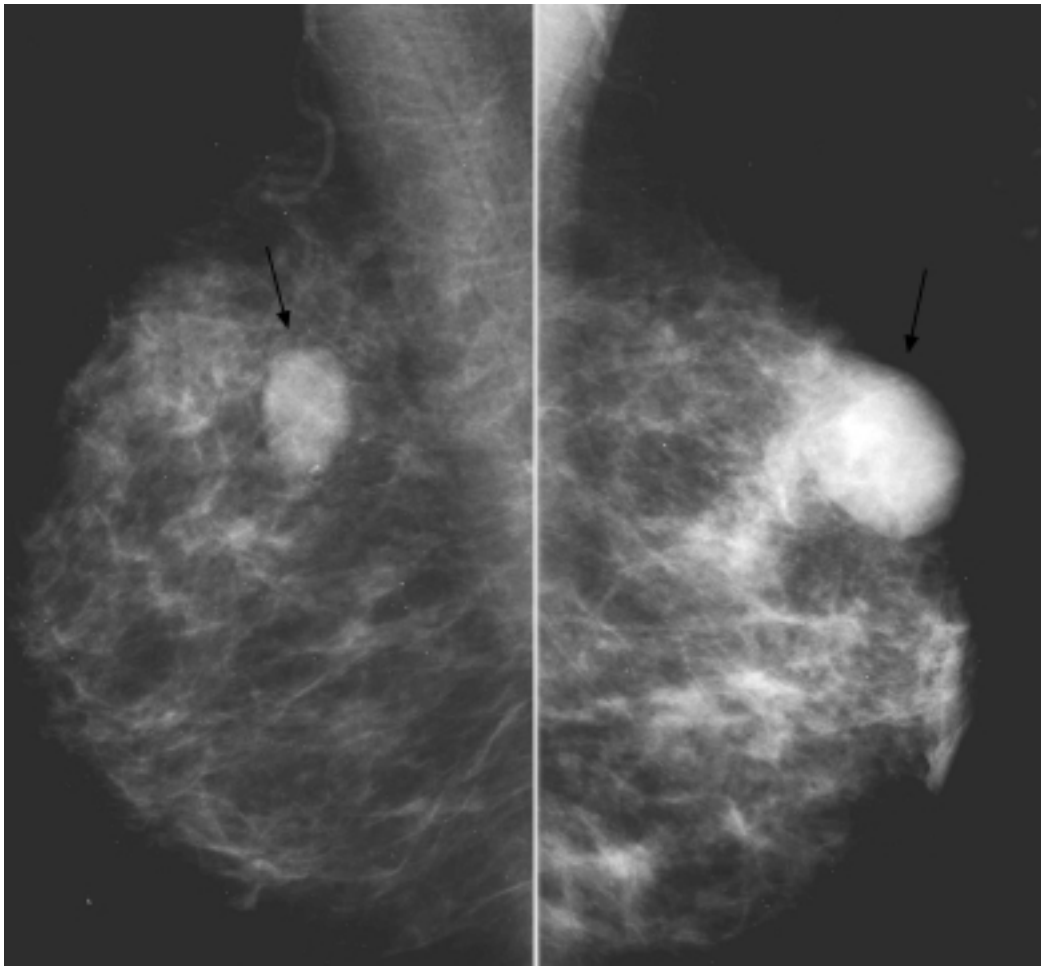

Figures 2a, 2b. Inflammatory carcinoma, common presentation. (a) Lateral oblique right mammogram shows a fibroadenoma (arrow) in an otherwise normal breast. In the counterpart (b), diffuse increase in breast density, trabecular thickening and architectural distortion are noticeable throughout the breast. The opacity on the upper side of the breast is a cyst (arrow)

Discussion

Diagnosis of IC was made, according to the most recently reported data, on clinical and pathological criteria.[1] Edema, erythema and breast heat occurred in 45.5% of examined cases and represented the common presentation of IC. Among the remaining cases, about 54.5% showed uncommon clinical findings such as palpable mass, and nipple discharge. In 2 cases, no clinical signs were observed. The pathological criteria utilized to diagnose IC were any subtype of breast carcinoma associated with emboli in the dermal lymphatics and/or in the vessels. All these findings are extremely important in the diagnosis of IC as this entity can be diagnosed even in cases of uncommon clinical presentation. In fact, not all women with clinical findings suggestive of IC have dermal lymphatic involvement at skin biopsy.

The most common clinical findings are

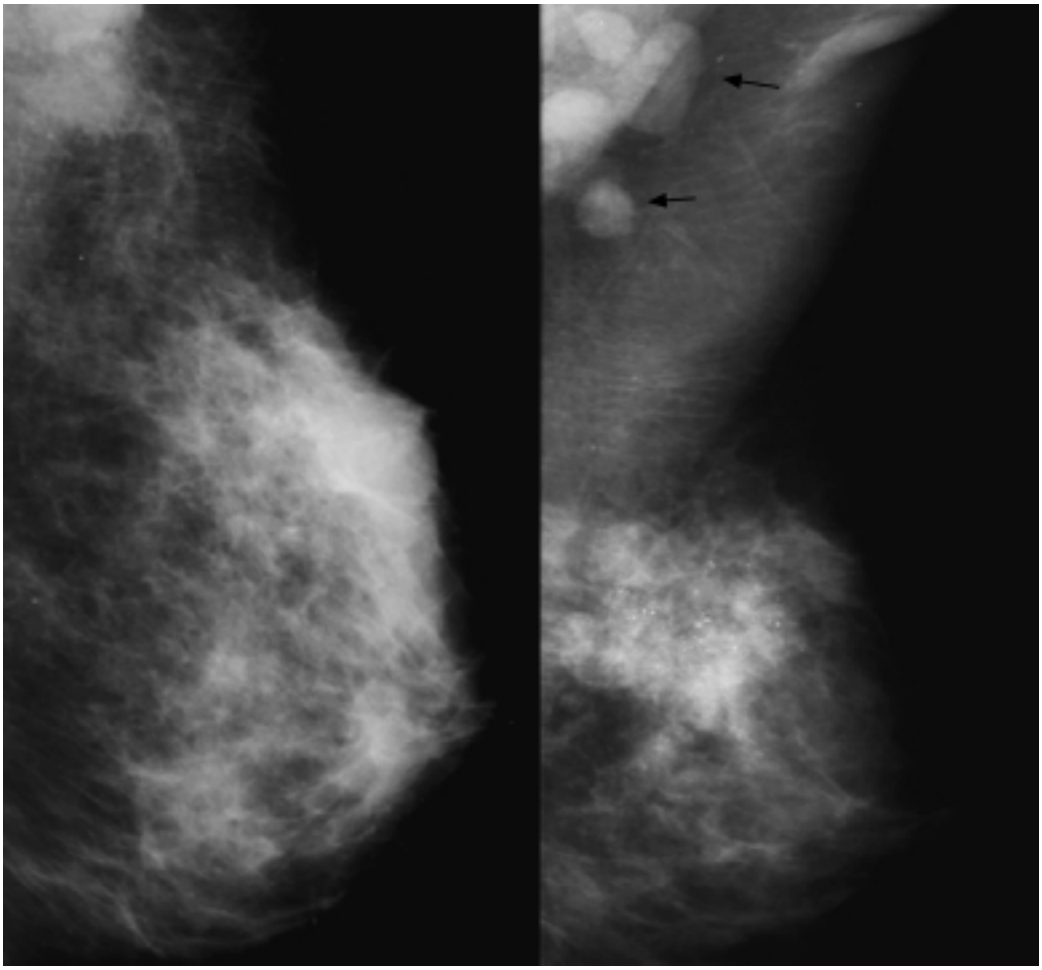

Figures 3a, 3b. Inflammatory carcinoma, uncommon presentation. (a) Mediolateral oblique left mammogram. A dense mass is seen in the upper part of the breast. (b) Another case, mediolateral oblique mammogram. In the lower part of the breast, a mass with calcifications is present. In the axilla, some lymph nodes are also appreciable (arrows).

usually, but not always, associated with diffuse increase in breast density, trabecular thickening and blurring of structure caused by edema on the mammograms. These mammographic findings[2] are not specific and can also be seen in other diseases, such as acute inflammatory process, post lumpectomy radiation changes and trauma. With the exception of the one patient in our series who had a negative mammogram, the other women had an uncommon presentation: a mass and/or malignant-type calcifications. These results support the concept that primary IC of the breast has different mammographic appearances; consequently, the diagnosis is made by biopsy.[3,4]

We correlated the two mammographic groups, common and uncommon, with the histological findings, but there were no significant differences between the two groups.

All the patients were treated with the same multimodality therapy. The disease-free survival rate for the patients with uncommon presentation is significantly better compared

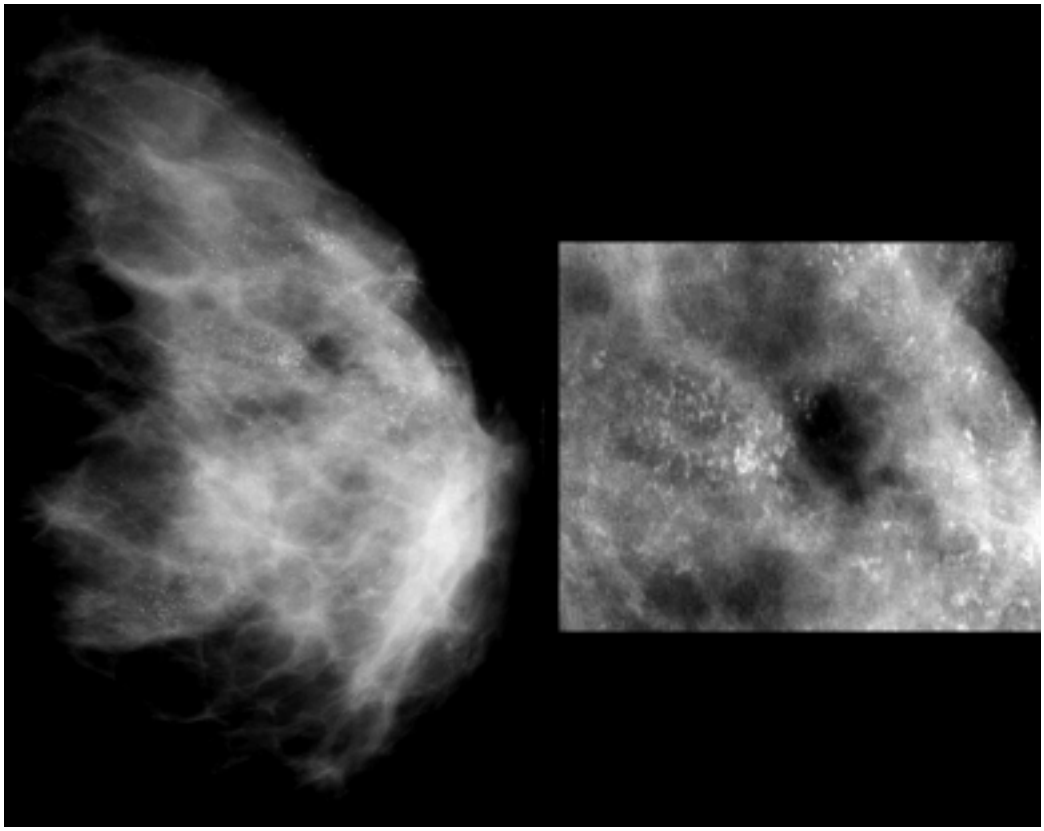

Figure 4. Inflammatory carcinoma, uncommon presentation. Malignant pleomorphic calcifications are scattered throughout the breast, but in particular in the deep upper region of the gland (magnification view).

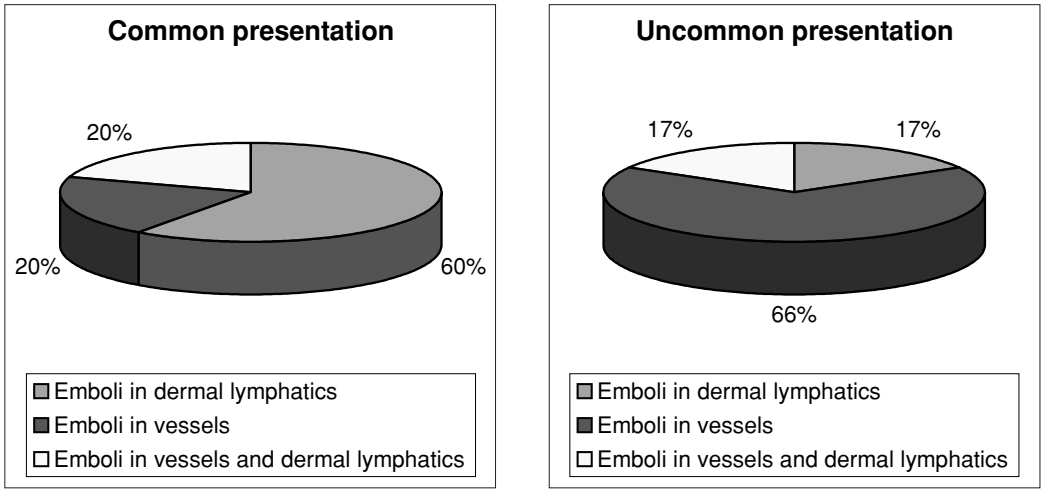

Figures 5a, 5b. Graphs showing the incidence of the different anatomo-pathologic findings encountered in the common (a) and uncommon (b) presentations.

to that of patients with common presentation. This discrepancy is probably a result of the stage of the disease: early in the uncommon presentation, advanced in the common one.

Conclusions

The clinical and mammographic findings suggesting the presence of an IC, with erythema, oedema and breast heat together with skin and trabecular thickening and blurring of structures were present in only 45.4% of the patients. These aspects cannot be considered pathognomonic as they can also be present in non-neoplastic diseases.

Diagnosis of IC can be carried out only an histological specimen. The histological aspects are different to the clinical and radiographical signs of the tumour.

The radiological aspect seems to indicate, after similar treatment, a different tumour prognosis, resulting better in those with an uncommon appearance.

The relationship that exists between the common and uncommon presentations is not clear. The second could be the earlier stage of the first.

References

1. Gardenosa G. *Breast imaging companion.* Washington: Lippincott Williams & Wilkins: 2001.

2. Dershaw DD, Moore MP, Liberman L. Inflammatory breast carcinoma: mammographic findings. Radiology 1994; **190:** 831-4.

3. Kushwaha AC, Whitman GJ, Stelling CB, Cristofanilli M, Buzdar AU. Primary inflammatory carcinoma of the breast: retrospective review of mammographic findings. *Am J Roentgenol AJR* 2000; **174:** 535-8.

4. Tardivon AA, Viala J, Rudelli AC, Guinebretiere J-M, Vanel D. Mammographic patterns of inflammatory breast carcinoma: a retrospective study of 92 cases. *Eur J Radiol* 1997; **24:** 124-30.

Radiol Oncol 2002; 36(4): 281-90.

Endovascular management of splanchnic arteries bleeding in pancreato-biliary disease

Mirko D'Onofrio[1], Giancarlo Mansueto[1], Anna Gasparini[1], Simone Vasori[1], Massimo Falcon[2], Carlo Procacci[1]

[1]*Department of Radiology and*
[2]*Department of Surgery, University Hospital »G.B. Rossi«, Verona, Italy*

Background. *Splanchnic artery bleeding is a life-threatening condition, especially in high-risk patients. The purpose of this study is to evaluate the efficacy of endovascular treatment of splanchnic artery bleeding in pancreato-biliary disease, considered as survival at the 3-month follow-up.*

Patients and methods. *From 1992 to 2001 39 patients with upper splanchnic arterial lesion due to acute and chronic pancreatitis after surgery or percutaneous procedures, or as a complication of aneurysms or trauma, were treated using endovascular techniques. The patients underwent CT control immediately after the procedure, after seven days and then at the 3, 6 and 12-month-follow-up.*

Results. *In some patients, more than one angiography was necessary to identify the source of bleeding. Bleeding was stopped in all treated patients. Fatal re-bleeding occurred in 6 patients and, in the first part of the study, 2 patients died of hepatic failure after hepatic artery embolization.*

Conclusions. *Splanchnic artery bleeding is a life-threatening condition. Endovascular treatment can reach a clinical success rate of up to 75% at three months.*

Key words: pancreatitis - complications; biliary tract disease - complications; mesenteric arteries - angiography; haemorrhage - therapy; embolization, therapeutic

Introduction

Splanchnic artery bleeding is a life-threatening condition. Although mortality and morbidity associated with major pancreatic and biliary surgery have diminished with recent advances in surgical techniques, post-operative complications, especially following pancreatoduodenectomy, are still common.[1] The incidence of hemorrhagic complications due to arterial disruption after pancreatic surgery, especially pancreatoduodenectomy, has not changed in the last 20 years (2%-18%).[2] Bleeding is the second most serious complication after sepsis due to the dehiscence of the pancreatic anastomosis. When arterial disruption related to pancreatitis, ruptured aneurysm or trauma occurs, the mortality rate

Received 22 July 2002
Accepted 6 August 2002

Correspondence to: Mirko D'Onofrio, Department of Radiology, University Hospital »G.B. Rossi«, Piazza L.A. Scuro, 10 37134 Verona, Italy; Phone: +39 (0)45 582 445; Fax: +39 (0)45 827 7808; E-mail: mk.don@libero.it

is high and can reach 70%.[3] Surgical intervention for upper splanchnic artery bleeding, including ligation of the proximal and distal portions of the lesion, may be critical in debilitated and high-risk patients. The upper splanchnic artery bleeding in pancreato-biliary disease can be managed by endovascular techniques.

Patients and methods

From 1992 to 2001, 39 patients with upper splanchnic arterial lesion due to acute and chronic pancreatitis after surgery or percutaneous procedures, or as a complication of aneurysms or trauma were treated using endovascular techniques.

The aetiology of the hemorrhage was assumed on the basis of the non-invasive vascular imaging (CT angiography, MR angiography, color-Doppler Ultrasonography) and the angiographic features as well as the case history (Table 1).

In 29 patients, the procedure was performed in emergency owing to unstable hemodynamic conditions. During the procedure, the hemodynamic parameters and pulse-oxymetry were monitored. In all patients, an intravenous infusion of acetate ringer was administered through a 16-gauge cannula needle inserted into a peripheral vein at an infusion rate of 15ml/kg/hr. In all patients, the procedure was carried out with anesthesiological support. A central venous catheter was positioned for infusions and pressure monitoring. Colloid solutions and packed red blood cells were administered as needed. Antibiotic prophylaxis was performed in all the patients by intravenous one-day administration of a second-generation cephalosporin.

Written consent was obtained from each patient before arteriography. At first, celiac arteriography, superior mesenteric arteriography and arterial portography were performed with a 5F catheter. The endovascular treatment was performed with the coaxial catheterism technique in all cases. For the embolization, 5F catheter was used for the selective catheterization of the vessel afferent to the arterial lesion and a microcatheter (Tracker-18 unibody Target Therapeutics, Fremont, CA, USA) for positioning the coils (Tornado Embolization Coils, W Cook Europe, Bjaeverskov, Denmark) or to inject the acrylic glue (Histoacryl B/Braun, Melsungen, Germany) added to Lipiodol UF (Guerbet, Aulnay-Sous-Bois, France). For artery repair a balloon-expandable covered stent (Jostent Peripheral Stent Graft, Jomed Implantate GmbH, Rangendingen, Germany) was used.

The patients underwent CT control immediately after the procedure, after seven days and then at the 3, 6 and 12-month-follow-up.

Table 1. Patient data: ethiology of haemorrage and distribution of the arterial lesion

Bleeding Artery	Acute Pancreatitis	P-B Surgery	Percutaneous Procedure	Chronic Pancreatitis	Aneurysm	Trauma	Total
Hepatic	-	3	7	-	2	1	13
Gastroduodenal	2	5	1	2	-	-	10
Splenic	5	-	-	1	1	-	7
Middle Colic	3	1	-	-	-	-	4
Pancreatico duodenal	1	-	-	2	-	-	3
Left Gastric	-	-	-	1	-	-	1
Gastroepiploic	1	-	-	-	-	-	1
Total	**12**	**9**	**8**	**6**	**3**	**1**	**39**

Results

From our experience, some patients required more than one angiography to identify the source of bleeding. The distribution of the arterial lesions is summarised in Table 1. The hepatic and gastroduodenal arteries were the most common locations of bleeding after surgery (Figures 1a, 1b). On the contrary, in pancreatitis, the distribution of the arterial lesions is quite uniform (Figures 2a, 2b, 3a, 3b, 3c). Bleeding was stopped in all treated patients. Different radiological endovascular techniques were used. The treatment modality depended on the vessel involved. Embolization, both proximal and distal to the bleeding site was performed whenever possible.

Embolization of the artery afferent to the arterial disruption using coils up and downstream of the arterial lesion (endovascular ligation) was performed in 21 cases (Figures 2c, 2d). The embolization with coils (Figures 2c 2d, 3d) was enough to stop the bleeding in about 50% of cases (Table 2). Acrylic glue with coils was used in 5 cases to achieve haemostasis more quickly. The embolization of the bleeding vessel just with acrylic glue was applied as endovascular treatment modality in 8 cases (Table 2). The embolization with acrylic glue alone was performed when selective catheterization downstream of the arterial lesion was impossible or in order to achieve an instant embolization (Figure 4). In 3 patients, an exclusion of the arterial disruption (Figures 1b, 1c, 1d) was achieved using a balloon-expandable covered stent (Jostent Peripheral Stent Graft, Jomed Implantate GmbH, Rangendingen, Germany). In acute pancreatitis, an artery dissection following selective catheterization resulted in bleeding stoppage in 2 cases of arterial lesion. These 2 cases were not considered as technical successes. After the procedure, fatal rebleeding occurred in 6 patients and, in the first part of the study, 2 patients died of he-

Table 2. Materials and techniques

Aetiology	Coils	Coils + glue	Glue	Covered stent	Dissection
Acute pancreatitis	6/12	1/12	3/12	0/12	2/12
P-B Surgery	2/9	3/9	1/9	3/9	0/9
Percutaneous procedure	8/8	0/8	0/8	0/8	0/8
Chronic pancreatitis	4/6	0/6	2/6	0/6	0/6
Aneurysm	0/3	1/3	2/3	0/3	0/3
Trauma	1/1	0/1	0/1	0/1	0/1
Total	**21/39 (54%)**	**5/39 (14%)**	**8/39 (20%)**	**3/39 (7%)**	**2/39 (5%)**

Table 3. Outcomes

Etiology	Mortality		Clinical Success
	Fatal Rebleeding	Fatal Complication	
Acute pancreatitis	4*/12	0/12	6/12
P-B Surgery	2/9	1/9	6/9
Percutaneous procedure	0/8	0/8	8/8
Chronic pancreatitis	0/6	0/6	6/6
Aneurysm	0/3	1/3	2/3
Trauma	0/1	0/1	1/1
Total	**6/39 (16%)**	**2/39 (5%)**	**31/39 (79%)**

* bleeding stoppage after artery dissection

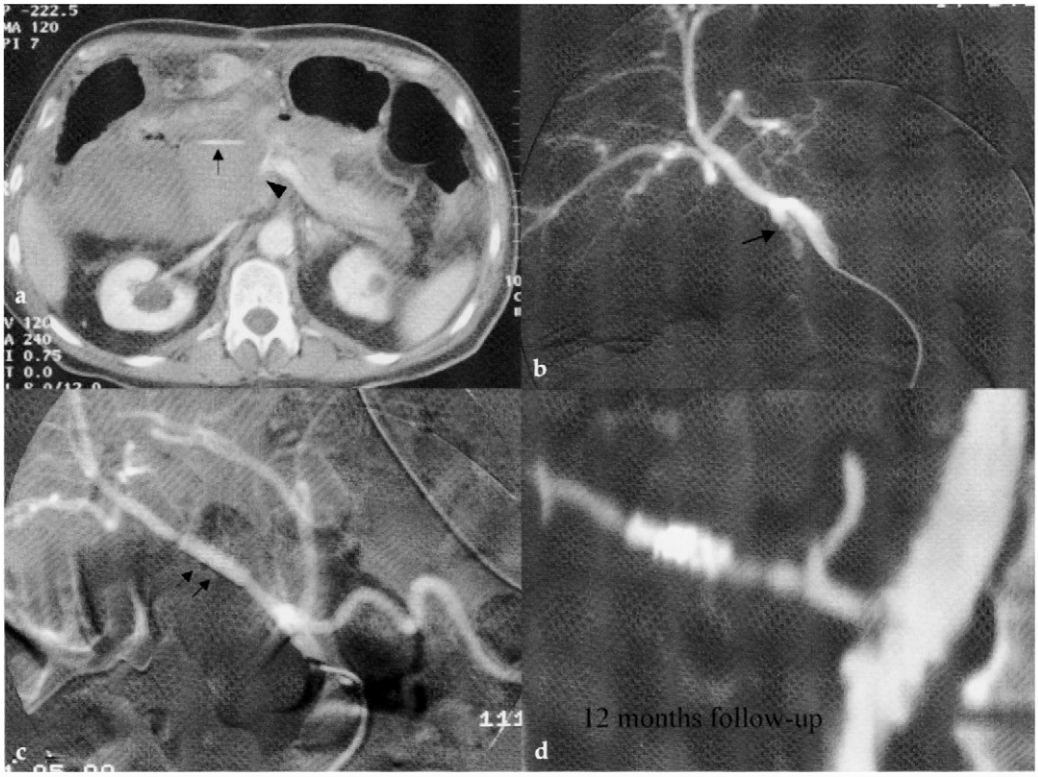

Figure 1a. Splanchnic artery bleeding after pancreatoduodenectomy (two cases). Axial CT scan, carried out in the venous contrastographic phase, highlights a voluminous subhepatic hematoma with intraperitoneal spread of contrast medium resulting in a contrast-blood level (arrow). The spleno-portal confluence (arrowhead) is compressed by the huge hematoma.

Figure 1b. Selective angiography of the hepatic artery, in another case, shows rupture of the hepatic artery involving the gastruoduodenal artery stump at the origin (arrow).

Figure 1c. In the same case, selective angiography after the placement of two covered stents (arrows) with a slight overlap in the hepatic artery for hepatic artery repair demonstrates bleeding stoppage and patency of the hepatic artery.

Figure 1d. In the same patient, at the 12-month follow-up the patency of the hepatic artery was still present at CT angiography.

patic failure after hepatic artery embolization (Table 3).

Discussion

Rupture of a pseudoaneurysm and bleeding into the abdominal cavity or gastrointestinal tract as a result of a different aetiology, although with a different clinical presentation, is often associated with massive, life-threatening haemorrhage.

The majority of pseudoaneurysms occur in pancreatitis, in association with or in close proximity to, pancreatic pseudocysts. In particular, although the natural history of pseudocyst in chronic pancreatitis is unpredictable, it can gradually erode the vascular wall of the adjacent vessels. This erosion has a double pathogenetic mechanism, enzymatic and mechanic. In the first case, the activated proteolytic enzymes in the liquid of the pancreatic pseudocyst cause necrotizing arthritis with a maceration of the vessel wall and

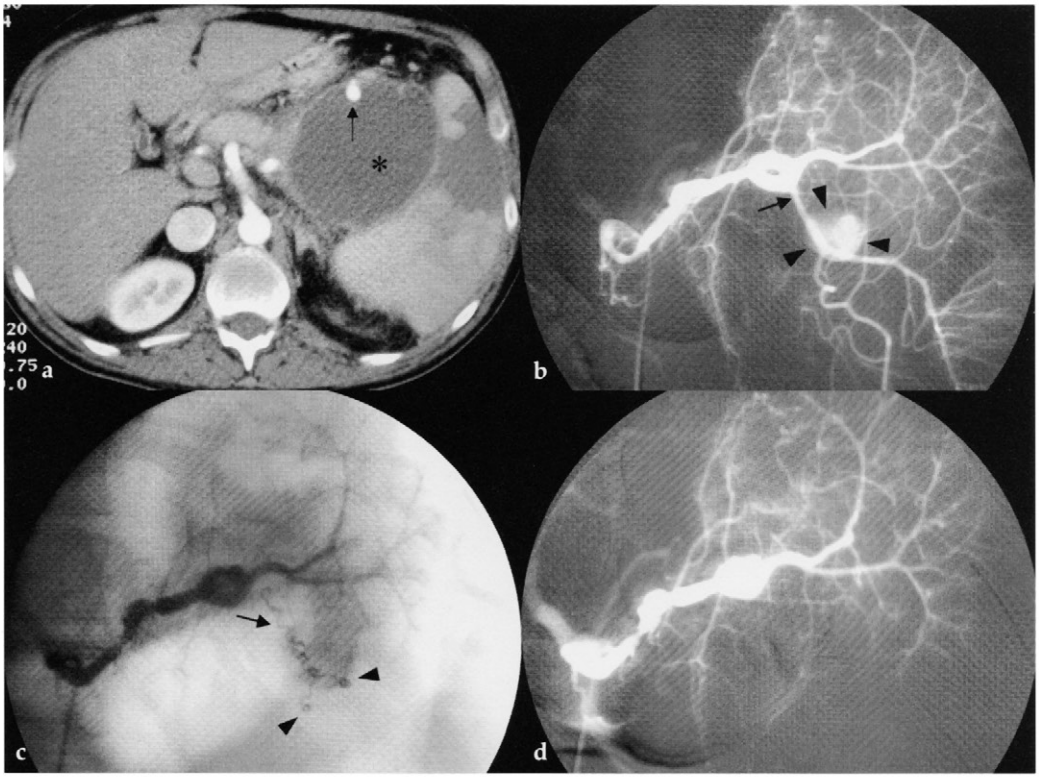

Figure 2a. Bleeding pancreatic pseudocyst. Axial CT scan in the arterial contrastographic phase demonstrates pseudocyst of the pancreatic tail (asterisk) involving the splenic artery. A small pseudoaneurysm is visible in front of the pseudocyst (arrow).
Figure 2b. Selective angiography of the splenic artery shows the pseudoaneurysm (arrowheads) slightly down-stream of the left gastroepiploic artery origin (arrow).
Figure 2c. After placing coils both up- (arrow) and down-stream (arrowheads) the pseudoaneurysm, at selective splenic arteriography.
Figure 2d. A complete exclusion of the lesion is present

bleeding inside the pseudocyst. The size of the pseudocyst is decisive in developing the type of the lesion: bleeding in a small pseudocyst is necessarily contained and more commonly ends up as a pseudoaneurysm; in case of a larger pseudocyst, rupture of the pseudoaneurysm and bleeding into the gastro-intestinal tract or into the peritoneal and/or retroperitoneal spaces can occur. Angiography reports the presence of pseudoaneurysm, without bleeding, in 10-21% of patients with chronic pancreatitis.[4] The occurrence is higher (10-31%) in patients with pseudocyst.[5,6] Hemorrhagic complications are expected in 6-31% of patients with pancreatic pseudocyst[7] and in 7-14% of those suffering from chronic pancreatitis.[8] The preventive vascular study of patients with pancreatic pseudocyst must be carried out since arterial pseudoaneurysm, although infrequent, is a potentially catastrophic complication. The risk vs. benefit balance when using angiography in this respect is, however, debatable and non-invasive vascular imaging is preferable (Doppler US, multidetectors CT, MRA).[9] Although in inflammatory pancreatic disease gastro-intestinal bleeding is frequently sustained by concurrent peptic disease, the

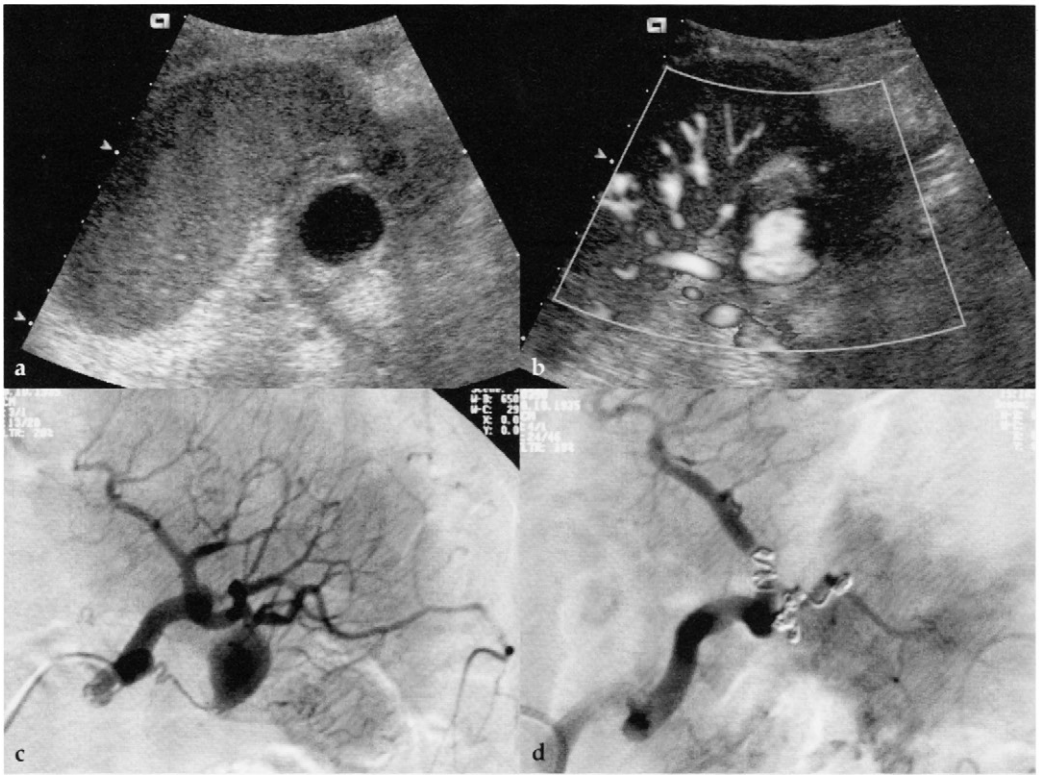

Figure 3a. Bleeding pancreatic pseudocyst. Ultrasonography shows a fluid-filled mass (asterisk) at the level of the pancreatic tail, adjacent to the splenic hilum.
Figure 3b. At power-Doppler, image blood flow within the pseudocystic lesion is present.
Figure 3c. Selective splenic angiography shows the presence of a pseudoaneurysm (asterisk) involving the splenic artery at the splenic hilum.
Figure 3d. after embolization with coils the selective angiographic control demonstrates the pseudoaneurysm exclusion

suspicion of vascular origin, apart from the negative findings of the endoscopic examination, above all correlates with the intermittence of the bleeding. Usually haemorrhagic shock is the clinical presentation of ruptured pseudoaneurysm, with a mortality rate of 50%.[10] Thanks to the most recent image reconstruction programs (MPR; MIP; SSD; VR), it is, nowadays, possible to obtain a well-defined arterial map of the pancreatic region thus identifying the lesion's vessel of origin with CT, particularly the multi-slice technique, or with MR, by means of 3D sequences in contrastographic phases. Angiography therefore plays no role in the diagnostic phase but is immediately used for treating lesions identified with non-invasive imaging. Embolization has a high possibility of success in the treatment of these lesions. With this aim it is above all necessary to define the afferent and efferent arteries involved. Only the occlusion of all efferences and therefore afferences to the pseudoaneurysm results in the certain and definite exclusion of the lesion from the arterial flow and its subsequent progressive collapse. The pseudoaneurysm has a pseudo-wall of variable thickness, which can derive from the fibrotic wall of the pseudocyst. It is better not to place coils inside the pseudoaneurysm, unless this is tech-

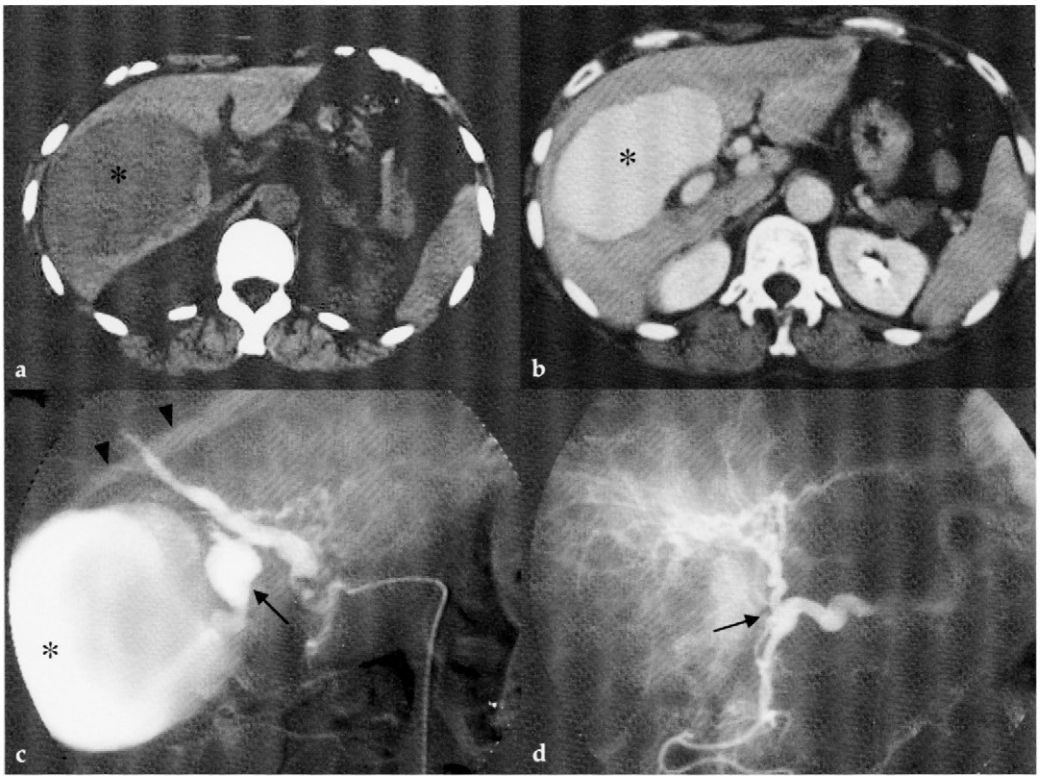

Figure 4a. Ruptured aneurysm of the right hepatic artery. CT scans in the pre- contrastographic phases show the presence of a huge intrahepatic hematoma (asterisk)

Figure 4b. Ruptured aneurysm of the right hepatic artery. CT scans in the post- contrastographic phases show the presence of a huge intrahepatic hematoma (asterisk)

Figure 4c. Selective common hepatic artery angiography demonstrates a ruptured aneurysm (arrow) arising from the right hepatic artery with the formation of a huge intrahepatic hematoma (asterisk) partially drained into the right hepatic vein (arrowheads).

Figure 4d. Selective common hepatic artery angiography following embolization with acrylic glue shows the occlusion of the right hepatic artery at the origin (arrow) with complete haemostasis.

nically indispensable to occlude the efferent vessels that would otherwise be inaccessible,[11] but to proceed to the occlusion of the afferent and efferent vessels with a technique similar to surgical tying.

Arterial bleeding in acute pancreatitis is a dramatic occurrence, subject to a high mortality rate. Stopping it may be very difficult, both surgically and radiologically. Emergency surgery is associated with a rather high degree of failure and mortality. In particular, there is more than an 80% occurrence of further bleeding,[12-14] while surgical resection is subject to more than 50% mortality.[8] The radiological treatment of acute bleeding from an arterial disruption in acute pancreatitis can fail due to the excessive extent of the maceration of the vessel or the involvement of several arterial branches. Once again the interventional procedure foresees the embolization of the bleeding vessel or vessels. The embolization of the vessel proximally or distally with respect to the site of bleeding is a condition for success not to be ignored. On the contrary, the embolization of the bleeding vessel with spongostan is subject to a high re-

lapse rate since the fibrin sponge is sensitive to the lytic action of the activated pancreatic enzymes.[15] The embolization with coils is a solution only when they are placed up and downstream of the breach in the bleeding arterial vessel where the wall is not affected by enzymatic erosion. From personal experience, when haemodynamic instability required a rapid embolic action, or when catheterization of the vessel downstream of bleeding was impossible, acrylic glue proved to be the most efficient embolizing agent.[16] Injected upstream of the arterial lesion and correctly diluted, the glue is able to reach the arterial tract downstream and, with its progressive polymerization, brings about a proximal and distal occlusion and, at the same time, fills the pseudoaneurysm.

The incidence of haemorrhagic complications due to arterial disruption after pancreatic surgery, especially pancreatoduodenectomy, has not changed in the last 20 years (2%-18%).[3] Bleeding is the second most serious complication after sepsis due to the dehiscence of the pancreatic anastomosis. Early bleeding, in the first two weeks, due to insufficient intra-operative hemostasis at the abdominal vessel level or in correspondence with the anastomosis, requires a second laparotomy. Late bleeding, after the first-second week, is more difficult to diagnose, and its treatment is less codified. It can follow arterial disruption by erosion after the dehiscence of the pancreato-jejunal anastomosis. More than two weeks after surgery, even modest bleeding must make anastomotic dehiscence a suspect. This slight bleeding is defined as »sentinel bleeding« because it often precedes, by 6 hours to 10 days, massive hemorrhage from the erosion of a large arterial branch. Rumstat *et al*[3] suggest immediate surgical intervention with a revision of the pancreatic-digestive anastomosis when »sentinel bleeding« appears at the drainage or the gastro-intestinal tract. When the dehiscence of the anastomosis occurs, the massive hemorrhage causes mortality in 15% to 58% of cases.[3,17] The frequent presence of anastomotic dehiscence requires an embolization technique similar to that used in acute pancreatitis. The most commonly involved vessels are the gastroduodenal artery stump or the common hepatic artery.[3,17-20] The embolization with coils leads to definite stoppage of the bleeding only when the gastroduodenal artery is occluded in a tract not involving septic maceration or, alternatively, the common hepatic artery is directly occluded. Embolization is sometimes used as a temporary procedure to stop or slow down bleeding so that the patient can be operated on electively rather than in emergency.

Considering the possible complication of the endovascular embolization, the vessels that can generally be embolized safely in this region include the left gastric, gastroduodenal, gastroepiploic, and pancreaticoduodenal arteries.[21] The occlusion of the common hepatic artery, with normal patency of the portal vein has no clinical consequences; embolization is, however, unadvisable in the presence of thrombosis or compression of the portal vein.[22] Moreover, the presence of a biliary-enteric anastomosis is considered a risk factor for developing a hepatic abscess following a hepatic artery embolization.[23] The treatment of bleeding from the common hepatic artery or from the short stump of the gastroduodenal artery following a pancreatoduodenectomy is often problematic for the surgeon, and the radiologist should decide to go ahead with classic embolization. But compression, even to the point of thrombosis, of the portal vein is common due to the presence of adjacent hematic collection. In these cases, the alternative treatment to embolization is positioning covered stents that maintain the patency of the hepatic artery in emergency (Figure 1). Although very significant, there are still only a few reports in literature concerned with the use of this technique.[24,25] Occlusion of the stent over time due to hy-

perplasia of intima is predictable. Nevertheless, the treatment stops the bleeding immediately and maintains the hematic contribution to the liver. The slow occlusion of the stent can then be compensated by the recruitment of collateral intra-hepatic arterial circulation and the return to normal portal flow or the growth of a collateral portal network.

Conclusions

Considering the high mortality rate of splanchnic artery bleeding in pancreato-biliary diseases and the poor results of surgical intervention, the endovascular approach, with embolization or repair of the bleeding vessel, has to be considered as the treatment of first choice. In our series, the endovascular treatment of splanchnic artery bleeding in pancreato-biliary disease resulted as clinically successful in up to 75% of cases at the three-month follow-up.

References

1. Shibata T, Sagoh T, Ametani F, Maetani Y, Itoh K, Konishi J. Transcatheter microcoil embolotherapy for ruptured pseudoaneurysm following pancreatic and biliary surgery. *Cardiovasc Intervent Radiol* 2002; **25:** 180-5.

2. Rumstadt B, Schwab M, Korth P, Samman M, Trede M. Hemorrhage after pancreatoduodenectomy. *Ann Surg* 1998; **227:** 236-41.

3. Messina LM, Shanley CJ. Visceral artery aneurysms. *Surg Clin North* Am 1997; **77:** 425-42.

4. Burke JW, Erickson SJ, Kellum CD, Tegtmeyer CJ, Williamson BRJ, Hansen MF. Pseudoaneurysms complicating pancreatitis: detection by CT. *Radiology* 1986; **161:** 447-50.

5. Frey CF, Stanley JC, Eckhauser F. Hemorrhage. In: Bradley EL, editor. *Complications of pancreatitis.* Philadelphia: WB Saunders Co; 1992. p. 96-123.

6. Kiviluoto T, Kivisaari L, Kivilaakso E, Lempinen M. Pseudocysts in chronic pancreatitis. Surgical results in 102 consecutive patients. *Arch Surg* 1989; **124:** 240-3.

7. Sankaran S, Walt AJ. The natural and unnatural history of pancreatic pseudocyst. *Br J Surg* 1975; **62:** 37-44.

8. Bresler L, Boissel P, Grosdidier J. Major haemorrhage from pseudocysts and pseudoaneurysms caused by chronic pancreatitis: surgical therapy. *World J Surg* 1991; **15:** 649-52; 652-3.

9. Ammori BJ, Alexander DJ, Madan M. Haemorrhagic complications of pancreatitis: presentation, diagnosis and management. *Ann R Coll Surg Engl* 1998; **80:** 316-25.

10. Lendrum R. Chronic pancreatitis. In: Misiewicz JJ, Pounder RE, Venables CW, editors. *Diseases of the gut and pancreas.* London: Blackwell Scientific Publications; 1994. p. 441-54.

11. Schoder M, Cejna M, Langle F, Hittmaier K, Lammer J. Glue embolization of a ruptured celiac trunk pseudoaneurysm via the gastroduodenal artery. *Eur Radiol 2000;* **10:** 1335-7.

12. Stabile BE, Wilson SE, Dibas HT. Reduced mortality from bleeding pseudocysts and pseudoaneurysms caused by pancreatitis. *Arch Surg* 1983; **118:** 45-51.

13. El Hamel A, Parc R, Adda G, Bouteloup PY, Huguet C, Malafosse M. Bleeding pseudocysts and pseudoaneurysms in chronic pancreatitis. *Br J Surg* 1991; **78:** 1059-63.

14. Stanley JC, Frey CF, Miller TA, Lindenauer SM, Child CG. Major arterial hemorrhage. *Arch Surg* 1976; **111:** 435-8.

15. Golzarian J, Nicaise N, Deviere J, Ghysels M, Wery D, Dussaussois L, et al. Transcatheter embolization of pseudoaneurysms complicating pancreatitis. *Cardiovasc Intervent Radiol* 1997; **20:** 435-40.

16. Yamakado K, Nakatsuka A, Tanaka N, Takano K, Matsumura K, Takeda K. Transcatheter arterial embolization of ruptured pseudoaneurysms with coils and n-butyl cyanoacrylate. *JVIR* 2000; **11:** 66-72.

17. Sato N, Yamaguchi K, Shimizu S, Morisaki T, Yokohata K, Chijiiwa K, et al. Coil embolization of bleeding visceral pseudoaneurysms following pancreatectomy: the importance of early angiography. *Arch Surg* 1998; **133:** 1099-102.

18. Aranha GV, Prinz RA, Greenlee HB, Freeark RJ. Gastric outlet and duodenal obstruction from inflammatory pancreatic disease. *Arch Surg* 1984; **119:** 833-5.

19. Brodsky JT, Turnbull AD. Arterial hemorrhage after pancreatoduodenectomy. The »sentinel bleed«. *Arch Surg* 1991; **126:** 1037-40.

20. Balladur P, Christophe M, Tiret E, Parc R. Bleeding of the pancreatic stump following pancreatoduodenectomy for cancer. *Hepatogastroenterology* 1996; **43:** 268-70.

21. Rosen RJ, Sanchez G. Angiographic diagnosis and management of gastrointestinal hemorrhage Current Concepts. *Radiol Clin North Am* 1994; **32:** 951-67.

22. Cardella JF, Vujic I, Tadavarthy SM, Beltran M, Castañeda-Zúñiga WR. Gastrointestinal bleeding. Part 1. Vasoactive drugs and embolotherapy in the management of gastrointestinal bleeding. In: Castañeda-Zúñniga WR, editors. *Interventional radiology*. 3rd ed. Baltimore: Williams & Wilkins; 1997. p. 207-52.

23. Okajima K, Kohno S, Tamaki M, Hosono M, Kawamoto M, Nishiyama Y, et al. Bilio-enteric anastomosis as a risk factor for postembolic hepatic abscess. *Cardiovasc Intervent Radiol* 1989; **12:** 128-30.

24. BŁrger T, Halloul Z, Meyer F, Grote R, Lippert H. Emergency stent-graft repair of a ruptured hepatic artery secondary to local postoperative peritonitis. *J Endovasc* Ther 2000; **7:** 324-7.

25. Paci E, Antico E, Candelari R, Alborino S, Marmorale C, Landi E. Pseudoaneurysm of the common hepatic artery: Treatment with a stent-graft. *Cardiovasc Intervent Radiol* 2000; **23:** 472-84.

Radiol Oncol 2002; 36(4): 291-5.

case report

Cerebral hyperperfusion syndrome after carotid angioplasty

Zoran Miloševič[1], Bojana Žvan[2], Marjan Zaletel[2], Miloš Šurlan[1]

[1]Institute of Radiology, [2]University Neurology Clinic,
University Medical Center, Zaloška cesta 7, Ljubljana, Slovenia

Background. *Cerebral hyperperfusion syndrome after carotid endarterectomy is an uncommon but well-defined entity. There are only few reports of »hyperperfusion injury« following carotid angioplasty.*
Case report. *We report an unstable arterial hypertension and high-grade carotid stenosis in a 58-year-old, right-handed woman. After a stroke in the territory of middle cerebral artery carotid angioplasty was performed in the patient. Among risk factors, the long lasting arterial hypertension was the most pronounced. Immediately after the procedure, the patient was stable without any additional neurologic deficit. The second day, the patient had an epileptic seizure and CT revealed a small haemorrhage in the left frontal lobe.*
Conclusions. *The combination of a high-grade carotid stenosis and unstable arterial pressure is probably an important prognostic factor in the pathogenesis of hyperperfusion syndrome.*

Key words: carotid artery diseases; angioplasty - adverse effects; reperfusion injury, hyperperfusion syndrome; hypertension

Introduction

Cerebral hyperperfusion after carotid endarterectomy is an uncommon, but well-defined entity.[1] Despite the increasing use of carotid anigoplasty, there are only few reports of »hyperperfusion injury« following carotid angioplasty in the literature.[2-5] The syndrome occurs in a number of clinical settings and is characterised by the diagnostic triad of unilateral headache, seizures, and intracranial haemorrhage. In our case, the patient developed typical signs of hyperperfusion syndrome detected from typical computed tomography (CT) findings.

Received 25 October 2002
Accepted 4 November 2002

Correspondence to: Zoran Miloševič, MD, University Medical Center, Institute of Radiology, Zaloška 7, SI-1525 Ljubljana, Slovenia; Phone: +386 1 432 2346; E-mail: zoran.milosevic@guest.arnes.si

Case report

In September 2001, a 58-year-old, right-handed woman was referred to our Department after an ischemic stroke. In 1995, she had an anterior circulation cerebrovascular accident but she has made a good recovery. Her medical history included long-lasting arterial hypertension for more than 20 years and hyperlipoproteinemia. There was no history of cigarette smoking or excessive alcohol intake. In spite of regular ACE-inhibitor treatment, her blood pressure fluctuated. She had been treated with Aspirin 100 mg daily and statin 20 mg.

When assessed in our hospital before carotid angioplasty she had a residual expressive dysphasia, as well as a mild weakness in the face and limb on the right. Her blood pressure was 180/110 mm Hg. Computed tomography scan (CT) of the brain revealed widened liquor spaces, pre-existed ischemic lesions up to 1 mm in size, located deep in the left cerebral hemisphere, in the left frontal lobe and subcortically in the left parietal lobe. There was no evidence of haemorrhage. All haematological and biochemical tests were normal with a normal platelet count and coagulation screen. Duplex ultrasonography made in 2001 revealed a 90-per-cent stenosis of the left internal carotid artery (ICA) produced by echolucent plaque, type I (according to the accepted international classification). The plaque was unstable and had an irregular surface (Figure 1).

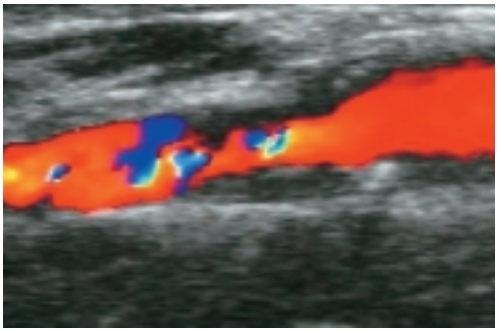

Figure 1. Colour Doppler ultrasound shows a 90-per-cent stenosis of the left internal carotid artery.

The patient underwent the left carotid angioplasty through the femoral approach under local anaesthesia. Intra-arterial digital subtraction angiography confirmed a 95-per-cent stenosis of the left ICA (Figure 2a). The patient was given 5000IU of heparin IV. The stenosis was crossed with a flexible coronary guidewire (V-18 Control Wire; Boston Scientific Corp). Glycopyrrolate and 0.5 mg atropine IV were administered during the procedure. The stenosis was predilated with a low-profile coronary balloon (4 x 20 mm Bypass Speedy Monorail Catheter, Boston Scientific Corp) and stented with a 7 x 30 Carotid Wallstent Monorail (Boston Scientific Corp). The stent was dilated with a 5.5 x 20 mm Bypass Speedy Monorail Catheter (Boston Scientific Corp) that embedded it firmly into the vessel wall.

The blood pressure varied between 160/90 mm Hg and 175/105 mm Hg during the procedure, but there were no residual adverse neurological *sequelae*. Postprocedural angiogram showed no significant stenosis or dissection (Figure 2b). In the following 24 hours, the patient was treated with Aspirin

Figure 2a. Digital subtraction angiography. Lateral views of the left carotid artery bifurcation. High grade circumferential, atherosclerotic stenosis of the internal carotid artery origin before carotid stenting.

and clopidogrel, her blood pressure varied between 140 and 160/95 mm Hg and she was clinically stable. On the following day she was dismissed. She did not continue antihypertensive therapy when she was at home because she was convinced that she did not need this therapy after carotid stenting.

After 2 days she was urgently re-admitted because of a grand mal type epileptic seizure. After the seizure she had a transient left right-sided hemiplegia. Blood pressure at the time of admission was 180/100 mm Hg. An urgent brain CT revealed a small haemorrhage in the left frontal lobe (Figure 3). Colour Doppler ultrasound of the ICA revealed a visibly patent vessel (Figure 4). The peak systolic velocity rose to 2.3 m/s, with the end diastolic velocity of 1.2 m/s. The patient was managed conservatively. Hypertension was easily controlled with 10 mg enalapril twice daily. The antiepileptic therapy was introduced. She recovered completely after two weeks.

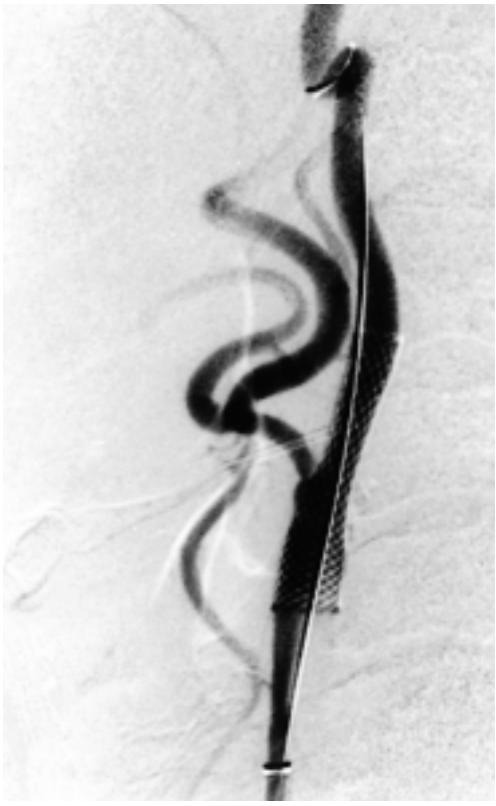

Figure 2b. Digital subtraction angiography. Lateral views of the left carotid artery bifurcation. No residual stenosis after carotid stenting.

Discussion

Cerebral hyperperfusion syndrome (CHS) may manifest as ipsilateral headaches, seizures, or intracerebral haemorrhages. Risk factors such as high-grade stenosis, contralateral carotid occlusion, poor collateral flow, chronic ipsilateral hypoperfusion, preoperative and postoperative hypertension, and perioperative use of anticoagulant or antiplatelet agents have been reported.[1] In our case, we do not have pathologic evidence to support hyperperfusion injury as a cause of the haemorrhage after CAS, but clinical feature and postprocedural systemic hypertension, together with the lobar appearance of the haemorrhage, indicate to the mechanism of hyperperfusion injury. Angioplasty performed in the patients with high degree carotid stenosis proved that the stenosis was associated with poststenotic drop in perfusion pressure. Therefore, it is likely that the patient suffered a chronic ischemia, which can cause a loss of autoregulation. This could be an important pathophysiologic mechanism of hyperperfusion injury.[6]

CHS has been defined as cerebral blood flow (CBF) in excess of that required for metabolic needs or a postoperative increase greater than 100% of the preoperative cerebral blood flow.[7] Therefore, when cerebral autoregulation is impaired, the elevated blood pressure could increase CBF. In our case, the patient had unstable arterial pressure with tendency toward high pressure. During hospitalisation, the arterial pressure did not exceed 145/90 mm Hg and the patient did not use antihypertensive medication. According to our experiences, the heart rate

and arterial pressure in most of the patients decrease after the carotid angioplasty. The reason could be iatrogenic stimulation of carotid baroreceptors, which seems to improve in the next few days. Thus, the arterial pressure could rise to hypertensive levels in the days after carotid stenting, thereby increasing regional CBF in the presence of impaired autoregulation and causing CHS.

CHS has also been widely reported in the surgical literature as an infrequent complication of carotid endarterectomy (CEA) with an incidence of approximately 0.6%.[6] In our opinion and previous experiences, it may also occur after percutaneous transluminal carotid angioplasty and stenting with causal mechanism and clinical features similar to those of CEA.[5,8] One cannot completely exclude the possibility of embolism and silent cerebral infarction with subsequent haemorrhagic transformation in response to hyperperfusion, but the CT scan appearances do not indicate to such a mechanism.

Conclusions

In conclusion, CHS may occur after carotid stenting. The combination of a high-degree carotid stenosis and unstable arterial pressure is probably an important cause in the pathogenesis of hyperperfusion syndrome. The arterial blood pressure monitoring seems to be important after carotid angioplasty of high-degree stenosis.

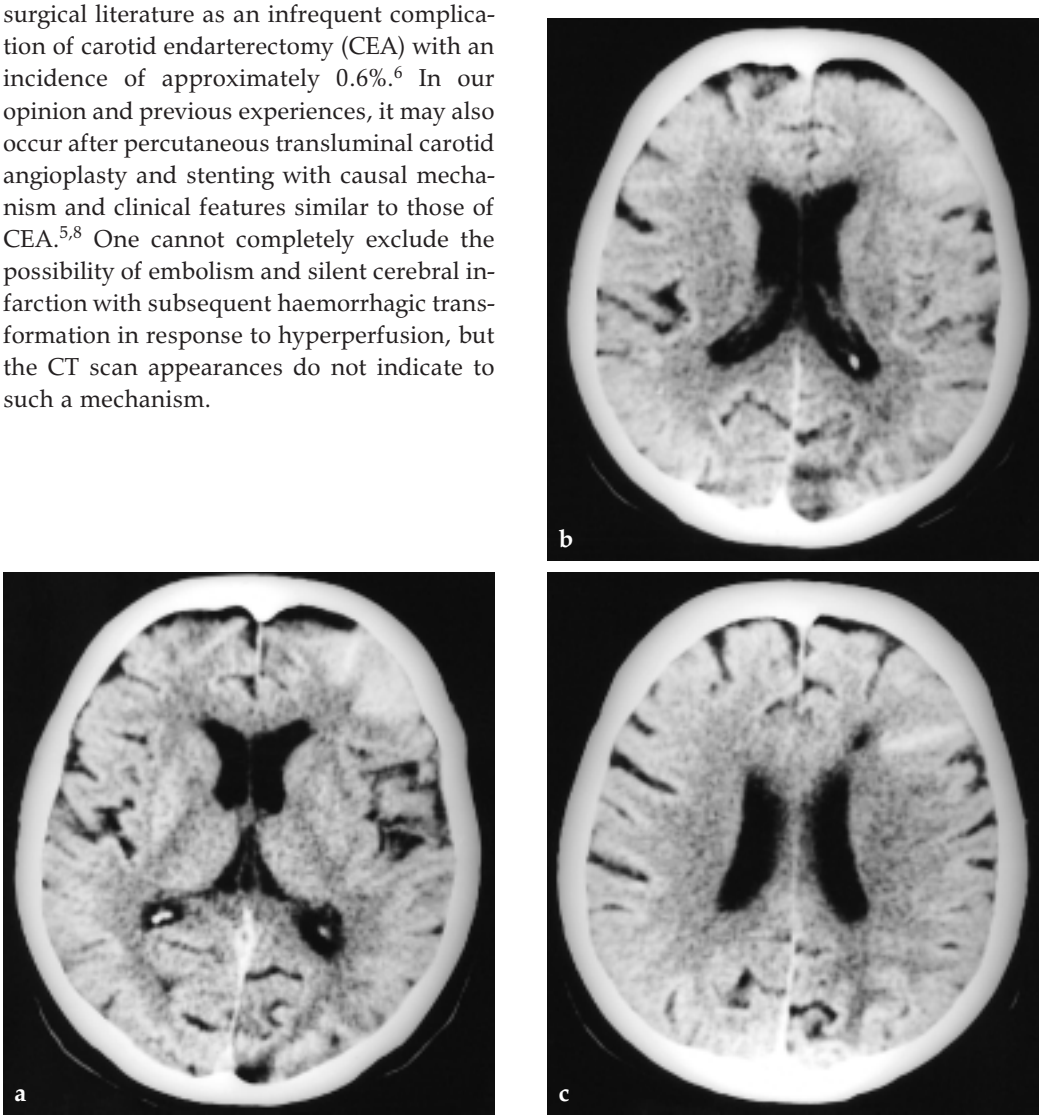

Figure 3a, 3b, 3c. CT of the brain demonstrates small haemorrhage in the left frontal region.

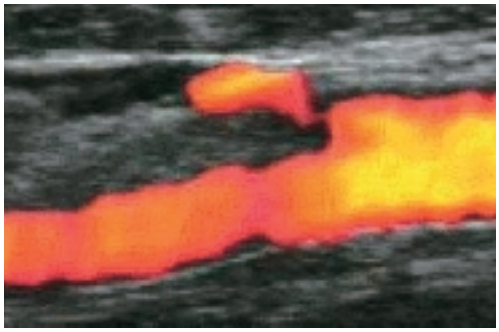

Figure 4. Colour Doppler ultrasound of the internal carotid artery shows a visibly patent vessel.

References

1. Keunen R, Nijmeijer HW, Tavy D, Stam K, Edelenbosch R, Muskens E, et al. An observational study of pre-operative transcranial Doppler examinations to predict cerebral hyperperfusion following carotid endarterectomies. *Neurol Res* 2001; **23:** 593-8.

2. Milosevic ZV, Zvan B, Zaletel M, Surlan M. Cerebral hyperperfusion syndrome after carotid stenting. [Online]. Mar 22, 2002. URL: http://www.eurorad.org/case.cfm?UID=1563 Luxembourg, Euromedia.

3. Chuang YM, Wu HM. Early recognition of cerebral hyperperfusion syndrome after carotid stenting - a case report. *Kaohsiung J Med Sci* 2001; **17:** 489-94.

4. Morrish W, Grahovac S, Douen A, Cheung G, Hu W, Farb R, et al. Intracranial hemorrhage after stenting and angioplasty of extracranial carotid stenosis. *AJNR Am J Neuroradiol* 2000; **21:** 1911-6.

5. McCabe DJ, Brown MM, Clifton A. Fatal cerebral reperfusion hemorrhage after carotid stenting. *Stroke* 1999; **30:** 2483-6.

6. Hosoda K, Kawaguchi T, Shibata Y, Kamei M, Kidoguchi K, Koyama J, et al. Cerebral vasoreactivity and internal carotid artery flow help to identify patients at risk for hyperperfusion after carotid endarterectomy. *Stroke* 2001; **32:** 1567-73.

7. Nakase H, Sakaki T, Kempski O. A scanning technique to measure regional cerebral blood flow and oxyhemoglobin level. *Neurosurgery* 2001; **48:** 1335-42.

8. Mansoor GA, White WB, Grunnet M, Ruby ST. Intracerebral hemorrhage after carotid endarterectomy associated with ipsilateral fibrinoid necrosis: a consequence of the hyperperfusion syndrome? *J Vasc Surg* 1996; **23:** 147-51.

Radiol Oncol 2002; 36(4): 297-303.

Cortico-basal ganglionic degeneration: radiological and functional features

Maja Ukmar[1], Rita Moretti[2], Paola Torre[3], Rodolfo M. Antonello[3], Renata Longo[4], Antonio Bava[2], Roberto Pozzi Mucelli[1]

[1]Department of Radiology, [2]Department of Physiology and Pathology, [3]Department of Internal Medicine and Clinical Neurology, [4]Department of Physics, University of Trieste

Background. *Cortico-basal ganglionic degeneration is a rare degenerative pathology that involves parietal areas and gradually determines frontal involvement. The aim of our work was to describe the main radiological findings in this pathology and to evaluate the cortical activation in these patients by f-MRI during simple and complex movements.*

Patients and methods. *We have evaluated eight patients with morphological and functional magnetic resonance by using a 1.5 T imager.*

Results. *Morphological evaluation: We found an asymmetric perirolandic cortical atrophy in seven patients, a mild hyperintensity in the perirolandic cortex in five patients, a mild atrophy of the basal ganglia in seven patients and, in one, a hypointensity in the lenticular nuclei. In one patient the morphological aspect was normal. Functional evaluation: The most important aspect was the hypoactivation of the parietal areas during the movement with the affected hand in all the patients.*

Conclusions. *We consider f-MRI a helpful tool for the diagnosis and follow-up of this pathology.*

Key words: basal ganglia diseases, cortico-basal degeneration; magnetic resonance imaging; fluorine radioisotopes, f-MRI; movement, apraxia, parietal lobe

Introduction

Cortico-basal ganglionic degeneration (CBGD) has become a more widely recognized entity: it has been considered as a degenerative movement disorder since its first description by Rebeiz thirty years ago.[1] Since then, one hundred cases have been reported,[2] but it remains a rare disease of unknown incidence and prevalence.[3,4]

CBGD usually presents after the fifth decade of life, with a varied combination of symptoms including stiffness, clumsiness, jerking, segmental dystonia, bradykinesia and usually ideomotor apraxia which can progress to the complete development of an »alien hand syndrome«. Other symptoms, such as action-induced and stimulus sensitive

Received 25 October 2002
Accepted 4 November 2002

Correspondence to: Maja Ukmar, MD, Department of Radiology, University of Trieste, Trieste, Italy

focal reflex myoclonus may precede or accompany the development of dystonic postures.[5] Invariably, it leads to a progressive disability (both motor and cognitive) which gradually leads to immobilization and institutionalisation.

Logistic regression analysis identified two models that contributed to distinguish these disorders and predicted the diagnosis of CBGD. The first one included asymmetric Parkinsonism as symptom onset and instability and falls at first clinic visit. The other one included cognitive disturbances, asymmetric parkinsonism within the first year of symptom onset and speech disturbances at the first clinic visit.[6] A recent evaluation[7] suggests that cognitive signs of disruption, which comprise a marked impairment of daily living functions, may be the commonest presentation of CBGD, rather than the better recognised perceptual-motor syndrome, described previously.

Radiological evaluation seems to be important as a diagnostic and clinical follow-up instrument. The most constant expression of the pathological features are: an important atrophy of the perirolandic gyri, particularly in the postrolandic cortex, associated with a mild atrophy of the basal ganglia,[8-10] and an almost evident, though not constant hypointensity of the lenticular nuclei.[8-10]

The possibility of a direct and functional evaluation of cortical activation during hand motion, registered in CBGD patients, seems to us very interesting. This was the aim of our study: we discussed the results with an overview of literature.

Patients and methods

During the period between 1st January 1997 and 1st January 2002, eight patients (three males and five females) were included into our observation. Their mean age was 62.1 years old (SD + 6.9), all of them were right-handed (average score at Briggs and Nebes Test: + 22.56).[11]

The past history of all the patients was completely mute for cerebrovascular disease, hypertension and metabolic disorders. No signs of addiction could be found. Their most common complain was the relatively recent development of an asymmetric akinetic syndrome (55% of cases), affecting in all the eight patients their left superior limb, ideomotor apraxia (43% of cases), bradykinesia (36% of cases), alien-limb syndrome (16% of cases), slurred speech (5% of cases) and gait difficulty (5% of cases). Only two of the subjects (35% of cases) showed action tremor and one of them (13% of cases) supranuclear gaze palsy affecting vertical and horizontal gazes (evidenced at oculomotor evaluation). All the patients underwent a complete oculomotor evaluation: a normal saccadic velocity (considering anti-saccades, reflexive saccades and voluntary saccades), with increased latency of saccades (especially of voluntary saccades) and preserved pursuit and optokinetic nystagmus were globally evidenced.

The mean duration of symptoms dated from 7.62 + 5.32 months prior to their admission.

From the cognitive perspective, intelligence performances were within normal ranges (111 + 2.34) as stated by the average score obtained in Raven Standard Progressive Matrices;[12] the patients recognised right/left personal and extrapersonal hemispace, and no signs of tactile agnosia and of bucco-facial apraxia were found. Wechsler Adult Intelligence Scale (WAIS) average results demonstrated a mild general tendency to global deterioration (21.1% SD + 2.34%).[13] All the patients could reproduce Koh's Block quite well, by copy and by memory. Wechsler Memory Scale (WMS)[14] put in evidence an MQ average score of 56.35 (SD + 5. 41), underlying a mild deterioration of logical, procedural and verbal memory strategies. All the subjects could not pantomime to

verbal command of the examiner: all together showed signs of ideomotor apraxia with the left, affected hand. On the contrary, they did not show signs of ideational apraxia. All the patients showed moderate insight into their general situation, but principally into their motion disruption.

All the patients underwent brain-MRI, performed by a 1.5 T magnet. For the morphological evaluation an axial SE PD/T2 (TR/TE=2709/20-80) and a turbo-FLAIR (TR/TE/TI=9832/150/2000) sequences were performed.

In order to obtain a dynamic acquisition of cortical activation during complex and acquired motor process, we decided to study our patients with f-MRI. After training, subjects had to oppose the thumb to the other fingers in a sequential task, in a 2, 3, 4, 5 sequence and in a complex, alternating sequence, 1-2, 1-4, 1-3 and 1-5 sequence.

The total acquisition time was equally divided into three-motor task periods, alternated with a three-rest period. Seven images per period were collected; so, in each measurement, 42 images were acquired. The images were oriented transversally. The major parameters of the 2D gradient-echo MR pulse sequence were the following: TR=60 ms, TE=40ms, Flip Angle=25, FOV=160x144 mm^2, Slice Thickness=4 mm, Scan Matrix=128x 128. The T1 contrast enhancement option was activated.[15]

An MR angiography acquisition was performed per each T1-GRE f-MRI acquisition. The major parameters of the angiographic sequence were the following: TR=shortest, Flip Angle=20, FOV=the same of the T1-gre, Slice Thickness=1 mm, Scan Matrix=256x256, Slices=12, Slice Thickness=1 mm, Phase Contrast Technique.

The image analysis is performed by a program developed in IDL environment (Interactive Data Language, Research System Inc., USA). The basic analysis consists of the calculation of the correlation coefficient between the time-intensity behavior of each pixel and the square wave model function.

In order to exclude transient hemodynamic responses, 5 images per block (from the 3rd to the 7th of each block) are included in the analysis. A raw activation map was obtained by applying a correlation analysis ($p<0.001$) and a cluster filtering (at least 5 pixels). The raw map was affected by flow artefacts; to eliminate these artefacts, activation map and MR angiography were compared and activation clusters related to the vessels were rejected. Whole-head high-resolution T1-weighted images (TR/TE=500/15) were then acquired to be used as an anatomical reference for the transformations into the Talairach space.[16]

Results

In seven patients, the morphological examination showed an important, asymmetric perirolandic and postrolandic cortical atrophy (Figure 1) associated to a mild atrophy of the basal ganglia. Subtle MRI T2 hyperin-

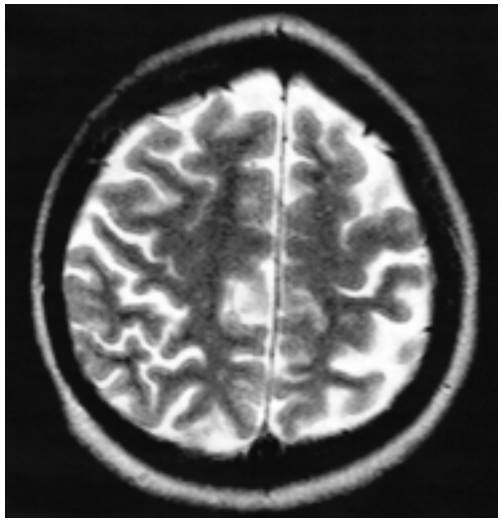

Figure 1. Axial SE T2 image: Diffuse brain atrophy particularly marked at the level of the right perirolandic cortex.

tense lesions in the primary motor cortex, compatible with underlying gliosis, were found in five patients (Figures 2a, 2b), hypointensity in the lenticular nuclei in one case only. In one patient the morphological aspect was normal.

During simple motor task carried out with the non-affected hand, we could observe a good activation of the contralateral rolandic cortex, associated with a discrete activation of the supplementary motor area (SMA) and of the parietal regions, as well as with a discrete activation of the right prefrontal region, but without significant difference from those in healthy population.

On the contrary, during a simple task of opposing the fingers executed with the affected hand, an evident hypo-activation of the homolateral and contralateral perirolandic cortex, associated with an evident hypo-activation of the contralateral SMA and with the affected parietal region, was observed. It was significantly different from the healthy control subjects.

During the complex sequence execution by the non-affected hand, an obvious bilateral activation of rolandic areas, of the parietal areas, of the SMA, and of the contralateral frontal region could be seen. These observations are similar to those in healthy controls.

When the complex sequence was executed by the affected hand, the observed activation was limited to the bilateral rolandic region, to SMA, and to a very modest activation of the parietal regions. Quantitatively, hypoactivation was significantly different from that in healthy population.

Qualitatively, the movement of the affected hand was impaired and not fluent at all despite more training exercises. Moreover, it was obvious that the patients had to see the entire procedure when they were performing the exercise with the affected hand. Without receiving the visual input that controlled the motor act the movement was even more impaired.

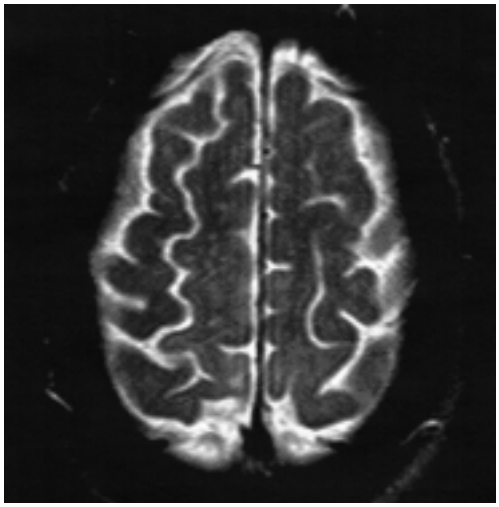

Figure 2a. Slight hyperintensity at the level of the right perirolandic cortex shown on the T2 weighted image.

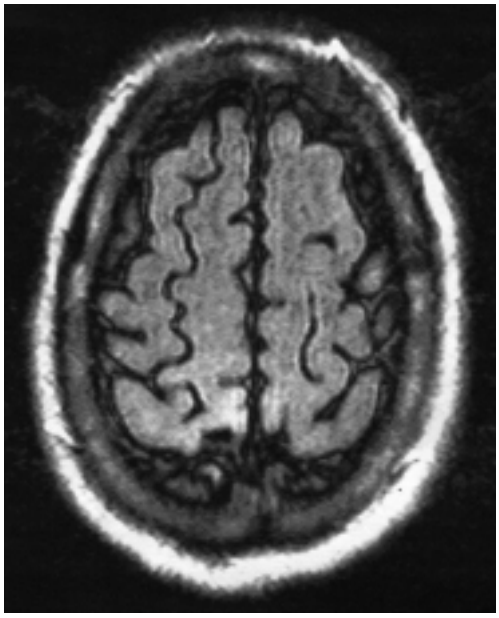

Figure 2b. Slight hyperintensity at the level of the right perirolandic cortex better shown on the FLAIR image.

Discussion

The patients with progressive focal cortical syndromes are being recognized with increasing frequency. CBGD is a degenerative disor-

der, involving primarily parietal areas, and gradually extending to frontal areas. The patients with CBGD revealed a mild to moderate global deficits including a frontal dysexecutive syndrome, explicit learning deficits without retention difficulties and displayed prominent deficits on the tests of sustained attention/mental control and verbal fluency.[17]

Different neuroimaging studies have been conducted on CBGD, using conventional computed tomography (CT) and magnetic resonance imaging (MRI),[4,18] and demonstrating an asymmetric pericentral cortical atrophy in approximately 50% of cases. On the contrary, another recent MRI study, comparing clinically diagnosed cases of CBGD with progressive supranuclear palsy (PSP), found that 87.5% patients with CBGD (but none of the PSP group) had asymmetric fronto-parietal atrophy while midbrain atrophy was seen in 6.3% and 89.3% of the same cases respectively.[18]

Another radiological observation[4] revealed that pathologically proven PSP, frontal lobe dementia and AD with clinical features of CBGD had similar MRI cortical changes.

The only possible conclusion is that, due to the distribution of pathological changes, the static imaging simply correlates with the predominant clinical presentation and not with the specific underlying pathological substrate.

Functional imaging studies were done with positron emission tomography (PET), but results did not seem to be conclusive.[18]FDG-PET studies demonstrated a greater heterogeneity of the metabolic patterns including diffuse hypometabolism despite asymmetrical clinical features. F-Dopa PET demonstrated a severe asymmetric reduction in striatal F-Dopa uptake which tended to be equal in putamen and caudate consistent with widespread substantia nigra neuron loss.[19] From these studies, the general suggestion is that (18F)-fluorodeoxyglucose (FDG) and (^{18}F)-fluoro-dopa (F-Dopa)-PET must be utilized at the same time, in the same patient.[19,20]

Our study is the first one on f-MRI in CBGD: the most interesting part is the dynamic acquisition which gives information on how the cortex works when the affected arm is moving.

The results obtained from this selected group of eight patients confirmed the results, reported previously.[21-25]

Our f-MRI evaluation revealed, while the patients executed the simple task of opposing the fingers with the affected hand, a hypo-activation of the homolateral and contralateral perirolandic cortex, associated with an evident hypo-activation of the contralateral SMA and of the affected parietal region. During the complex motor skills with the affected hand, a drastic reduction of activation of premotor and motor areas (perirolandic region) of the contralateral cortex, associated with a very modest activation of the supplementary motor area of the same hemisphere were noted.

It is interesting to see a very modest activation of motor areas, associated with the reduced activity of the parietal area: the latter is largely preventable, but the former is rather unexpected.

The imaging studies on both monkeys and humans report of the activation in the region of the supplementary motor area, globus pallidus, and parietal cortex during the performance of sequential movements.[26] Neurons of the globus pallidus also discharge during specific phases of a sequential performance.[26] This does not involve uniquely motor speed and correct execution, but also attention, coordination and dynamic adjustment to the situation. The hypoactivity of the cortical areas we have reported does match with previous finding.

Nevertheless, there is an unresolved question: our patients indisputably presented with a parietal (postrolandic) atrophy: considering that the parietal damage is the cause, why should the pure motor areas should hy-

poactivated? We maintain that the brisk stop due to the disconnection of the parietal cortex and the SMA because of degenerative alteration of parietal areas causes an interruption of the neural net to putamen and pallidus, ending in frontal and prefrontal areas.

Therefore, f-MRI, with its constant demonstration of hypoactivity of motor cortical areas, SMA and parietal areas, while affected arm is moving, might be a valid supportive tool for the diagnosis of CBGD: a positive correlation with hypoactivation of motor areas could be found even in modest, and initial stages of disease.

Having assessed that the accuracy of neurologists' clinical diagnosis of CBGD is very low, even in specialized centers[2] (at first visit mean sensitivity for CBGD 35%, specificity 99.6% and at the last visit mean sensitivity 48.3% while specificity remained stable), then MRI and f-MRI might be suggested as an adjunctive tool of the diagnosis refinement.

References

1. Rebeiz JJ, Kolodny EH, Richardson EP. Corticodentatonigral degeneration with neuronal achromasia. *Arch Neurol* 1968; **18:** 20-33.

2. Litvan I, Agid Y, Goetz C, Jankovic J, Wenning GK, Brandel JP, et al. Accuracy of the clinical diagnosis of corticobasal degeneration: a clinicopathologic study. *Neurology* 1997; **48:** 119-25.

3. Lippa CF, Smith TW, Fontneau N. Corticonigral degeneration with neuronal achromasia. *J Neurol Sci* 1990; **98:** 301-10.

4. Lang A. *Cortico-basal ganglionic degeneration.* San Diego: American Academy of Neurology; 2000.

5. Thompson PD, Day BL, Rothwell JC, Brown P, Britton TC, Marsden CD. The myoclonus in corticobasal degeneration. Evidence for two forms of cortical reflex myoclonus. *Brain* 1994; **117:** 1197-207.

6. Litvan I, Grimes DA, Lang AE, Jankovic J, McKee A, Verny M, et al. Clinical features differentiating patients with postmortem confirmed progressive supranuclear palsy and corticobasal degeneration. *J Neurol* 1999; **246(Suppl 2):** 1-5.

7. Grimes DA, Lang AE, Bergeron C. Dementia is the most common presentation of cortical-basal ganglionic degeneration. *Neurology* 1998; **50(Suppl 4):** a96.

8. Hauser R., Murtaugh F, Akhter K, Gold M, Olahow C. Magnetic resonance imaging of corticobasal degeneration. *J Neuroimaging* 1996; **6(4):** 222-6.

9. Otsuki M, Sama Y, Yoshimuro N, Tsuji S. Slowly progressive limb-kinetic apraxia. *Eur Neurol* 1997; **37(2):** 100-3.

10. Tokumaru AM, O'uchi T, Kuru Y, Maki T, Murayama S, Horichi Y. Corticobasal degeneration: MR with histopathologic comparison. ASNR 1996; **17(10):** 1849-52.

11. Briggs GC, Nebes RD. Patterns of hand preference in a student population. *Cortex* 1975; **11:** 230-8.

12. Raven JC. *Standard progressive matrices.* London: Lewis; 1938.

13. Wechsler D. *Wechsler adult intelligence scale manual.* New York: Grune & Stratton; 1976.

14. Wechsler D. A standardized memory scale for clinical use. *J Psychol* 1945; **19:** 87-97.

15. Sobol WT, Gauntt DM. On the stationary states in gradient echo imaging. *J Magn Reson Imaging* 1996; **6:** 384-98.

16. Talairach J, Tornoux P. *Co-planar stereotaxic atlas of the human brain.* Thieme: Stuttgart; 1988.

17. Kertesz A, Munoz DG. Clinical and pathological overlap between frontal dementia, progressive aphasia and corticobasal degeneration - the Pick complex. *Neurology* 1997; **48:** 293-300.

18. Gimenez-Roldan S, Mateo D, Benito C, Grandas F, Perez-Gilabert Y. Progressive supranuclear palsy and corticobasal ganglionic degeneration: differentiation by clinical features and neuroimaging techniques. *J Neural Transm* 1994; **98(Suppl 42):** 79-90.

19. Brooks DJ. Pet studies on the early and differential diagnosis of Parkinson's disease. *Neurology* 1993; **43(Suppl 6):** S6-16.

20. Eidelberg D. Differential diagnosis of parkinsonism with (18-f)fluorodeoxyglucose FDG and PET. [abstract]. *Mov Disord* 1996; **11:** 349.

21. Moretti R, Ukmar M, Torre P, Antonello RM, Longo R, Nasuelli D, et al. Cortical-basal ganglionic degeneration: a clinical, functional and cognitive evaluation (1-year follow-up). *J Neurolog Sci* 2000; **182:** 29-35.

22. Moretti R, Torre P, Antonello RM, Ukmar M, Cazzato G, Bava A. Valutazione con risonanza magnetica funzionale dell'attivazione corticale durante compiti motori fini in soggetti con degenerazione cortico-basale. *Nuova Rivista di Neurologia* 2001; **11(3):** 73-9.

23. Moretti R, Torre P, Antonello RM, Bava A. Deterioramento cognitivo nella sindrome corticobasale. *Dementia Update* 2002; **11:** 49-52.

24. Moretti R, Torre P, Antonello RM, Ukmar M, Longo R, Cazzato G, et al. Complex distal movement in cortico-basal ganglionic degeneration. A functional evaluation. *Funct Neurol* 2002; **17(2):** 71-6.

25. Jeannerod M, Arbib MA, Rizzolatti G, Sakata H. Grasping objects: the cortical mechanisms of visuomotor transformation. A review. *Trends Neurosci* 1995; **18:** 314-20.

26. Lu MT, Preston JB, Strick PL. Interconnections between the prefrontal cortex and the premotor areas in the frontal lobe *J Comp Neurol* 1994; **341:** 375-92.

Radiol Oncol 2002; 36(4): 305-12.

Breast MRI of ductal carcinoma in situ: Is there MRI role?

Giuliana E. Francescutti, Viviana Londero, Ilaria Berra, Chiara Del Frate, Chiara Zuiani, Massimo Bazzocchi

Department of Medical and Morphological Research, Institute of Radiology, University of Udine

Background. *The purpose of this study is to report our personal experience of 22 cases of ductal carcinoma in situ (DCIS) studied with magnetic resonance imaging (MRI).*

Patients and methods. *From September 1995 to December 2001, 22 women diagnosed with DCIS lesions underwent contrast enhanced MRI within 7 days after mammographic examination.*

Dynamic MRI was performed with a 1 T system, using a three dimensional fast low angle shot (FLASH) pulse sequence before and after contrast media administration. We evaluated the morphologic features of the enhancement, the enhancement rate and the signal time intensity curve. Pathology was obtained in all cases.

Results. *The results of histopatological examination included: 15 DCIS and 7 DCIS with associated microinvasive component or microfoci of invasive ductal carcinoma (IDC).*

On MRI, 21 of 22 (95%) DCIS lesions showed contrast enhancement. Fourteen out of 15 pure DCIS lesions demonstrated respectively a low (3), undeterminate (5), and strong (6) enhancement. Morphologically, the enhancing lesion was focal in 7, segmental in 4, and with linear branching in 3 cases. Wash out was found in 4 cases, plateau curve in 8 and Type I curve in 2 cases. Multifocality was present in 5 cases.

All DCIS with associated microinvasion demonstrated contrast enhancement: 1/7 cases showed a low enhancement, 2/7 showed an indeterminate enhancement and 4/7 showed a strong enhancement. Morphologically, the enhancing lesion was focal in 3/9, segmental in 5 and with linear branching in 1 case. The wash out was demonstrated in 3/7 cases, plateau curve in 3 and Type 1 curve in 1case. Multifocality was present in 3 cases.

Conclusions. *In conclusion, the sensitivity of MRI for DCIS detection is lower than that achieved for invasive breast cancer; however, contrast-enhanced MRI can depict foci of DCIS that are mammographically occult. The MRI technique is of complementary value for a better description of tumor size and detection of additional malignant lesions.*

Key words: breast neoplasms; carcinoma, ductal, noninfiltrative; carcinoma in situ, minimally invasive breast cancer; magnetic resonance imaging

Received: 7 June 2002
Accepted: 17 June 2002

Correspondence to: Professor Massimo Bazzocchi, Istituto di Radiologia, APUGD via Colugna nį 50, 33100 Udine, Italy; Phone: +39 43 25 59 266; Fax: +39 43 25 59 867; E-mail: massimo.bazzocchi@med.uniud.it

Introduction

Ductal carcinoma in situ (DCIS) is histologically not considered as a single entity, but as a heterogeneous group of lesions that differ in their histopathologic features, growth pattern, clinical presentation and biological behavior. Before the advent of widespread mammographic screening, DCIS was rarely detected and accounted for only 0.8%-5.0% of all breast cancers.[1] With the introduction of mammographic screening, DCIS accounted for 15-20% of all detected breast cancers, and for 25%-56% of all clinically occult cancers.[1,2]

Seventy percent of DCIS presents as a cluster of microcalcifications; therefore, mammography is the primary and most sensitive technique to identify DCIS. Nevertheless, in many cases, it is not accurate either in assessing the real cancer's extent (underestimation of 46% of cases) or detecting multifocal lesions.[3]

The potential of magnetic resonance imaging (MRI) in the detection of DCIS is well documented in many recent trials,[4-6] where encouraging data about the role of MRI have been shown. Unfortunately, these data are not always concordant with others in different studies, reporting of varying in sensitivities. The explanation is likely related to the extreme variability in histologic features of a tumor, tumor size, tumor grade, different MRI parameters used, different technical factors involved in performing breast MR imaging and image interpretation.

The purpose of this study is to report our personal experience on 22 cases of DCIS studied with MRI.

Patients and methods

We retrospectively reviewed the MRI and mammographic (Mx) examinations performed from September 1995 to December 2001on 22 women (aged between 75 and 43 years, mean 53 years) affected by DCIS.

Bilateral mammograms (mediolateral oblique and craniocaudal views) were obtained on a standard mammographic unit (Mammo DIAGNOST UC, Philips medical Systems Inc., Best Netherlands). In most cases, additional mammograms (e.g. spot views) were obtained in both projections.

The following mammographic features were specifically assessed in each examination:

- Focal nodular mass;
- Microcalcifications: distribution, characteristics, size, association with mass (suspicious of malignancy if: clustered, pleomorphic, mixed density or associated with mass or area of architectural distortion);
- Associated features: architectural distortion, parenchymal distortion.

Breast MRI was performed within 7 days from the Mx, with a 1 T system (Magneton Impact Siemens, Erlangen Germany), with a dedicated bilateral breast surface coil. A three-dimensional fast low-angle shot (FLASH) pulse sequence was used: 14 ms repetition time (TR), 7 ms echo time (TE), 25° flip angle, 2.5 mm effective slice thickness, 192x256 matrix, and 84 sec acquisition time. Images were acquired in coronal plane, with rectangular FOV (4/8). The entire breast was imaged before and five times after intravenous injection of 0.1-mmol of Gd-DTPA/Kg body weight (Magnevist; Schering Berlin, Germany).

The post-processing procedures included:

- Digital image subtraction: subtraction of pre-contrast from the second acquisition of the post-contrast images. The subtraction enables to obtain the signal suppression of fat tissue and to identify the enhancing areas (malignant lesions with neoangiogenetic activity);
- Maximum intensity projection (MIP) permits to obtain a 3D-image rotating on axial and on sagittal plane, based on the subtracted images;

- Multiplanar reconstruction (MRP) permits to obtain axial images, based on the coronal acquisition.

Semi-quantitative analysis of the signal intensity to time relation was performed with the region of interest technique. The region of interest (ROI) (2-5 pixel) was placed within the tumoral area, where the highest signal intensity enhancement was seen.

The percentage of signal intensity increase was defined as:

SI Increase lesion = (SI post-SI pre)/SI pre x 100

SI = signal intensity; »pre« and »post« mean before and after contrast administration.

With respect to enhancement kinetics, the enhancement rate that is referred to as a relative signal intensity increase that occurs in a certain period of time (usually identified in the first contrast minute) was calculated.

The optimal threshold value above which the enhancement level should be considered suggestive of malignancy is still debated. According to recent studies, a relative signal increase below 70% is usually considered as an index of no or minimal enhancement; a relative signal increase ranging between 70% and 140% is considered as intermediate, and a relative signal increase over 140% is considered as strong.[4]

The three types of time-intensity curve, which have been previously described,[7,8] were used:
- Type 1 (continuous signal intensity increase): a persistent increase in SI was present beyond 2 minutes after the contrast media injection;
- Type II (plateau): the maximum signal intensity was achieved in the first 2 minutes and then remained fairly constant;
- Type III (wash out): the maximum signal intensity was achieved in the first 2 minutes and went decreasing over time

The morphology of the enhancement[7] was classified as:
- Focal enhancement corresponding to a well-defined mass;
- Ductal enhancement corresponding to a linear/linear branching configuration, which can be related to a single enhancing duct (»galactogram«);
- Segmental enhancement usually present in the lesions confined to the territory of a duct or of a ductal system, of a triangular shape with the tip pointing toward the nipple;
- Regional or diffuse enhancement corresponding to the areas of confluent enhancement that do not respect the borders of ductal system.

In 6 patients, the histological diagnosis was obtained by surgical biopsy, following the placement of a mammorep under Mx or US guidance, while in the other 16 patients, histological diagnosis was provided by core needle biopsy. The patients underwent definitive surgical treatment within 14 days after MRI. Finally, in all patients, the definitive histological diagnosis was made from the pathologic specimen (mastectomy or breast-conservative surgery).

Results

Pathology demonstrated the presence of DCIS in 15 cases (68%), and of DCIS with associated microinvasive component or microfoci of invasive ductal carcinoma (IDC) in 7 cases (32%). In 12 patients an isolate focus was diagnosed. Twenty-one out of 22 lesions (95%) showed enhancement after contrast media administration at MRI.

DCIS

The diagnosis of pure DCIS was made by histopathology in 15 lesions; 2 lesions were

classified as comedo type and 13 as non-comedo type DCIS.

Mammography demonstrated clusters of exclusively pleomorphic round and branching microcalcifications in 12 cases (3 associated with mass) (86%), and achitectural distortion or opacity in 2 (14%). One patient had negative mammograms, but ultrasonography (US) revealed abnormal findings.

On MRI, 14/15 (93%) lesions revealed the uptake of contrast media, while 1 (7%) lesion was not identified at MR imaging. Nevertheless, Mx demonstrated microcalcifications typical for malignancy in this false negative at MRI. In five out of the 14 enhancing lesions patients were affected by multiple foci of DCIS.

Among the 14 enhancing lesions, 3 (21%) showed a low, 5 (36%) an indeterminate, and 6 (43%) a strong enhancement (Table 1a). Morphologically, the enhancing lesion was focal in 7 (50%), segmental in 4 (27%) and with linear branching in 3 (21%) cases (Table 1b). Wash out was found in 4 (29%) cases, a plateau curve in 8 (57%), and type I curve in 2 (14%) cases (Table 1c).

In detail, the 2 comedo type DCISs showed a morphological pattern (ductal or segmental) and a enhancement behavior, strong typical for malignancy.

DCIS + DCI

In 7/22 lesions (32%), histology detected DCIS with associated minimally invasive carcinoma.

Mx was abnormal in all these patients (100%) who were suspicious for microcalcifications present in all cases (in one case, microcalcifications were associated with opacity).

All lesions demonstrated contrast enhancement at MRI: 1/7 (14%) showed a low enhancement, 2/7 (29%) an indeterminate enhancement, and 4/7 (57%) a strong enhancement (Table 1a).

Morphologically, the enhancing lesion was focal in 3/7 (43%) cases, segmental (Figure 1) in 3 (43%), and with linear branching in 1 (14%) case (Table 1b) (Figure2). Wash out was demonstrated in 3/7 (43%) cases, plateau curve in 3 (43%), and type I curve in 1 (14%) case (Table 1c).

Three out of 7 cases (43%) presented multiple foci of DCIS with associated microinvasion (Figure 3).

Table 1a. Enhancement rates in14 DCIS and 7 DCIS with associated minimum invasion.

Percentage of signal intensity increase	DCIS	DCIS+DCI	Total
<70%	3 (21%)	1(14%)	19%
70%-140%	5 (36%)	2 (29%)	33%
>140%	6 (43%)	4 (57%)	48%

Table 1b. Enhancement configuration in 14 DCIS and 7 DCIS with associated minimum invasion.

Configuration			
Focal mass like	7 (50%)	3 (43%)	48%
Segmental	4 (27%)	3 (43%)	33%
Linear-branching	3 (21%)	1 (14%)	19%

Table 1c. Signal intensity curve types in 14 DCIS and 7 DCIS with associated minimum invasion.

Signal intensity curve			
Type i	2 (14%)	1 (14%)	14%
Type ii	8 (57%)	3 (43%)	52%
Type iii	4 (29%)	3 (43%)	33%

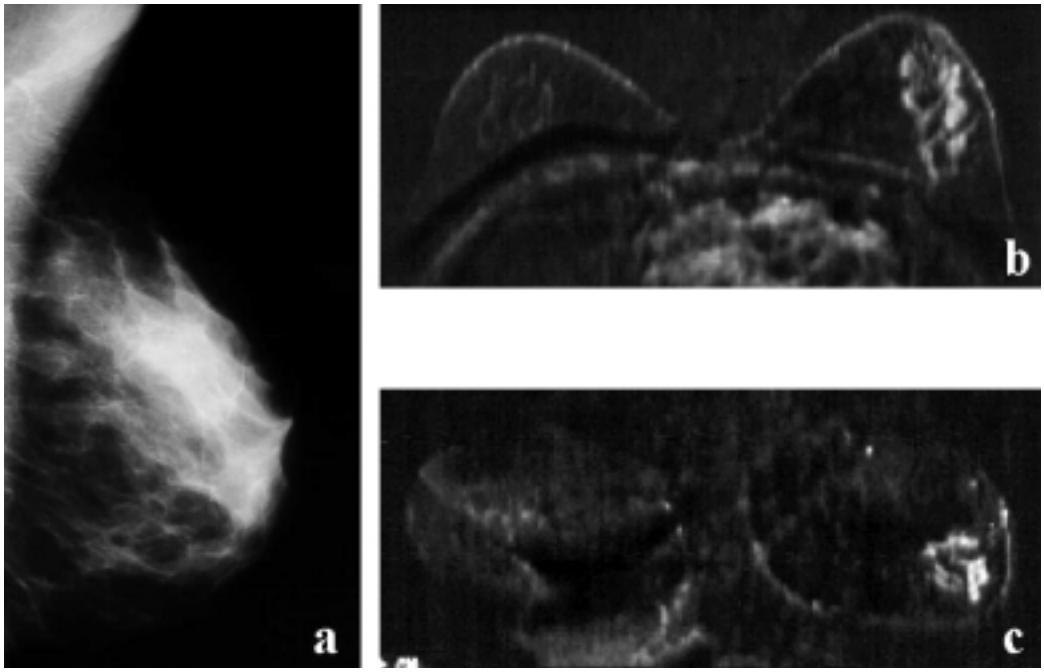

Figure 1. Segmental enhancement. A 54 year-old asymptomatic woman. Mammogram of the left breast, in mediolateral oblique view, did not show abnormalities (a). MRI revealed an area of segmental enhancement, well visible both in the coronal and in the MPR images (b,c). Histology proved DCIS with a focal area of minimally invasive component.

Discussion

Ductal carcinoma in situ is a heterogeneous group of histopathologic lesions, traditionally classified in two main subgroups, non-comedo (cribriform, micropapillary, clinging and solid), and comedo type, on the basis of the architectural growth pattern and cell type, and the presence or absence of comedo type necrosis within the ducts.

Recently, the new pathologic classifications proposed by Holland et al.[9] distinguish among well-, intermediately-, and poorly differentiated DCIS subtypes on the basis of cytonuclear differentiation and architectural growth pattern. Silverstain et al[10] have introduced the so-called Van Nuys classification in which the presence or absence of high nuclear grade and the presence or absence of comedo type necrosis is considered.

A new pathologic classification, considering the biological behavior of DCIS and playing an important role in recognizing more aggressive lesions for an optimal management of DCIS, should be recommended.

The value of mammography is well known seeing that 70% of DCIS become evident as a cluster of microcalcifications (usually linear, with linear branching or granular; Le Gal type IV-V), and that, in well-differentiated lesions, mammography is also very useful.

Several investigations demonstrated that contrast enhanced MRI has a very high sensitivity in invasive breast cancer detection, with the values reaching 100%, whereas the sensitivities for the identification of DCIS on MR images have been reported to be variable, ranging from 33 to 100%.[4] There are many potential explanations for the wide variability in reported sensitivities; according to one, it may be due to the differences in the size of DCIS lesions studied. It is obvious that MRI is

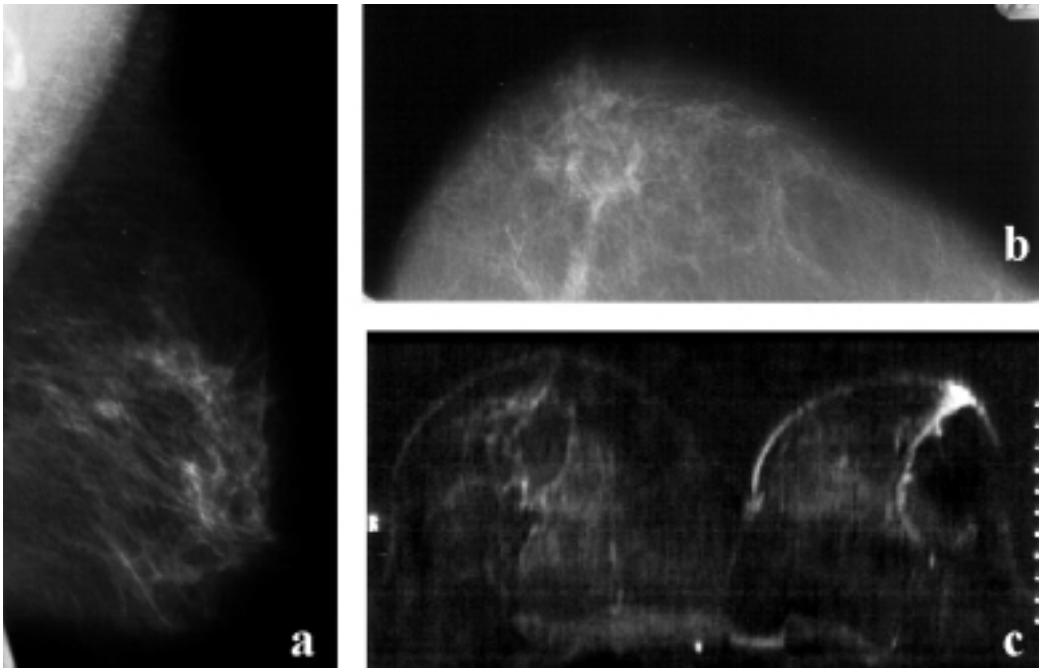

Figure 2. Linear branching enhancement. Images of a 58-year-old woman with a retracted mammary nipple on the left side. Mammography, in medio-lateral oblique and cranio-caudal views, demonstrated an area of subtle architectural distortion, better seen in the second projection (a, b). MPR image on axial plane revealed a typical linear branching enhancement pattern (c). Histology proved a pure DCIS.

not able to visualize tumors smaller than the slice thickness due to partial volume effect. Nevertheless, the size of lesions does not seem to be the only explanation for the variable detection of DCIS with MR imaging. In fact, false-negative results with tumor sizes ranging from 2 mm to 9 cm have been reported.

Another factor that could affect the sensitivity of MRI in DCIS detection is the histological type of the tumor. However, the histological subtype by itself is not sufficient to explain the presence or absence of contrast enhancement on MR images because false negative cases of both comedo type and non-comedo type DCIS have been reported. The degree of tumor angiogenesis is another histological variable that could influence the sensitivity of MRI in the depiction of DCIS. It is well known that malignant lesions release angiogenetic factors (e.g. vascular endothelial growth factor, VEGF) that induce sprouting and growth of pre-existing capillaries, and the ex novo formation of new vessels (angiogenetic activity). In dynamic breast MR imaging, invasive breast cancer is detectable due to its strong enhancement, whereas a certain degree of angiogenetic activity seems to be a prerequisite for tissue invasion, and it is not needed as long as the tumor stands in the preinvasive state (in situ). While invasive growth is almost invariably associated with contrast enhancement, this is not necessarily true for the in situ cancers. In fact, a weak tumor angiogenesis, found in the stroma and around the ducts involved in DCIS, can explain the lack of a significant enhancement behavior.

In addition to the size of the lesion, histological subtype and neoangiogenesis, differences in MRI technique (2D section selected sequence, 3D volume sequence, 3D volume

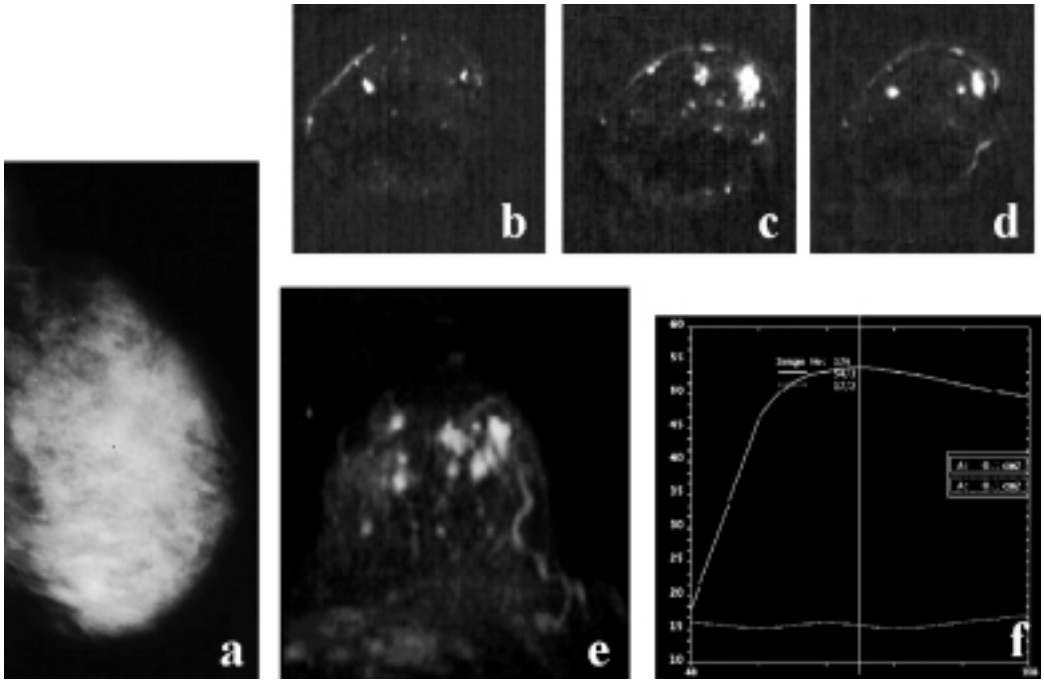

Figure 3. Multifocal, multicentric enhancement. Images of a 47-year-old woman. Mammogram of the left breast, in the medio-lateral oblique view, did not show any abnomality (a). MIP and several coronal MR images revealed multifocal and multicentric enhancement (b,c,d,e). The SI/T curve, relative to the lesion, presents a plateau-type curve (f). Histology proved DCIS with associated microinvasion.

fat suppressed technique, dynamic technique,...), and the differences in image interpretation (morphologic criteria to establish the degree of suspicion, threshold value of enhancement above which a lesion should be considered suggestive for malignancy) may also explain the variability in reported sensitivities.

Mammography, whose morphologic criteria of suspicion in a detected lesion are well known, does not use any criteria similar to those used in MR imaging. The enhancement configuration of DCIS is variable: DCIS lesions can present a focal, mass-like enhancement with ill-defined borders or can exhibit a linear or linear branching enhancement (duct-like configuration) or even a segmental enhancement with a configuration corresponding to a ductal system.[2,7]

In a recent study reported by Viehweg et al.[4], MRI detected 96% of DCIS lesions that exhibited at least some week enhancement. Only 4% of DCIS lesions did not show enhancement at all. The morphology of enhancement was focal (73%), diffuse (10%) or ductal (17%). In 65% of cases, the speed of enhancement was considered as delayed. In high-grade DCIS lesions (according to Van Nuys classification), comparing comedo subtype to non-comedo subtype, the behavior of enhancement was more often ill defined (83% vs. 43%), ductal (29% vs. 12%), and rapid (50% vs. 29%). Significant differences in the enhancement behavior were not found between high-grade and low-grade DCIS, nor were there any between comedo and non-comedo subtype lesions. Although 96% of DCIS showed the contrast enhancement on MRI, only 50% of DCIS lesions showed a »typical« enhancement behavior suspicious for malig-

nancy characterized by a strong and early enhancement, focal ill-defined enhancement or an enhancement with ductal configuration. Moreover, in the same work, MRI allowed the detection of 25 additional foci of DCIS.

In our study, the majority (95%) of DCIS lesions demonstrated at least some enhancement. The only false negative lesion at MRI was a pure non-comedo DCIS. On the other hand, MRI identified additional foci of DCIS that were mammographically occult in 8 cases. However, using the usual diagnostic algorithm, the enhancement rate was considered typical of malignancy, e.g. strong or at least indeterminate in 79% of pure DCIS and in 86% of microinvasive DCIS.

The configuration of DCIS was variable: linear branching enhancement, which is considered to be an important feature of malignancy, was present in only 21% of pure DCIS and in 14% of microinvasive DCIS. Early wash out, known as a typical feature of invasive malignancy was present in 29 % of pure DCIS and 43% of microinvasive DCIS. The non-enhancing DCIS was mammographically identified by the presence of microcalcifications. MR imaging, however, may contribute to the diagnosis of DCIS by detecting the lesions not visible on mammography.

In conclusion, the sensitivity of MRI for DCIS detection is lower than that achieved for invasive breast cancer; however, contrast enhanced MRI can depict mammographically occult foci of DCIS. Mammography remains the main diagnostic technique for breast examination. The MRI technique is of complementary value for better description of tumor size, in the detection of additional malignant lesions, and in the study of the dense breasts, poorly visible by mammography.

References

1. Stomper PC, Margolin FR. Ductal carcinoma in situ: the mammographer's perspective. *AJR* 1994; **162:** 585-91.

2. Orel SG, Mendonca ME, Reynolds C, Schnall MD, Solin LJ, Sullivan DC. MR imaging of ductal carcinoma in situ. *Radiology* 1997; **202:** 413-20.

3. Holland R, Hendriks JH, Vebeek AL, Mravunac M, Schuurmans Stekhoven JH. Extent, distribution and mammographic/ histological distribution of breast ductal carcinoma in situ. *Lancet* 1990; **335:** 519-522.

4. Viehweg P, Lampe D, Buchmann J, Heywang-Kobrunner SH. In situ and minimally invasive breast cancer: morphologic and kinetic features on contrast-enhanced MR imaging. *MAGMA* 2000; **11:** 129-37.

5. Soderstrom CE, Harms SE, Copit DS, Evans WP, Savino DA, Krakos PA, et al. Three-dimensional RODEO breast MR imaging of lesions containing ductal carcinoma in situ. *Radiology* 1996; **201:** 427-32.

6. Gilles R, Meunier M, Lucidarme O, Zafrani B, Guinebretiere JM, Tardivon AA, et al. Clustered breast microcalcifications: evaluation by dynamic contrast enhanced subtraction MRI. *J Comput Assist Tomogr* 1996; **20 (1):** 9-14.

7. Kuhl CK. MRI of breast tumors. *Eur Radiol* 2000; **10:** 46-58.

8. Kuhl CK, Mielcareck P, Klaschik S, Leutner C, Wardelmann E, Gieseke J, et al. Dynamic breast MR imaging: are signal intensity time course data useful for differential diagnosis of enhancing lesions? *Radiology* 1999; **211:** 101-10.

9. Holland R, Peterse JL, Millis RR, Eusebi V, Faverly D, van de Vijver MJ, et al. Ductal carcinoma in situ: a proposal a new classification. *Semin Diag Pathol* 1994; **11 (3):** 167-80.

10. Silverstein MJ, Poller DN, Waisman JR, Colburn WJ, Barth A, Gierson ED, et al. Prognostic classification of breast ductal carcinoma-in-situ. *Lancet* 1995; **345:** 1154-7.

Radiol Oncol 2002; 36(4): 313-8.

Magnetic resonance microscopy of trabecular bone

Maria Cova[1], Renato Toffanin[2,3], Agostino Accardo[4], Igor Strolka[5], Cristina Furlan[1], Roberto Pozzi-Mucelli[1]

[1] Department of Radiology, University of Trieste, Ospedale di Cattinara,
[2] Department of Biochemistry, Biophysics and Macromolecular Chemistry, University of Trieste,
[3]PROTOS Research Institute, Trieste, [4]DEEI, University of Trieste, Trieste, Italy
[5] Institute of Measurement Science, Slovak Academy of Sciences, Bratislava

Background. *Bone diseases such as osteoporosis lead to changes in the trabecular bone mass and architecture. Improved methods for the quantitative assessment of trabecular bone are needed to better understand the role of trabecular architecture in bone strength. MR microscopy (MRM), with its ability to achieve resolutions below 50 μm, has proved to be particularly useful for the ex vivo evaluation of the complex architecture of trabecular bone. In this study, we describe the use of projection reconstruction (PR) with MRM for the quantitative evaluation of the three-dimensional structure of trabecular bone explants and for the prediction of their biomechanical properties.*

Material and methods. *High-resolution 3D PR and trabecular bone explants were analysed to determine standard morphologic parameters such as trabecular bone volume fraction (BV/TV or Vv), trabecular thickness (Tb.Th) and trabecular separation (Tb.Sp). Segmentation of the high-resolution images into bone and bone marrow was obtained by using a Bayesian approach. The derived parameters were finally included in non-linear mathematical models for the prediction of Young's modulus (YM).*

Results. *The parameters derived from the PR spin-echo were found to be stronger predictor of YM (R^2 = 0.86) than those derived from the conventional spin-echo images (R^2 = 0.75) used for comparison.*

Conclusions. *This ex vivo approach should be readily adaptable to the studies in human subjects.*

Key words: bones - ultrastructure; magnetic resonance imaging, magnetic resonance microscopy; projection reconstruction, Young's modulus

Introduction

Bone diseases lead to changes in the trabecular bone structure that are not only characterised by reduction of bone mass but also by modifications of the bone architecture often accompanied by atraumatic fractures.[1] Osteoporosis is nowadays a problem of primary importance, which mainly affects women and elderly people. In Europe, the

Received 25 October 2002
Accepted 4 November 2002

Correspondence to: Maria Cova, Department of Radiology, University of Trieste, Ospedale di Cattinara, Strada di Fiume 447, I-34139 Trieste, Italy; Phone: +39 (0)40 399 4372; Fax: +39 (0)40 399 4500; Email: cova@gnbts.univ.trieste.it

number of bone fractures related to osteoporosis amounts to more than one million per year and this number is expected to rise dramatically over the coming years because the percentage of elderly people that is already high is still increasing. As a consequence, there is a great need to develop accurate methods for the evaluation of the status of bone tissue in order to achieve an early diagnosis of the disease and to determine the level of fracture risk as well as to provide therapeutic intervention in high risk patients and to monitor the effects of therapy. Several investigations have indicated that, besides bone mineral density (BMD), also trabecular architecture can be an important factor in assessing bone strength.[2,3]

The accurate in vivo observation of the microstructure of the bone is today not feasible, but the use of magnetic resonance imaging (MRI) techniques in the area of osteoporosis appears very promising.[4-6] Among these techniques, the most powerful methodology for the *ex vivo* study of trabecular bone is certainly magnetic resonance microscopy (MRM), which also able to provide detailed information on the trabecular bone structure. Recently, we have proposed the use of short-TE projection reconstruction (PR) MR microscopy for the study of healthy and osteoporotic bone explants.[7] The aim of this study was to verify the potential of the PR method in the characterisation of trabecular bone architecture and in the prediction of its mechanical properties.

Material and methods

Sixteen specimens consisting of cylindrical bone plugs (∅=4mm) were obtained from load-bearing and no-load-bearing regions of porcine humeral heads. The explants were examined at 7.05 T using a Bruker AM300 instrument equipped with a vertical wide-bore magnet and a microimaging accessory. All the explants were studied in the air using a 5mm diameter radio frequency (RF) coil. Short-TE proton MR microimages were acquired using a 3D spin-echo (TE = 3.0 ms, TR = 1.0 s) sequence according to the projection reconstruction (PR) method with constant gradient step and partial echo-acquisition already described.[8] This method provided images with a final voxel resolution of 41×41×82 μm^3. Spin-echo microimages (TE = 6.2 ms, TR = 1.0 s) were obtained on the same explants by the standard Fourier transform imaging method. The Young's modulus was measured on other sixteen bone specimens excised from adjacent areas to those used for the explants subjected to MR microscopy.

After interpolation to obtain an isotropic voxel resolution, the main standard structural parameters such as trabecular bone volume fraction (BV/TV or Vv), trabecular thickness (Tb.Th), and trabecular separation (Tb.Sp) were derived from contiguous cross sections of binary images using the *t3m* software.[9] Segmentation of the high resolution images into bone and bone marrow was obtained by adopting a Bayesian approach based on the Markov random field model where the likelihood function was locally adaptive.[10] The derived structural parameters were finally included in non linear mathematical models for the prediction of Young's modulus (YM) of the trabecular bone explants.

Results

Figure 1 shows a 2D section of a 3D PR microimage of an intact specimen of porcine trabecular bone. The morphologic parameters obtained from the PR images were compared with those extracted from the standard FT images. In Table 1, the morphologic parameters extracted from the PR and standard FT images of the load-bearing bone specimens are reported, whereas Table 2 presents the corresponding data derived for the bone speci-

mens excised from no-load-bearing regions. The best prediction of the mechanical properties of the examined trabecular bone explants were obtained by using the following non linear model derived from the equation proposed by Hwang et al.:[11]

$$YM=Vv*(a+b/Tb.Sp+c/Tb.Sp^2+d/Tb.Sp^3)+Tb.Th*(e+f/Tb.Sp+g/Tb.Sp^2+h/Tb.Sp^3)+k \quad [1]$$

which included simultaneously Vv, Tb.Th and 1/Tb.Sp. Figures 2 and 3 show the relationships between the Young modulus measured experimentally and that predicted using the structural parameters derived from the PR and standard FT images, respectively. The parameters extracted from the PR images were found to be stronger predictors of YM (R^2 = 0.86) than those derived from the standard FT images (R^2 = 0.75).

Discussion

In this study, short-TE PR method was adopted to minimise the susceptibility effect at the bone-marrow interface, which may lead to overestimation of the trabecular thickness as

Table 1. Standard morphologic parameters estimated from projection reconstruction (PR) and conventional FT spin-echo images of porcine trabecular bone explants from load-bearing regions.

	PR method			FT method		
Sample	**Vv**	**Tb.Th**	**Tb.Sp**	**Vv**	**Tb.Th**	**Tb.Sp**
	%	**mm**	**mm**	**%**	**mm**	**mm**
1	0.680	0.289	0.136	0.720	0.399	0.155
2	0.796	0.329	0.084	0.789	0.428	0.115
3	0.697	0.266	0.116	0.754	0.444	0.135
4	0.714	0.281	0.113	0.559	0.287	0.227
5	0.662	0.215	0.109	0.738	0.356	0.126
6	0.613	0.217	0.137	0.542	0.225	0.190
7	0.609	0.219	0.141	0.664	0.301	0.152
8	0.558	0.193	0.153	0.539	0.202	0.173
9	0.695	0.264	0.116	0.637	0.241	0.137
Mean	0.669	0.253	0.123	0.660	0.320	0.157
S.D.	0.070	0.044	0.021	0.097	0.090	0.035

Table 2. Standard morphologic parameters estimated from projection reconstruction (PR) and conventional FT spin-echo images of porcine trabecular bone explants from no-load-bearing regions.

	PR method			FT method		
Sample	**Vv**	**Tb.Th**	**Tb.Sp**	**Vv**	**Tb.Th**	**Tb.Sp**
	%	**mm**	**mm**	**%**	**mm**	**mm**
1	0.481	0.144	0.155	0.275	0.103	0.270
2	0.532	0.197	0.174	0.268	0.119	0.326
3	0.379	0.119	0.195	0.425	0.150	0.203
4	0.359	0.128	0.229	0.433	0.126	0.166
5	0.470	0.162	0.183	0.349	0.110	0.205
6	0.394	0.146	0.225	0.459	0.144	0.169
7	0.440	0.152	0.193	0.556	0.213	0.170
Mean	0.436	0.150	0.193	0.395	0.138	0.216
S.D.	0.062	0.025	0.027	0.104	0.037	0.061

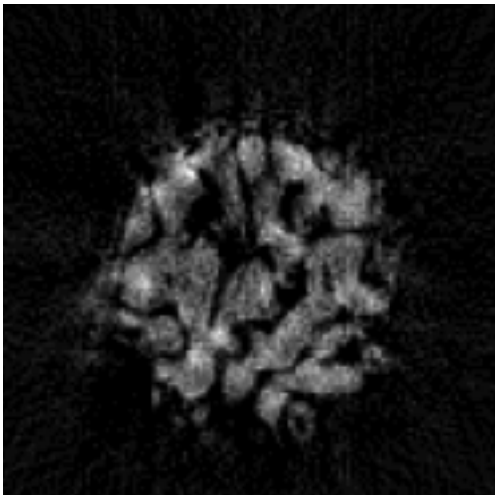

Figure 1. 2D section of a 3D projection reconstruction spin-echo image of a porcine trabecular bone specimen.

reported by Majumdar and co-workers.[12] The results reported in Table 1 and Table 2 do not seem to show significant differences in Tb.Th for the PR and FT method. This is probably due to the fact that the morphologic parameters were computed on isotropic image voxels with a 41 μm^3 resolution. However, the PR-derived structural data appear to be more accurate as their SD resulted lower than those calculated for the FT-derived values. Even though a spin-echo scheme was adopted in this study, we foresee that the PR method can also be of great advantage in the case of gradient-echo sequences. This implies that the PR method can be readily implemented on modern clinical MRI scanners. Moreover, our best model for the prediction of Young's

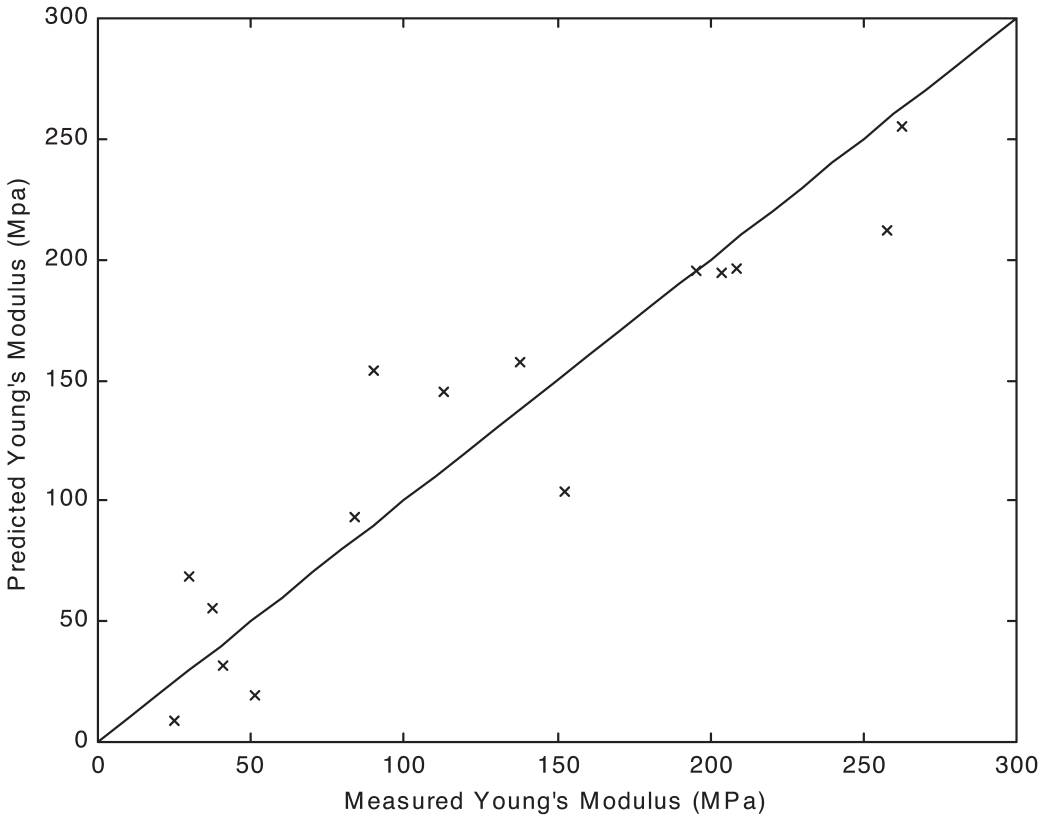

Figure 2. Experimental Young's modulus versus predicted Young's modulus. Predicted YM values were calculated including the morphologic parameters Vv, Tb.Th and 1/Tb.Sp derived from PR images in the equation 1 ($R^2 = 0.86$).

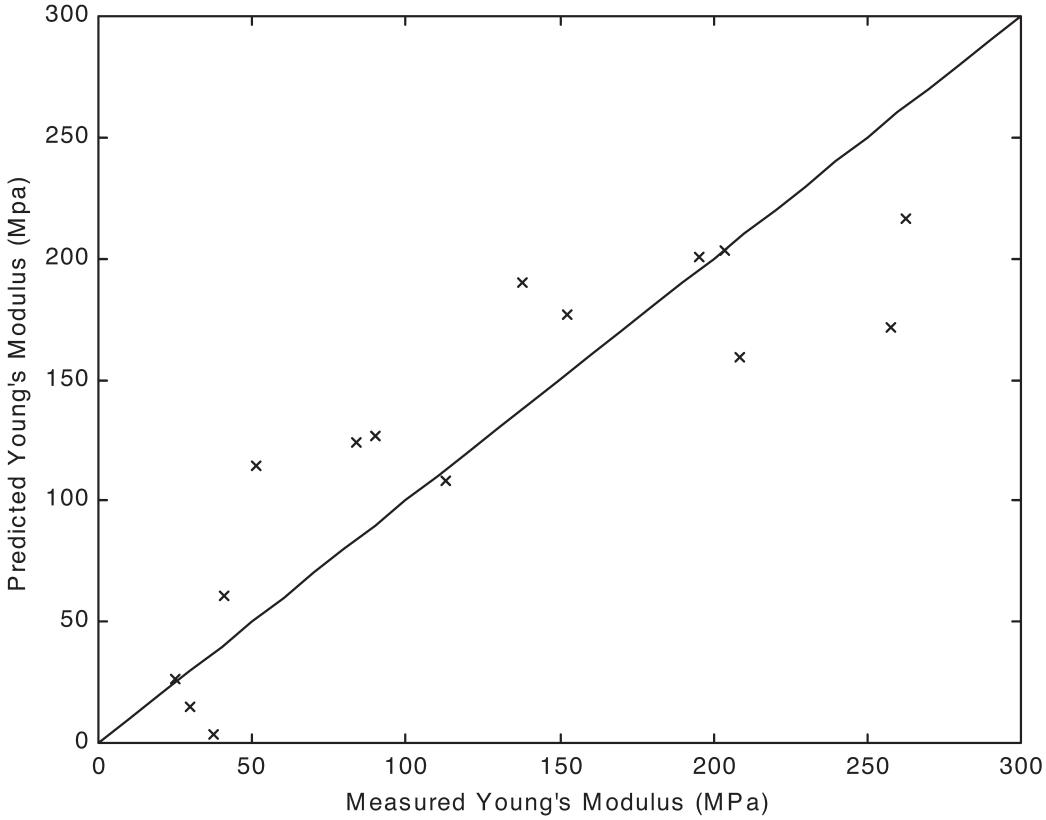

Figure 3. Experimental Youngīs modulus versus predicted Young's modulus. Predicted YM values were calculated including the morphologic parameters Vv, Tb.Th and 1/Tb.Sp derived from conventional FT images in the equation 1 (R^2 = 0.75).

modulus can contribute to a more accurate in vivo evaluation of the mechanical properties of the trabecular bone.

Since the risk of bone fractures seems to be strongly related to bone architecture, the described PR-based approach may provide a relevant contribution to the clinical MRI investigation of trabecular bone in ageing and osteoporosis.

Acknowledgements

Work supported by grants from the University of Trieste, from the Commissariato del Governo nella Regione Friuli-Venezia Giulia (Fondo Speciale per la Ricerca Scientifica e Tecnologica, P. 63-1997) and from the Slovak Academy of Sciences (VEGA 2/2040/22).

References

1. Melton LJ 3rd, Thamer M, Ray NF, Chan JK, Chesnut CH 3rd, Einhorn TA, et al. Fractures attributable to osteoporosis: report from the National Osteoporosis Foundation. *J Bone Miner Res* 1997; **12:** 16-23.

2. Mosekilde L. Vertebral structure and strength in vivo and in vitro. *Calcif Tissue Int* 1993; **53:** 121-6.

3. Odgaard A, Kabel J, van Rietbergen B, Dalstra M, Huiskes R. Fabric and elastic principal directions are closely related. *J Biomech* 1997; **30:** 487-95.

4. Gordon CL, Webber CE, Christoforou N, Nahmias

C. In vivo assessment of trabecular bone structure at the distal radius from high-resolution magnetic resonance images. *Med Phys* 1997; **24:** 585-93.

5. Wehrli F W, Hwang SN, Ma J, Song H K, Ford J C, Haddad J G. Cancellous bone volume and structure in the forearm: noninvasive assessment with microimaging and image processing. *Radiology* 1998; **206:** 347-57.

6. Link T M, Majumdar S, Augat P, Lin J C, Newitt D, Lu Y, et al. In vivo high resolution MRI of the calcaneus: differences in trabecular structure in osteoporosis patients. *J Bone Miner Res* 1998; **13:** 1175-82.

7. Toffanin R, Szomolányi P, Jellúš V, Cova M, Pozzi-Mucelli RS, Vittur F. Magnetic resonance microscopy of osteoporotic bone. In El-Genk MS, editor. *Space Technology and Applications International Forum - 2000*. American Institute of Physics; 2000. p. 295-9.

8. Jellúš V, Latta P, Budinsky L, Toffanin R, Jarh O, Vittur F. Projection-reconstruction method with constant gradient step. In: *Proceedings of the 5th Annual ISMRM Meeting*. Vancouver; April 12-18; 1997. p. 1987.

9. Hipp J, Jansujwicz A, Simmons C, Snyder B. Trabecular bone morphology from micro-magnetic resonance imaging. *J Bone Miner Res* 1996; **11:** 286-92.

10. Jansen M. Wavelet thresholding and noise reduction. *PhD dissertation*. Katholieke Universiteit Leuven, 2000.

11. Hwang SN, Wehrli FW, Williams JL. Probability-based structural parameters from three-dimensional nuclear magnetic resonance images as predictors of trabecular bone strength. *Med Phys* 1997; **24:** 1255-61.

12. Majumdar S, Newitt D, Jergas M, Gies A, Chiu E, Osman, et al. Evaluation of technical factors affecting the quantification of trabecular bone structure using magnetic resonance imaging. *Bone* 1995; **17:** 417-30.

Radiol Oncol 2002; 36(4): 319-25.

Real time compound ultrasound of the shoulder

Alessandro De Candia[1], Stefano Doratiotto[1], Francesco Pelizzo[1], Elio Paschina[2], Massimo Bazzocchi[1]

[1]*Department of Radiology,*
[2]*Department of Orthopedic Surgery, University Hospital of Udine, Udine, Italy*

Background. *The purpose of the study was to determinate the value of the ultrasound real time compound imaging in the evaluation of supraspinatus tendon in subacromial impingement disease.*
Patients and methods. *Preoperative ultrasound was performed on 180 shoulders in 157 patients with clinical suspicion of rotator cuff disease; 71 patients were surgically treated with acrimioplasty and cuff repair. The sonograms were obtained under static and dynamic examination using a 5-12 MHz high frequency linear array probe, and compound real time elaboration of multiple images from different viewing angles (Sono CT© - ATL). The supraspinatus morphology was classified into the following groups: the absence of tears, the presence of partial thickness tears and the presence of full thickness tears. In the absence of tears, the supraspinatus tendinopathy was classified into three classes according to the Neer stages. The ultrasound findings were compared to the surgical inspection results.*
Results. *Ultrasound showed 32 (96.9%) out of 33 full thickness tears, only one false negative in a patient with large body, and 9 (75%) out of 12 partial thickness tears. There were three false negative studies in supraspinatus tendons with superficial lesions. Ultrasound correctly showed 26 (100%) out of 26 rotator cuffs with the absence of tear.*
Conclusions. *Real time compound ultrasound is a useful tool in the evaluation of the supraspinatus tendon diseases; this technique permits the reduction of the presence of conventional ultrasound acoustic artefacts and provides necessary information for preoperative planning.*

Key words: shoulder joint - ultrasonography; rotator cuff; shoulder impingement syndrome - ultrasonography; real time compound ultrasound; sono CT

Introduction

Rotator cuff tears are usually described as common pathologic conditions we can meet while performing the ultrasonographic imaging of the shoulder.[1] Technical development in the last few years allowed ultrasonography to be considered one of the best imaging methods for studying those conditions. The newest full-digital equipments in fact allow to

Received 7 June 2002
Accepted 17 June 2002

Correspondence to: Alessandro De Candia, MD, Department of Radiology, University Hospital of Udine, APUGD Via Colugna 50, 33100 Udine, Italy; Phone: +39 43 25 59 266; Fax: +39 43 25 59 867; E-mail: alessandro.decandia@med.uniud.it

obtain a high quality of the ultrasonographic images as never before. High-resolution digital ultrasonography allows increasing the sensitivity, the specificity and the overall diagnostic accuracy in the shoulder lesions characterisation if compared to the conventional ultrasonographic methods.[2-6]

The aim of this paper is to describe the features of real time compound ultrasound technique and to introduce its potential benefits on the supraspinatus tendon study comparing sonographic images to surgical results.

Patients and methods

Between January 2000 and December 2000, we performed a prospective study on 180 shoulders in 157 patients (69 males and 88 females aged between 17 and 82 years; mean age of males 49.7 years; mean age of females 58.2 years) with clinical suspicion of rotator cuff tear.

Out of 157 patients 71, aged between 34 and 80 years (31 males, mean age 51.2 years; 40 females, mean age 55 years) underwent surgery on the day after sonography. Surgical intervention on the supraspinatus tendon with tear repair and acromioplasty was performed on all the 71 patients by the same operator who recorded the data using a standard method. The study was performed in a clinical setting with the approval of the Ethics Committee of our Institute.

Sonograms were obtained with an ATL 5000 scanner, using a 7 to 12 MHz linear array probe (Advanced Technology Laboratories, Bothell, WA) applying the soon CT digital algorithm.

This algorithm allows the digital real time image capturing along nine different lines of view at the same time for every point on the patient's shoulder on which the operator places the transducer. The nine virtual images that the transducer receives back at once from the patient are weighted in real time by a digital beamformer unit and melted into one final image which is the result of the nine different frames compound processing.[7,8]

In all patients, both the static and the dynamic evaluations were performed.

The static examination was performed on the patient's arm in standard position of the shoulder joint to evaluate the supraspinatus tendon as it is described in the first part of the dynamic evaluation. Dynamic images were obtained by moving passively the patients arm in intrarotated position first and then in extended position: during the first part of the dynamic evaluation, the patient's arm was placed in the abducted and intrarotated position, with the forearm flexed to the arm, and the back face of the fingertips pointing to the tip of the scapula. The second part of the dynamic evaluation was performed by moving the limb passively in adduction\extension but keeping the intrarotation of the forearm during the movement.[9,10] All the images of the 71 patients were stored digitally on the US unit.

Two radiologists performed separately the image evaluation. Both the observers evaluated each image set for the presence or absence of tendon tear and for the characterisation of the supraspinatus tendon features in the absence of sonographic proof of the tear.

The patients in whom ultrasonography revealed the presence of tendon tear were divided into two groups: the first group comprised the patients with complete rupture of the supraspinatus tendon, while the second group included the patients with partial rupture of the supraspinatus tendon.

In the absence of sonographic appearance of any type of tendon tear, the lesion grade based on the sonographic appearance of the tendon was established. We described tendons by grouping them into three sonographically determined classes. The first class included the tendons which appeared to be thickened with a hyperechogenic surface, but showing a normal fibrillar central region. The

subacromial bursa was thickened but without intratendinous calcifications. The second class grouped the tendons that showed to be thickened and had an irregular and inhomogeneous aspect of their central fibrillar region. This class included the shoulders with the thickened subacromial bursa and intratendinous calcifications. The third class comprised the patients in whom the supraspinatus tendon appeared diffusely hypoechoic, inhomogeneous and thinner. In this class, intratendinous calcifications were also present.

The ultrasonograpic findings were compared to surgery outcome, the latter being considered as the gold standard technique in characterising the presence or absence of tear.

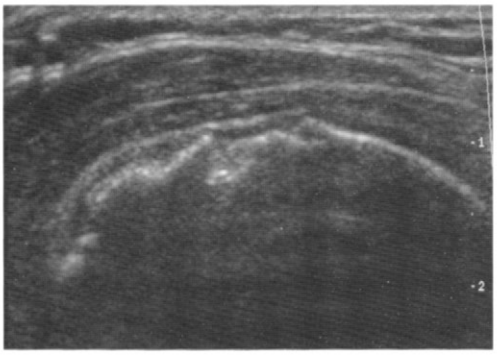

Figure 1. Transverse image of the supraspinatus tendon. Real time compound imaging shows a full thickness tear of the supraspinatus tendon with the deltoid muscle laying on the humeral head. Note the severe humeral head arthrosic degeneration.

Results

Considering the 71 patients who underwent surgery, the real time compound imaging correctly identified and characterized 32 (96.9%) out of 33 surgically confirmed full thickness tears of the supraspinatus tendon (Figures 1, 2). The study of the rotator cuff performed on one obese patient was not able to lead to the final right diagnosis (false negative). There was not any false positive study. The real

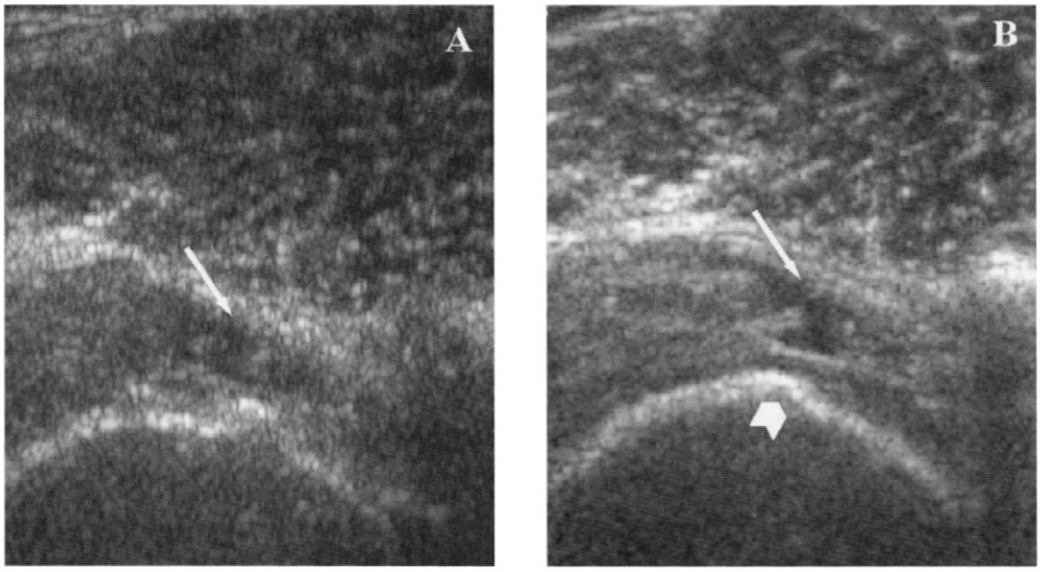

Figure 2. Transverse images of the supraspinatus tendon. A) Conventional ultrasound shows a small full thickness tear on the front side edge of the tendon (arrow); B) Real Tine Compound Imaging shows a remarkable increase in lesion conspicuousness and the broken tendon fibres as well (arrow). The cartilage surface is better displayed (arrowhead).

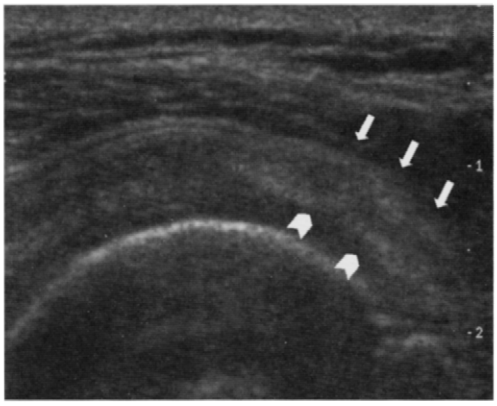

Figure 3. Transverse image of the supraspinatus tendon. Real Time Sono CT imaging is better showing the tendon structure focusing on the hypehogenic area of tendon suffering on the front side of the tendon (arrows) mixed to the superficial area of abrasive injury (arrowheads).

time compound imaging identified correctly 9 of 12 (75%) partial thickness tears diagnosed by surgery. There were 3 false negative studies (superficial partial thickness tears of the supraspinatus tendon on surgery). There were no false positive studies. The absence of tear was detected in 26 patients by ultrasonograpy (Figure 3). All these cases were confirmed by surgery as tearless tendons.

In 5 (29%) out of 26 patients, a first-class ultrasonographic aspect of the tearless tendon were described (3 women, two of them aged 39 and the third 79 years old; 2 men aged 41 and 51 years). Surgery on these 5 patients described one case as degeneration of the supraspinatus tendon with no tear, one case as abrasive lesion of the tendon due to impingement syndrome disease with no tear, and three cases without any lesion either in the tendon or in the bursa. In the first case, the surgeon described a hypertophic subacromial bursa, in the second one, the bursa was oedematous and swollen, and in the last three cases, the bursa was void of lesions.

Fifteen (57%) out of 26 patients had a second class-like tendon type on ultrasonography (9 men aging between 34 and 61 years; 6 women aging between 54 and 74 years). The surgical examination showed 2 cases of supraspinatus tendon degeneration, 1 case of oedema of the whole rotator cuff, 2 cases of hyperaemic cuff, 2 cases of swollen and hyperaemic cuff; 2 cases of hemorrhagic cuff. There were 6 cases without any lesion of the cuff. The subacromial bursa was described as swollen with oedema in 3 cases, hypertrofic in 4 cases, hypertrophic and hyperaemic in 4 cases, void of lesions in 3 cases. Both sonography and surgery showed one or more calcifications in 9 cases, while 6 cases did not have any calcification.

In 6 (24%) out of 26 patients, ultrasonography detected a third-class tendon (2 men aged 50 and 62 years and 4 women aged between 44 and 55 years). On surgery, the rotator cuffs were described as void of lesions in 2 cases, in the third patient, hyperaemic spot was detected on the rotator cuff (impingement site), the fourth had globally hyperaemic cuff, the fifth inflammation of the cuff, and the sixth degenerated cuff. Both sonography and surgery showed one or more intratendinous calcifications in 3 cases, while the other 3 cases did not have any calcification. The comparison between surgery and sono CT findings is shown on Table 1.

Table 1. Comparison between sono CT findings and surgery (gold standard) in shoulders with no tears, partial thickness tear and full thickness tear

		SURGERY			
		No tear	**Partial tear**	**Complete tear**	**Total**
SONO CT	No tear	26	3	1	30
	Partial tear	-	9	-	9
	Complete tear	-	-	32	32
	Total	**26**	**12**	**33**	

Discussion

MRI has always played an important role in the identification and characterization of musculoskeletal diseases.[2,3] The technical drawback of the past conventional sonographic devices was limited possibility to reach the end of the diagnostic path using sonography by itself and forcing the radiologist to get more hints from other imaging techniques because the specificity and sensitivity of ultrasound examination were too low. The ultrasonographic evaluation of the shoulder joint has been performed since late 80's to describe the rotator cuff tears. The sensibility of the sonographic images in those years was not comparable to the MRI ones.[2,11-13] In 1986, Middleton et al. performed a sonographic examination of the rotator cuff and described the drawbacks of sonography in evaluating the acute tears of the rotator cuff. The sensitivity and specificity obtained by those Authors was lower than 90%. In late 80's, standard criteria to describe the tears of the rotator cuff were not encoded yet.[12,14] In 1989, Miller et al. performed a study on 56 patients, but the sensitivity of 93%, the specificity of 53% and the overall accuracy of 77% of their study were still too low.[13]

The technical development of the 90's with the introduction of the digital units allowed the image capture to be faster and rich in spatial details and time resolution with no loss of information and opened the possibility of accessing the post-processing tasks.[5,6,10,15,16]

Those new features allowed Moriggl and Steinlechner to encode the sonographic criteria to describe the features of normal rotator cuff tendons.[17]

In our experience we noticed that, in particular, the reduction of noise and the increased overall image contrast resolution, given by the real time compound imaging technique, allowed us to study the supraspinatus tendon with the highest resolution and to reach the best agreement between sonography and surgical findings.

Our experience with Sono CT on 71 patients demonstrates that the visualization of the rotator cuff tendon tears is possible with a level of accuracy that allowed us to estimate the features of the rotator cuff tendons and describe them in detail.

The possibilities offered by the Sono CT algorithm permitted us to perform a precise measuring of the tendon thickness and of subacromial space, due to less image artefacts, such as he speckle or the image blurring, which no more affected the image quality. In our experience, it was also possible to describe in detail whether intratendinous calcifications and fluid collections in the subacromial bursa were present or not.

In our experience, the full thickness acute tears were the lesions that we could better describe because the borders of the tear into the broken tendon were always visible. It was also always possible to describe other signs of acute full thickness tear as peritendinous inflammation or fluid collection in the subacromial bursa and obtain a good concordance with the surgical results.

Partial thickness tears were visible, but it was not possible to describe any of them as well as the full thickness tears. Actually, partial lesions demonstrated to be better superficial erosions than proper lesions of the tendon and occurred strictly under the lower border of the acromion where the conflict was present.

The drawbacks of the compound technique are linked to those of sonography itself. In obese patients and in people with hypertrophic musculature of the rotator cuff, the tendons are too deep to perform a correct diagnostic study and the high frequency probes are obviously not able to visualize at best those deep structures. The shoulder is perhaps an anatomical district in which the operator can take the best advantage from the compound technique use.

One of the major drawbacks of the compound technology is given by the reduction of the frame rate because of the delay in the multiple image processing. This reduction is sometimes a great limitation, in particular when deep structures are studied (i.e. studying the liver) because the image persistence is often the main artefact affecting the investigation. There are also other artefacts, like the image blurring that may slow down the examination. This is not the case of the shoulder investigation because the superficial position of the structures allows to proceed the study at a higher frame rate, maintaining the real time effect on.[5,15,18]

Conclusions

The real time compound imaging technique is a full digital algorithm based on the digital beamformer unit. This unit permits the reduction of conventional sonography acoustic artefacts because there is no analogic digital conversion during the image capturing process, but the system is all-digital. The possibility to combine up to nine different digital images, captured in real time under nine different view angles, into a single final image increases the overall image definition. In particular, in the study of the rotator cuff, this new technique allows us to reach a better contrast resolution with smoother and more detailed images than conventional sonography ones. Those features, thanks to the new digital imaging capabilities, allow to obtain a good agreement between surgical findings and sonographic ones.

References

1. King LJ, Healy JC, Baird P. Imaging of the rotator cuff and biceps tendon. *J R Army Med Corps* 1999. **145:** 125-31.

2. Burk DL Jr, Karasick D, Kurtz AB, Mitchell DG, Rifkin MD, Miller CL, et al. Rotator cuff tears: prospective comparison of MR imaging with arthrography, sonography, and surgery. *AJR Am J Roentgenol* 1989; **153:** 87-92.

3. D'Erme M, De Cupis V, De Maria M, Barbiera F, Maceroni P, Lasagni MP. [Echography, magnetic resonance and double-contrast arthrography of the rotator cuff. A prospective study in 30 patients]. [Article in Italian]. *Radiol Med* 1993; **86:** 72-80.

4. Drakeford MK, Quinn MJ, Simpson SL, Pettine KA. A comparative study of ultrasonographic and arthrography in evaluation of the rotator cuff. *Clin Ortop* 1990; **253:** 118-22.

5. Fabis J, Synder M. [The sensitivity and specificity of sonographic examination in detection of rotator cuff tear]. [Article in Polish]. *Chir Narzadow Ruchu Ortop Pol* 1999; **64:** 19-23.

6. Farin PU, Jaroma H. Acute traumatic tears of the rotator cuff: value of sonography. *Radiology* 1995; **197:** 269-73.

7. Leotta DF, Martin RW. Three dimensional ultrasound of the rotator cuff: spatial compounding and tendon thickness measurement. *Ultrasound Med Biol* 2000; **26:** 509-25.

8. Leotta DF. Three dimensional spatial compounding of ultrasound scans with weighting by incidence angle. *Ultrason Imaging* 2000; **22:** 1-19.

9. Martino F, Mocci A, Rizzo A, Dicandia V, Strada A, Macarini L, et al. [Echography of the supraspinatus tendon: forced passive adduction maneuver]. [Article in Italian]. *Radiol Med* 1998; **95:** 298-302.

10. Teefey SA, Middleton WD, Bauer GS, Hildebolt CF, Yamaguchi K. Sonographic differences in the appearance of acute and chronic full-thickness rotator cuff tears. *J Ultrasound Med* 2000; **19:** 377-8.

11. Fabis J, Kowalska A. [The value of radiological examination in the diagnosis of rotator cuff tear]. [Article in Polish]. The value of radiological examination in the diagnosis of rotator cuff tear. *Chir Narzadow Ruchu Ortop Pol* 1999; **64:** 447-52.

12. Middleton WD, Reinus WR, Melson GL, Totty WG, Murphy WA. Pitfalls of rotator cuff sonography. *AJR Am J Roentgenol* 1986; **146:** 555-60.

13. Miller CL, Karasick D, Kurtz AB, Fenlin JM Jr. Limited sensitivity of ultrasound for the detection of rotator cuff tears. *Skeletal Radiol* 1989; **18:** 179-83.

14. Middleton WD, Reinus WR, Totty WG, Melson

CL, Murph. Ultrasonographic evaluation of the rotator cuff and biceps tendon. *J Bone Joint Surg Am* 1986; **68:** 440-5.

15. Teefey SA, Middleton WD, Yamaguchi K. Shoulder sonography. State of the art. *Radiol Clin North Am* 1999; **37:** 767-85.

16. Wallny T, Wagner UA, Prange S, Schmitt O, Reich H. Evaluation of chronic tears of the rotator cuff by ultrasound. *Bone Joint Surg Br* 1999; **81:** 675-8.

17. Moriggl B, Steinlechner M, Genser N. [Determining normal ultrasound values of the supra- and infraspinatus muscles]. [Article in German]. *Ultrashall Med* 1993; **14:** 52-7.

18. Thain L, Adler RS. Sonography of the rotator cuff and biceps tendon: technique, normal anatomy and pathology. *J Clin Ultrasound* 1999; **27:** 446-58.

Radiol Oncol 2002; 36(4): 327-9.

F-18-FDG PET in presurgical oro-maxillofacial carcinomas

Reingard M. Aigner,[1] Günter Schultes,[2] Gerald Wolf,[1] Thomas Schwarz,[1] Mark Lorbach[1]

[1]*Department of Radiology, Division of Nuclear Medicine,*
[2]*Division of Maxillofacial Surgery, Karl-Franzens University Graz*

Background. *We performed an analysis of the diagnostic impact of F-18-FDG-PET in presurgical oro-maxillofacial malignancies.*

Patients and methods. *The diagnosis of the malignant primary was made clinically and was histologically verified before FDG-PET and the cervical CT examinations were performed in 25 patients of this study. For the FDG-PET investigation a full ring PET scanner was used (ECAT EXACT HR+, Siemens). Thoracic CT was performed only if pathological findings on FDG-PET scans required it.*

Results. *The primary was clearly identified with FDG-PET in all patients. Active cervical lymph node sites were seen in 9/25 patients (ipsilateral: 8/25; ipsi- and contralateral: 1/25). Lung-metastases were found in 2/25 patients. Cervical CT: The primary was recognised in all patients. Artefacts caused by dental implants did not allow visualising the extension of the tumour in 9/25 patients. Ipsilateral lymph node sites were seen in 7/25 patients (size: 0.9-1.6 cm), and ipsi- and contralateral lymph node sites in 7/25 patients (size: 0.8-1.8 cm). The lung metastases primarily recognised with FDG were visualised with CT in both patients, too.*

Conclusion. *FDG-PET is a sensitive diagnostic modality for the preoperative visualisation of active, i.e. suspicious malignant lymph nodes. Distant metastases were demonstrated in 8% of the patients on whole body PET. The usefulness of FDG-PET and CT for establishing the diagnosis of the primary is limited. The preoperative importance of CT lies primarily in the accessibility of the algorithms for the intraoperative reconstruction of the facial structures.*

Key words: mouth neoplasms - diagnosis; maxillofacial neoplasms - diagnosis; tomography, emission - computed, fluorine radioisotopes; F18-FDG, PET

Received 25 October 2002
Accepted 13 November 2002

Correspondence to: Prof. Reingard M. Aigner, MD, Department of Radiology, Division of Nuclear Medicine, Karl-Franzens University Graz, Auenbruggerplatz 9, A-8036 Graz, Austria; E-mail: reingard.aigner@uni-graz.at

Introduction

Diagnosis of maxillofacial malignancies remains a special problem for diverse radiological imaging modalities, even in the preoperative stage. Artefacts caused by metallic crowns and dental implants reduce the diagnostic impact of magnetic resonance imaging (MRI) and of computed tomography (CT). We

analysed the diagnostic value of F-18-Fluoro-deoxy-glucose positron-emission-tomography (FDG- PET) as an alternative or additional method for preoperative evaluation of oro-maxillofacial malignant tumours.

Patients and methods

The series consisted of 25 patients, 17 males, and 8 females, aged between 38-69 years. The primaries were diagnosed clinically and histologically verified before FDG-PET and CT-examinations were performed. The serum glucose levels ranged between 70-110 mg/dl. F-18-FDG was injected intravenously in a dose of 333 -370 MBq. The acquisition on a full ring PET scanner (ECAT EXACT HR+, Siemens, Medical Systems/CTI, Knoxville, USA) with an axial field of view of 15.5 cm resulting in 63 transverse slices with a slice thickness of 2.5 mm started between 70-90 minutes after injection. The transmission scans were obtained with 68-Ge rod sources (4 min acquisition time per bed position) alternating with the emission scans of 8 min each. The transmission data were reconstructed with filtered back projection, the emission data were corrected for random events, dead time, scatter and attenuation, and were reconstructed with ordered subset iterative reconstruction (OSEM; 2 iterations, 8 subsets). The resulting in-plane image resolution of transaxial images was about 4 to 5 mm full with at half maximum. FDG-PET was done as whole body imaging method in all patients. Cervical CT was done in all patients, too. Thoracic CT was performed only if pathological findings on FDG-PET scans required it.

Results

FDG-PET: Intense localised pathological FDG-uptake indicating the primary was observed in 25/25 patients. Intense pathological FDG-uptake in ipsilateral lymph node sites was seen in 8/25 patients, in ipsi- and contralateral lymph node sites in 1/25 patient. Lung-metastases were found in 2/25 patients.

Cervical CT: The primary was recognised in all patients. Multiple artefacts caused by metallic crowns and dental implants did not allow visualising the extension of tumour in all patients. Ipsilateral lymph node sites were seen in 7/25 patients (size: 0.9-1.6 cm), ipsi- and contralateral lymph node sites were demonstrated in 7/25 patients (size: 0.8-1.8 cm). Radiologically unsuspected lymph nodes < 1 cm could be seen highly active on the FDG-PET study in 2/25 patients. On the other hand, lymph nodes > 1 cm were inactive on FDG-PET in 2/25 patients.

Thoracic CT was done after FDG-PET in 2/25 patients: the lung metastases recognised with FDG were visualised with CT in both patients, too.

Discussion

The majority of malignant oro-maxillofacial tumours are squamous cell carcinomas originating in mucosal structures.[1] The incidence of oro-maxillofacial malignancies is still increasing. The age of the patients is still de-

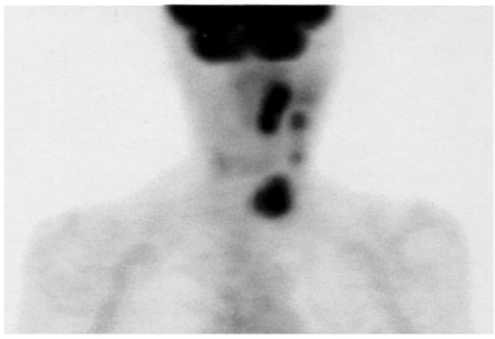

Figure 1. F18-FDG-PET scan of a 69 year old woman with squamous cell carcinoma of the left maxilla, infiltration of the left sinus maxillaris, left cervical lymph nodes, left supracervical lymph node bulk.

creasing at time of clinical presentation. The earliest possible diagnosis and subsequent treatment planning are essential parameters for better prognosis of these patients. Management and prognosis depend on the age of the patient, local tumour invasion, presence of local lymph nodes (ipsi- and contralateral cervical lymph nodes) and distant metastases at time of clinical presentation. Preoperative staging is essential in order to choose the individual therapeutic regime.[2-5]

We analysed the diagnostic value of FDG-PET as an alternative or additional method for preoperative evaluation of oral-maxillofacial malignant tumours knowing some data from the scientific literature.[6-8]

All in all, we found FDG-PET to be a quite sensitive, non-invasive diagnostic modality for preoperative staging of patients suffering from oro-maxillofacial malignancies. FDG-PET proved to be favourable for the visualisation of active, i.e. of suspicious malignant lymph nodes and for the detection of distant metastases in these patients. It is known that distant metastases are a rare condition at the initial staging of oro-maxillofacial malignancies. Nevertheless they were demonstrated in 8 % of our patients on the whole body PET-investigations.

On the other hand, the malignant primary is usually identified by means of clinical findings and confirmed to be malignant by biopsy. Therefore the usefulness of FDG-PET for recognition of the malignant primary itself and for establishing the diagnosis is limited. The radiological imaging modalities monitor the malignant tumours and their metastases by the size and structural changes and not by metabolic activities. And there is of course the well-established preoperative importance of CT for determining the algorithms needed for the intraoperative reconstruction of the facial structures. The diagnostic impact of FDG-PET is of extraordinary diagnostic importance in patients with artefacts caused by metallic crowns and dental implants.

References

1. Arnold WJ, Laissue JA, Friedman A, Naumann HH. Diseases of the head and neck, an atlas of histopathology. Stuttgart: Georg Thieme Verlag; 1987.

2. Rassekh CH. Tobacco cancer of the oral cavity and pharynx. *W V Med J* 2001; **97(1):** 8-12.

3. Macluskey M, Ogden GR. An overview of the prevention of oral cancer and diagnostic markers of malignant change: 2. markers of value in tumour diagnosis. *Dent Update* 2000; **27(3):** 148-52.

4. Goldenberg D, Ardekian L, Rachmiel A, Peled M, Joachims HZ, Laufer D. Carcinoma of the dorsum of the tongue. *Head Neck* 2000; **22(2):** 190-4.

5. Ferlito A, Mannara GM, Rinaldo A, Politi M, Robiony M, Costa F. Is extended selective supraomohyoid neck dissection indicated for treatment of oral cancer with clinically negative neck? *Acta Otolaryngol* 2000; **120(7):** 792-5.

6. Kunkel M, Wahlmann U, Grotz KA, Benz P, Kuffner HD, Spitz J, et al. [Value of (F18)-2-fluorodeoxyglucose PET scanning in staging mouth cavity carcinoma. Comparative evaluation of PET findings before and after preoperative radiochemotherapy with histological and computerized tomography findings]. *Mund Kiefer Gesichtschir* 1998; **2(4):** 181-7. [German].

7. Stuckensen T, Kovacs AF, Adams S, Baum RP. Staging of the neck in patients with oral cavity squamous cell carcinomas: a prospective comparison of PET, ultrasound, CT and MRI. *J Craniomaxillofac Surg* 2000; **28(6):** 319-24.

8. Braams JW, Pruim J, Nikkels PG, Roodenburg JL, Vaalburg W, Vermey A. Nodal spread of squamous cell carcinoma of the oral cavity detected with PET-tyrosine, MRI and CT. *J Nucl Med* 1996; **37(6):** 897-901.

Radiol Oncol 2002; 36(4): 275-80.

Klinično koristna retrospektivna primerjava radioloških in patomorfoloških sprememb pri vnetnem raku dojke

Caumo F, Manfrin E, Bonetti F, Pinali L, Procacci C

Izhodišča. Namen naše študije je bil opisati klinične, mamografske in patomorfološke značilnosti vnetnega raka dojke.

Bolniki in metode. Pregledali smo klinične in mamografske značilnosti pa tudi patomorfološke slike 22 bolnic starih od 28 do 60 let, z vnetnim rakom dojke, ki so bile obravnavane v obdobju štirih let.

Rezultati. Klinične značilnosti so bile: pri desetih bolnicah kožna rdečina, edem in zadebelitev ter vroča dojka; pri devetih bolnicah je bila tipna zatrdlina; pri eni bolnici izcedek iz bradavice; brez izrazitih kliničnih znakov pa sta bili dveh bolnici.

Patomorfološke značilnosti so bile: pri osmih bolnicah embolizmi v kožnih limfatičnih žilah; pri desetih bolnicah tumorsaki embolizmi v krvnih žilah; pri štirih bolnicah tumorski embolizmi v limfatičnih in krvnih žilah.

Običajne radiološke spremebe so bile: pri desetih bolnicah zadebelitev kože, trabekularna zgostitev in zabrisanost strukture mamarnega tkiva. Neobičajne radiološke spremembe pa so bile: pri devetih bolnicah tumorska masa in pri dveh bolnicah maligni tip kalcinacij. Pri eni bolnici nismo našli radioloških sprememb.

Po 18 mesecih sledenja bolezni samo ena bolnica iz skupine z običajnimi radiološkimi spremembami ni imela lokalne ali sistemske ponovitve bolezni, ter osem bolnic iz skupine z neobičajnimi radiološkimi spremembami.

Zaključki. Običajne klinične in mamografske značilnosti, opisovane pri vnetnem raku dojke, se javljajo le pri 45,4% bolnic. Naša študija kaže, da so radiološke spremembe povezane z različno prognozo bolnic. Tiste z neobičajnimi radiološkimi spremembami za vnetni rak dojke imajo boljšo prognozo.

Radiol Oncol 2002; 36(4): 281-9.

Endovaskularno zdravljenje krvavitve iz splanhnične arterije pri bolnikih z pankreatobiliarnim obolenjem

D'Onofrio M, Mansueto G, Gasparini A, Vasori S, Falconi M, Procacci C

Izhodišča. Krvavitev iz splanhnične arterije je nevarno obolenje še zlasti pri močno ogroženih bolnikih. Z raziskavo smo nameravali oceniti učinkovitost endovaskularnega zdravljenja krvavitve iz splanhnične aterije pri bolnikih s pankreatobiliarnim obolenjem. Če so bolniki preživeli 3 mesece, smo smatrali, da je bil poseg uspešen.
Bolniki in metode. Od 1992 do 2001 smo z endovaskularno metodo zdravili 39 bolnikov s poškodbo zgornje splanhnične arterije zaradi akutnega ali kroničnega vnetja trebušne slinavke, kirurškega zdravljenja oz. perkutanih posegov, zaradi zapletov ob anevrizmi ali poškodbi. Bolnike smo napotili na pregled z računalniško tomografijo takoj po posegu in nato še sedmi dan po posegu ter po 3, 6 in 12 mesecih.
Rezultati. Pri nekaterih bolnikih je bilo potrebno angiografijo večkrat ponoviti, da smo lahko odkrili mesto krvavitve. Pri vseh bolnikih smo krvavitev zaustavili. Ponovljena krvavitev je bila pri 6 bolnikih usodna. V prvem raziskovalnem obdobju sta umrla 2 bolnika zaradi jetrne odpovedi po embolizaciji arterije.
Zaključki. Krvavitev iz splanhnične arterije je zelo nevarno obolenje. Z endovaskularnim zdravljenjem lahko dosežemo do 75-odstotono preživetje po treh mesecih.

Radiol Oncol 2002; 36(4): 291-5.

Sindrom hiperperfuzije možganov po karotidni angioplastiki

Miloševič Z, Žvan B, Zaletel M, Šurlan M

Izhodišča. Sindrom hiperperfuzije možganov po kirurški karotidni endarterektomiji je redek pojav, vendar v literaturi pogosto opisan. Hiperperfuzijska poškodba možganov po znotrajžilni karotidni angioplastiki je prav tako redek pojav, opisi v literaturi pa so še redkejši.
Prikaz primera. Avtorji poročajo o 58-letni bolnici, ki je imela nekontrolirano arterijsko hipertenzijo in močno zožitev leve notranje karotidne arterije. Bolnica je bila desničarka in je že prebolela manjšo možgansko kap v povirju srednje možganske arterije na strani zožitve. Odločili so se za karotidno angioplastiko. Takoj po posegu je bila bolnica stabilna in brez dodatnih nevroloških izpadov. Dva dni po posegu je prišlo do epileptičnega napada. Računalniška tomografska preiskava možganov pa je pokazala manjšo krvavitev v področju levega frontalnega režnja velikih možganov.
Zaključki. Kombinacija hude zožitve notranje karotidne arterije in nekontrolirane arterijske hipertenzije lahko povzroči hiperperfuzijo možganov po karotidni angioplastiki.

Radiol Oncol 2002; 36(4): 331-7.

Radiol Oncol 2002; 36(4): 297-303.

Degeneracija kortikobazalnih ganglijev: radiološke in funkcionalne značilnosti

Ukmar M, Moretti R, Torre P, Antonello RM, Longo R, Bava A, Pozzi Mucelli R

Izhodišča. Degeneracija kortikobazalnih ganglijev je redka degenerativna bolezen, ki prizadene parietalne predele in postopno preide v frontalno prizadetost. Namen študije je bil opisati glavne radiološke značilnosti te bolezni in s funkcionalno magnetno resonančno preiskavo oceniti kortikalno aktivacijo bolnika med enostavnimi in kompleksnimi gibi.
Bolniki in metode. Ocenili smo osem bolnikov z morfološko in funkcionalno magnetno resonanco ob uporabi slik posnetih pri 1,5 T.
Rezultati. *Morfološka ocena:* Pri sedmih bolnikih smo našli asimetrično perirolandsko kortikalno atrofijo, pri petih blago hipersenzitivnost perirolandskega korteksa, pri sedmih blago atrofijo bazalnih ganglijev in pri enem hiposenzitivnost lentikularnega jedra. Pri enem bolniku so bili morfološki aspekti normalni. *Funkcionalna ocena:* Najpomembnejša je hipoaktivacija parietalnih predelov pri gibih s prizadeto roko, kar smo ugotovili pri vseh bolnikih.
Zaključki. Funkcionalna magnetna resonančna preiskava je potencialno koristno orodje pri diagnozi in spremljanju degeneracije kortiko-bazalnih ganglijev.

Radiol Oncol 2002; 36(4): 305-12.

MRI dojke pri duktalnem karcinomu in situ

Francescutti GE, Londero V, Berra I, Del Frate C, Zuiani C, Bazzocchi M

Izhodišča. Namen te študije je bil proučiti naše izkušnje pri obravnavi 22 bolnic z duktalnim karcinomom in situ (DCIS), pri katerih smo opravili magnetno resonančno slikanje (MRI).
Bolniki in metode. Med septembrom 1995 in decembrom 2001 smo pri 22 bolnicah z DCIS opravili s kontrastom ojačan MRI. Preiskavo smo naredili v 7 dneh po mamografiji.
Dinamični MRI smo opravili s sistemom 1T in s tridimenzionalno (FLASH) pulzno sekvenco pred in po uporabi kontrastnega sredstva. Ocenjevali smo morfološke značilnosti, stopnjo ojačanja in krivuljo jakosti signala v času. Pri vseh primerih smo proces verificirali še histološko.
Rezultati. Histopatološka preiskava je pokazala 15 DCIS in 7 DCIS s pridruženo mikroinvazivno komponento ali pridruženimi mikrootočki invazivnega duktalnega karcinoma.
Od 22 lezij jih je 21 (95%) pokazalo kontrastno ojačanje; 14 od 15 lezij, ki so vsebovale samo DCIS, je pokazalo nizko ojačanje 3 lezij, nedoločeno 5 in močno 6.
Morfološko so bile ojačane fokalne lezije v 7 od 14 primerov, segmentne v 4 od 14 in linearno razvejene v 3 od 14 primerov. Izplavljanje smo odkrili v 4 od 14 primerov, plato krivulje v 8 od 14 in krivuljo tipa I v 2 od 14 primerov. Pet primerov je bilo multifokalnih.
Vsi DCIS s pridruženo mikroinvazijo so se kontrastno ojačali: 1 od 7 primerov je pokazal nizko, 2 od 7 nedoločeno in 4 od 7 močno ojačanje. Morfološko so bile ojačane fokalne lezije v 3 od 9 primerov, segmentne v 5 primerih in linearno razvejane v enem. Izplavljanje smo odkrili v 3 od 7 primerov, v 3 od 7 plato krivulje in krivuljo tipa I v 1 od 7 primerov. Trije primeri so bili multifokalni.
Zaključki. Občutljivost MRI je pri DCIS nižja kakor pri invazivnem karcinomu dojk; lahko pa s kontrastom ojačana MRI prikaže mamografsko okultne otočke DCIS. MRI je dopolnilna preiskava za boljši prikaz velikosti tumorja in odkrivanje dodatnih zloveščih lezij.

Radol Oncol 2002; 36(4): 313-8.

Magnetnoresonančna mikroskopija trabekularnih kosti

Cova M, Toffanin R, Accardo A, Strolka I, Furlan C, Pozzi-Mucelli R

Izhodišča. Kostne bolezni, kot je osteoporoza, vodijo v spremembe trabekularne mase in arhitekture kosti. Za boljše razumevanje trabekularne strukture in kostne moči potrebujemo izboljšane **kvantitativne metode.** MR mikroskopija (MRM) se je s svojo zmožnostjo doseči resolucijo pod 50 μm izkazala za zelo uporabno pri *ex vivo* oceni kompleksne arhitekture trabekularnih kosti. V pričujoči študiji opisujemo uporabo projekcijske rekonstrukcije (PR) z MRM pri kvantitativni oceni tridimenzionalne trabekularne strukture kostnih eksplantatov in pri napovedovanju njihovih biomehaničnih značilnosti.

Material in metode. Analizirali smo 3D PR visoke ločljivosti in eksplantate trabekularnih kosti, da bi določili standardne morfološke parametre kot so volumska frakcija trabekularne kosti, debelina trabekul in trabekularna separacija. Razločevanje slik visoke ločljivosti na kost in na kostni mozeg smo opravili z uporabo »Bayesianskega« pristopa. Pridobljene parametre smo na koncu vključili v nelinearen matematični model za določitev Youngovega modula (YM).

Rezultati. Ugotovili smo, da so parametri, ki smo jih dobili pri spinskem odboju PR močnejši napovedovalci Youngovega modula (R^2 = 0.86) kot parametri pridobljeni z konvencionalnimi spinskimi odbojnimi slikami (R^2 = 0.75), ki smo jih uporabljali za primerjavo.

Zaključki. Opisani ex vivo pristop bi lahko zlahka prilagodili in vivo študijam.

Radiol Oncol 2002; 36(4): 319-25.

Ultrazvočna preiskava rame

De Candia A, Doratiotto S, Pelizzo F, Paschina E, Bazzocchi M

Izhodišča. Namen raziskave je bil določiti vrednost dinamične ultrazvočne preiskave s sestavljanjem slik (real time compound ultrasound) pri bolnikih, ki so imeli bolezensko spremenjene tetive supraspinatusa ramenskega sklepa.

Bolniki in metode. Ultrazvočno smo preoperativno pregledali 180 ramen pri 157 bolnikih, ki so imeli klinično sumljive znake poškodbe rotatorne manšete; 71 bolnikov je bilo nato kirurško zdravljenih. Bolnike smo pregledali s statičnim in dinamičnim ultrazvokom in pri tem uporabljali visokofrekvenčno (5-12 MHz) linearno sondo, dinamična ultrazvočna preiskava pa je sestavljala različne slike pod različnimi koti (Sono CT● - ATL). Morfologijo supraspinatusov smo opredelili v skupine: ni raztrganine, delna raztrganina in popolna raztrganina. Kadar nismo našli raztrganine, smo supraspinatovo tendinopatijo razvrstili v 3 skupine glede na Neerove stadije. Na koncu smo opredelitve ob ultrazvočnih preiskavah primerjali z ugotovitvami ob kirurških posegih.

Rezultati. Ultrazvočna preiskava je ugotovila 32 (96,9%) od 33 popolnih raztrganin. Samo pri enem bolniku, ki je bil prekomerno hranjen, smo ugotovili lažno negativni rezultat. Pri 9 (75%) od 12 bolnikih pa smo pravilno ugotovili delno raztrganino. Pri treh bolnikih, kjer je bila poškodba površinska, je bil rezultat lažno negativen. Ultrazvočna preiskava 26 bolnikov je prav tako pravilno pokazala, da noben od 26 bolnikov (100%) ni imel raztrganine, tako da nismo zasledili lažno pozitivnih razultatov.

Zaključki. Dinamična ultrazvočna preiskava s sestavljanjem slik (real time compound ultrasound) je koristna pri ocenjevanju bolezni supraspinatusnih tetiv. Pri takšni preiskavi je manj akustičnih artefaktov, ki so sicer prisotni pri konvencionalni ultrazvočni preiskavi, takšna preiskava omogoča bolj natančno opredelitev poškodbe oziroma lažje načrtovanje kirurškega zdravljenja.

Radiol Oncol 2002; 36(4): 327-9.

Diagnostičen pomen F-18-FDG PET pri oro-maksilofacialnih malignomih pred kirurškim zdravljenjem

Aigner RM, Schultes G, Wolf G, Schwarz T, Lorbach M

Izhodišča. Analizirali smo diagnostični pomen FDG-PET pri oro-maksilofacialnih malignomih pred kirurškim zdravljenjem.

Bolniki in metode. Pri 25 bolnikih, vključenih v študijo, smo klinično in histološko potrdili primarni maligni tumor še preden smo opravili FDG-PET in cervikalni CT. Pri FDG-PET smo uporabili krožni PET čitalnik (ECAT EXACT HR+, Siemens). CT prsnih organov smo opravili samo pri tistih bolnikih, kjer je FDG-PET pokazal patološke spremembe.

Rezultati. Primarni tumor smo s FDG-PET identificirali pri vseh bolnikih. Pri 9/25 bolnikih smo prikazali aktivne vratne bezgavke (ipsilateralne 8/25; ipsi- in kontralateralne1/25). Pri 2/25 bolnikih smo našli pljučne metastaze. Prav tako smo s cervikalnim CT-jem identificirali primarni tumor pri vseh bolnikih. Artefakti povzročeni z zobnimi vsadki so preprečili prikaz razširjenosti tumorja pri 9/25 bolnikih. Ipsilateralne bezgavke smo prikazali pri 7/25 bolnikih (velikosti 0,9-1,6 cm), ipsi- in kontralateralne bezgavke pa pri 7/25 bolnikih (velikost 0,8-1,8 cm). Pljučne zasevke prikazane s FDG smo prikazali tudi s CT-jem pri obeh bolnikih.

Zaključki. FDG-PET je občutljiva diagnostična metoda za preoperativni prikaz aktivnih, torej sumljivih bezgavk. Oddaljene zasevke smo dokazaki pri 8 % bolnikov, ko smo naredili PET celega telesa. Uporabnost FDG-PET in CT-ja za postavljanje diagnoze primarnega tumorja je omejena. Preoperativni CT nam je v veliko pomoč predvsem za določanje algoritmov, potrebnih pri intraoperativni rekonstrukciji obraznih struktur.

Notices

Notices submitted for publication should contain a mailing address, phone and/or fax number and/or e-mail of a ***Contact*** *person or department.*

Lung cancer

January 14-19, 2003

The »1st IASLC/ASCO International Conference on Molecular Targeted Therapies in Lug Cancer« will take place in Marbella Spain.

Contact Dr. Fred R. Hirsch, call +1 303 315 3007; or fax +1 303 315 3304; or e-mail fred.hirsch@uchsc.edu

Breast cancer

January 16-18, 2003

The »19th Annual Breast Surgery Symposium« will take place in Atlanta, USA

Contact Secretariat, Southeastern Society of Plastic and Reconstruction Surgery, 4900 B South 31st Street, Arlington, VA - 22206, USA; or fax +1 703 931 4520.

Oncology

January 19-24, 2003

The »European Winter Oncology Conference (EWOC-8)« will be offered in Flims, Switzerland.

Contact Secretariat, FECS Conference Unit, Federation of European Cancer Societies, Avenue E. Mounier, 83, Brussels - B-1200, Belgium; or phone +32 2 775 02 02; or fax +32 2 775 02 00

Magnetic resonance

January 24-25, 2003

The »4th Japanese Society for Magnetic Resonance in Medicine. International Symposium on Oncologic MR Imaging »will be held in Hyogo, Japan.

Contact Secretariat, Japanese Society for Magnetic Resonance in Medicine, c/o Congress Corporation; 3-6-13 Awajimachi, Chuo-ku, Osaka - 541-0047; Japan; or phone +81 6 622 925 55; or fax +81 6 622 130 71.

Radiation therapy

January 26-27, 2003

The »CRT 2003, Seven Concurrent Scientific Courses« will take place in Washington, DC, USA.

Contact Cardiovascular Research Institute, CRT 2003; 110 Irving Street, NW Suite 6D; Washington, DC 20010, USA; or call +202 877 8574; or fax +202 877 8141; or e-mail mikki.aashin@medstar.net; or see http://www.crtonline.org

Blood and marrow transplantation

January 30 - February 3, 2003

The »American Society for Blood and Marrow Transplantation Annual Meeting« will take place in Keystone, Colorado, USA.

Contact Secretariat, American Society for Blood and Marrow Transplantation, West Algonquin Road 85, Suite 550, Arlington Heights, IL, USA; or phone +1 847 427 0224, or fax +1 847 427 9656.

Oncology

February 1-4, 2003

The »14th International Congress on Anti-Cancer Treatment« will be offered in Paris, France.

Contact Travel Congress Organisation, 2 rue de la Pépiniere, Paris 75008, France.

Gynaecological oncology

February 1-5, 2003

The »Annual Meeting of the Society of Gynecological Oncologists« will be held in New Orleans, USA.

Contact Secretariat, Society of Gynecological Oncologists (SGO), 401 North Michigan Ave, Chicago, IL 60611-4267, USA.

Nasopharyngeal carcinoma

February 14-16, 2003

The »4th International UICC Symposium on Nasopharyngeal Carcinoma held in conjunction with the 8th Annual Scientific Symposium of The Hong Kong Cancer Institute: UICC NPC WORKSHOP 20032 will take place in Hong Kong SAR, China.

Contact Ms Nicole Ngan, Hong Kong Cancer Institute, Sir Y.K. Pao Centre for Cancer, Prince of Wales Hospital, Shatin, Hong Kong SAR, China; or phone +852 2632 1043; or fax +852 2632 5816; or see http://www.clo.cuhk.edu.hk

Pain medicine

February 18-23, 2003

The »19th Annual Meeting of the American Academy of Pain Medicine« will be offered in New Orleans, USA

Contact Secretariat, American Academy of Pain Medicine, 4700 W Lake, Glenview, IL 60025, USA; or fax +1 847 375 633.

Radiotherapy

March 9-13, 2003

The ESTRO teaching course »Radiotherapy Treatment Planning: Principles and Practice« will be held in Dublin, Ireland.

Contact ESTRO office, Avenue E. Mounier, 83/12, B-1200 Brussels, Belgium; or call +32 775 93 40; or fax +32 2 779 54 94; or e-mail info@estro.be; or see http://www.estro.be

Radiation oncology

March 15-19, 2003.

The »2nd International Conference on Translation Research and Pre-Clinical Strategies in Radiation Oncology, ICTR 2003« will be offered in Lugano, Switzerland.

Fax +41 91 820 9044, or e-mail jbernier@pop.eunet.ch, or see http://www.osg.ch/ictr2003.html

Radiation oncology

March 16-19, 2003

The »2nd International Conference on Translation Research and Pre-Clinical Strategies in Radiation Oncology« will take place in Lugano, Switzerland.

Contact Mr. Jacques Bernier, Oncology Institute of Southern Switzerland, San Giovanni Hospital, CH-6504 Bellinzona, Switzerland; or fax +41 91 820 9044; or e-mail jbernier@pop.eunet.ch; or see http://www.osg.ch/ictr2003.html

Brachytherapy

March 23-27, 2003

The ESTRO teaching course »Modern Brachytherapy Techniques« will be offered in Cairo, Egypt.

Contact ESTRO office, Avenue E. Mounier, 83/12, B-1200 Brussels, Belgium; or call +32 775 93 40; or fax +32 2 779 54 94; or e-mail info@estro.be; or see http://www.estro.be

Biomedicine

April 2-4, 2003.

The »5th International Conference on Simulations in Biomedicine« will be offered in Ljubljana, Slovenia.

Contact Ms. Gabriella Cossutta, Conference Secretariat, Biomedicine 2003, Wessex Institute of Technology, Ashurst Lodge, Ashurst, Southampton, SO40 7AA, UK; or call +44 238 029 3232; or fax +44 238 029 2853; or e-mail gcossutta@wessex.ac.uk; or see http://www.wessex.ac.uk/conferences/2003/biomed03

Radiation oncology

May 4-8, 2003

The ESTRO teaching course »Radiation Oncology: a Molecular Approach« will take place in Tenerife, Spain.

Contact ESTRO office, Avenue E. Mounier, 83/12, B-1200 Brussels, Belgium; or call +32 775 93 40; or fax +32 2 779 54 94; or e-mail info@estro.be; or see http://www.estro.be

Radiotherapy

May 6-10, 2003

The ESTRO teaching course »Dose Determination in Radiotherapy: Beam Characterisation, Dose calculation and Dose Verification« will be held in Barcelona, Spain.

Contact ESTRO office, Avenue E. Mounier, 83/12, B-1200 Brussels, Belgium; or call +32 775 93 40; or fax +32 2 779 54 94; or e-mail info@estro.be; or see http://www.estro.be

Brachytherapy

May 15-17, 2003

The Annual Brachytherapy Meeting GEC-ESTRO will take place in Luebeck, Germany.

Contact ESTRO office, Avenue E. Mounier, 83/12, B-1200 Brussels, Belgium; or call +32 775 93 40; or fax +32 2 779 54 94; or e-mail info@estro.be; or see http://www.estro.be

Radiotherapy

May 25-29, 2003

The ESTRO teaching course »Physics for Clinical Radiotherapy« will be offered in St. Petersburg, Russia.

Contact ESTRO office, Avenue E. Mounier, 83/12, B-1200 Brussels, Belgium; or call +32 775 93 40; or fax +32 2 779 54 94; or e-mail info@estro.be; or see http://www.estro.be

Clinical oncology

May 31 - June 3, 2003

The »39th ASCO Annual Meeting« will take place in Chicago, Illinois, USA.

Call ASCO Member Services at +1 888 282 2552 or +1 703 299 0158; or e-mail info@asco.org; or see http://www.asco.org

Radiobiology

June 1-3, 2003

The 2nd ESTRO workshop on biology in radiation oncology will be offered in Berg en Dal / Nijmegen, the Netherlands.

Contact ESTRO office, Avenue E. Mounier, 83/12, B-1200 Brussels, Belgium; or call +32 775 93 40; or fax +32 2 779 54 94; or e-mail info@estro.be; or see http://www.estro.be

Radiotherapy

June 1-5, 2003

The ESTRO teaching course »Imaging for Target Volume Determination in Radiotherapy« will be held in Nice, France.

Contact ESTRO office, Avenue E. Mounier, 83/12, B-1200 Brussels, Belgium; or call +32 775 93 40; or fax +32 2 779 54 94; or e-mail info@estro.be; or see http://www.estro.be

Allergology and clinical immunology

June 7-11, 2003

The »22nd Congress of the European Academy of Allergology and Clinical Immunology« will take place in Paris, France.

Contact Congrex Sweden AB, Attn: EAACI 2003, Linnegatan 89A, P.O. Box 5619, SE-114 86 Stockholm, Sweden, or call +46 8 459 66 00; or fax +46 8 661 91 25; or e-mail eaaci2003@congrex.se; or see http://www.eaaci.org

Paediatric radiation oncology

June 18-20, 2003

The »First International Congress of Pediatric Radiation Oncology« will take place in Lyon, France.

Contact Thomas Garmier, Package Organisation, 140, Cours Chalemagne, 69002 Lyon, France; or call +33 4 72 77 45 50; or fax +33 4 72 77 45 77; or e-mail package@package.fr

Radiotherapy

June 22-26, 2003

The ESTRO teaching course »IMRT and other Conformal Techniques in Practice« will be held in Amsterdam, the Netherlands.

Contact ESTRO office, Avenue E. Mounier, 83/12, B-1200 Brussels, Belgium; or call +32 775 93 40; or fax +32 2 779 54 94; or e-mail info@estro.be; or see http://www.estro.be

Small Cell Lung Cancer

June 25-28, 2003

The »4th IASLC Workshop on Small Cell Lug Cancer« will take place in Helsingor, Denmark.

Contact Dr. Heine H. Hansen, The Finsen Center, 5072, The National University Hospital, Blegdamsvej 9, DK-2100 Copenhagen, Denmark; or phone +45 3545 4090; or fax +45 3535 6906; or e-mail 4th-sclc@iaslc.org

Oncology

August 3-8, 2003

The »12th World Conference on Tobacco or Health« will be offered in Helsinki, Finland.

Contact Ms. Aira Raudesoja, CongCreator CC Ltd., P.O. Box 762, FIN-00101 Helsinki, Finland; or call +358 9 454 2190; or fax +358 9 4542 1930; or e-mail secretariat@congcreator.com

Lung cancer

August 10-14, 2003

The »10th World Conference of the International Association for the Study of Lung Cancer« will be offered in Vancouver, Canada.

Contact 10th World Conference of Lung Cancer, c/o International Conference Services, 604-850 West Hastings, Vancouver BC Canada V6C 1E1, or call +1 604 681 2153; or fax +1 604 681 1049; or e-mail conference@2003worldlungcancer.org

Prostate cancer

August 31 - September 2, 2003

The ESTRO teaching course »Brachytherapy for prostate Cancer« will take place in Kiel, Germany.

Contact ESTRO office, Avenue E. Mounier, 83/12, B-1200 Brussels, Belgium; or call +32 775 93 40; or fax +32 2 779 54 94; or e-mail info@estro.be; or see http://www.estro.be

Radiotherapy

August 31 - September 4, 2003

The ESTRO teaching course »Physics for Clinical Radiotherapy« will be held in Leuven, Belgium.

Contact ESTRO office, Avenue E. Mounier, 83/12, B-1200 Brussels, Belgium; or call +32 775 93 40; or fax +32 2 779 54 94; or e-mail info@estro.be; or see http://www.estro.be

Radiotherapy

September 13-18, 2003

The 7th Biennial ESTRO Meeting on Physics for Clinical Radiotherapy / ESTRO Meeting on Radiation Technology for Clinical Radiotherapy will take place in Geneva, Switzerland.

Contact ESTRO office, Avenue E. Mounier, 83/12, B-1200 Brussels, Belgium; or call +32 775 93 40; or fax +32 2 779 54 94; or e-mail info@estro.be; or see http://www.estro.be

Oncology

September 21-25, 2003

The ESTRO 22 / ECCO 12 Meeting will take place in Copenhagen, Denmark.

Contact FECS office, Av. E. Mounier, 83/4, B-1200 Brussels, Belgium; or call +32 7759340; or fax +32 2 7795494; or e-mail info@estro.be; or see http://www.fecs.be

Radiobiology

October 12-16, 2003

The ESTRO teaching course »Basic Clinical Radiobiology« will be offered in Santorini, Greece.

Contact ESTRO office, Avenue E. Mounier, 83/12, B-1200 Brussels, Belgium; or call +32 775 93 40; or fax +32 2 779 54 94; or e-mail info@estro.be; or see http://www.estro.be

Radiation therapy

October 19-23, 2003

ASTRO Annual meeting will be held in Salt Lake City, Utah, USA.

Contact American Society for Therapeutic Radiology and Oncology Office, 1891 Preston White Drive, Reston, VA 20191, USA; or see http://www.astro.org

Radiation oncology

November 9-14, 2003

The ESTRO teaching course »Evidence-Based Radiation Oncology: Methodological Basis and Clinical Application« will take place in Lisbon, Portugal.

Contact ESTRO office, Avenue E. Mounier, 83/12, B-1200 Brussels, Belgium; or call +32 775 93 40; or fax +32 2 779 54 94; or e-mail info@estro.be; or see http://www.estro.be

Surgical oncology

March 31 - April 3, 2004

The 12th ESSO Congress will be held in Budapest, Hungary.

See http://www.fecs.be/conferences/esso2004

Oncology

April 15-17, 2004
The European Oncology Nursing Society EONS Spring Convention will be held in Edinburg, UK.
See http://www.fecs.be/conferences/eons4

Oncology

July 3-6, 2004
The 18th EACR (European Association for Cancer Research) Congress will be held in Innsbruck, Austria.
See http://www.fecs.be/conferences/eacr18

Paediatric oncology

September, 2004
The International Society of Paediatric Oncology - SIOP Annual Meeting will be held in Oslo, Norway.
See http://www.siop.nl

Radiation therapy

October 3-7, 2004
ASTRO Annual meeting will be held in Atlanta, USA.
Contact American Society for Therapeutic Radiology and Oncology Office, 1891 Preston White Drive, Reston, VA 20191, USA; or see http:// www.astro.org

Therapeutic radiology and oncology

October 24-28, 2004
The 23rd ESTRO Meeting will be held in Amsterdam, the Netherlands.
Contact ESTRO office, Av. E. Mounier, 83/4, B-1200 Brussels, Belgium; or call +32 7759340; or fax +32 2 7795494; or e-mail info@estro.be; or see http://www.estro.be

Medical oncology

October 29 - November 2, 2004
The 28th ESMO Congress will be held in Vienna, Austria.
See http://www.esmo.org

As a service to our readers, notices of meetings or courses will be inserted free of charge.
Please send information to the Editorial office, Radiology and Oncology, Zaloška 2, SI-1000 Ljubljana, Slovenia.

Reviewers in 2002

Bilban Jakopin C, Ljubljana, Slovenia — Bilban M, Ljubljana, Slovenia — Brenčič E, Ljubljana, Slovenia — Budihna M, Ljubljana, Slovenia — Čemažar M, Ljubljana, Slovenia — Fidler V, Ljubljana, Slovenia — Gale N, Ljubljana, Slovenia — Hertl K, Ljubljana, Slovenia — Jereb B, Ljubljana, Slovenia — Jevtič V, Ljubljana, Slovenia — Kadivec M, Ljubljana, Slovenia — Kocijančič I, Ljubljana, Slovenia — Koren A, Ljubljana, Slovenia — Kovač V, Ljubljana, Slovenia — Lah T, Ljubljana, Slovenia — Lesničar H, Ljubljana, Slovenia — Lipovšek M, Maribor, Slovenia — Majdič E, Ljubljana, Slovenia — Miklavčič L, Valdoltra, Slovenia — Miloševič Z, Ljubljana, Slovenia — Pavlin-Košir S, Ljubljana, Slovenia — Petrič P, Ljubljana, Slovenia — Podkrajšek M, Ljubljana, Slovenia — Rener M, Ljubljana, Slovenia — Serša G, Ljubljana, Slovenia — Swartz HM, Hanover, Germany — Šoba E, Ljubljana, Slovenia — Tomšič-Demšar R, Ljubljana, Slovenia — Umek B, Ljubljana, Slovenia — Velenik V, Ljubljana, Slovenia — Žumer-Pregelj M, Ljubljana, Slovenia

Editors greatly appreciate the work of the reviewers who significantly contributed to the improved quality of our journal.

Author Index 2002

Subject Index 2002

FONDACIJA "DOCENT DR. J. CHOLEWA"
JE NEPROFITNO, NEINSTITUCIONALNO IN NESTRANKARSKO ZDRUŽENJE POSAMEZNIKOV, USTANOV IN ORGANIZACIJ, KI ŽELIJO MATERIALNO SPODBUJATI IN POGLABLJATI RAZISKOVALNO DEJAVNOST V ONKOLOGIJI.

MESESNELOVA 9
1000 LJUBLJANA
TEL 01 519 12 77
FAKS 01 251 81 13

ŽR: 50100-620-133-05-1033115-214779

Activity of "Dr. J. Cholewa" Foundation for Cancer Research and Education - A Report for the Fourth Quarter of 2002

With the year 2002 slowly coming to the end, the members of the "Dr. J. Cholewa Foundation" for Cancer Research and Education are considering some of the new approaches in contacts and communications with prospective donors. The new approaches are believed to enable the Foundation's members to achieve more beneficial results with regard to the donations needed in the future. In this context, new circumstances and problems associated with maintaining regular contacts with the donors have been taken into consideration and are regularly discussed by the Foundation's members.

The decision to increase the amount of the "Dr. J Cholewa Foundation for Cancer Research and Education" annual prize in order to give further incentive to young researchers in Slovenia, has resulted in some high quality research work in oncology and related scientific fields being submitted. It is hoped by the members of the Foundation, that the results of cancer research supported by the Foundation, may find its way to the practical application in hospital wards across Slovenia significantly easier, and that in this way also the attempts to publish and present the research results in respectable international scientific oncology journals, international meetings and conferences, and other events of scientific importance, may continue and receive further encouragement. It is also a common consensus among the members of the Foundation that cancer research should be further encouraged in all parts of Slovenia, where the interest to promote such research exists.

The Foundation continues to support the regular publication of "Radiology and Oncology" international scientific journal that is edited, published and printed in Ljubljana, Slovenia. With this in mind, a number of grants was also awarded to experts from various parts of Slovenia in order to attend various conferences and meetings in the field of oncology in Slovenia and around the world. The Foundation continues to command all its experience and knowledge in promotion of basic, epidemiological and clinical cancer research, and in promoting cancer education in general in order to increase its impact in general population and among scientists, especially interested in the topic of cancer research. The Foundation also supported the already traditional "Oncology Weekend" Scientific Meeting, that took place in the city of Laško on November 22nd-23rd, 2002. The first day of the Meeting was dedicated to research and clinical problems associated with lymphomas, while on the second day the same topics associated with problems of gynaecological cancers were discussed in detail.

Tomaž Benulič, MD
Borut Štabuc, MD, PhD
Andrej Plesničar, MD

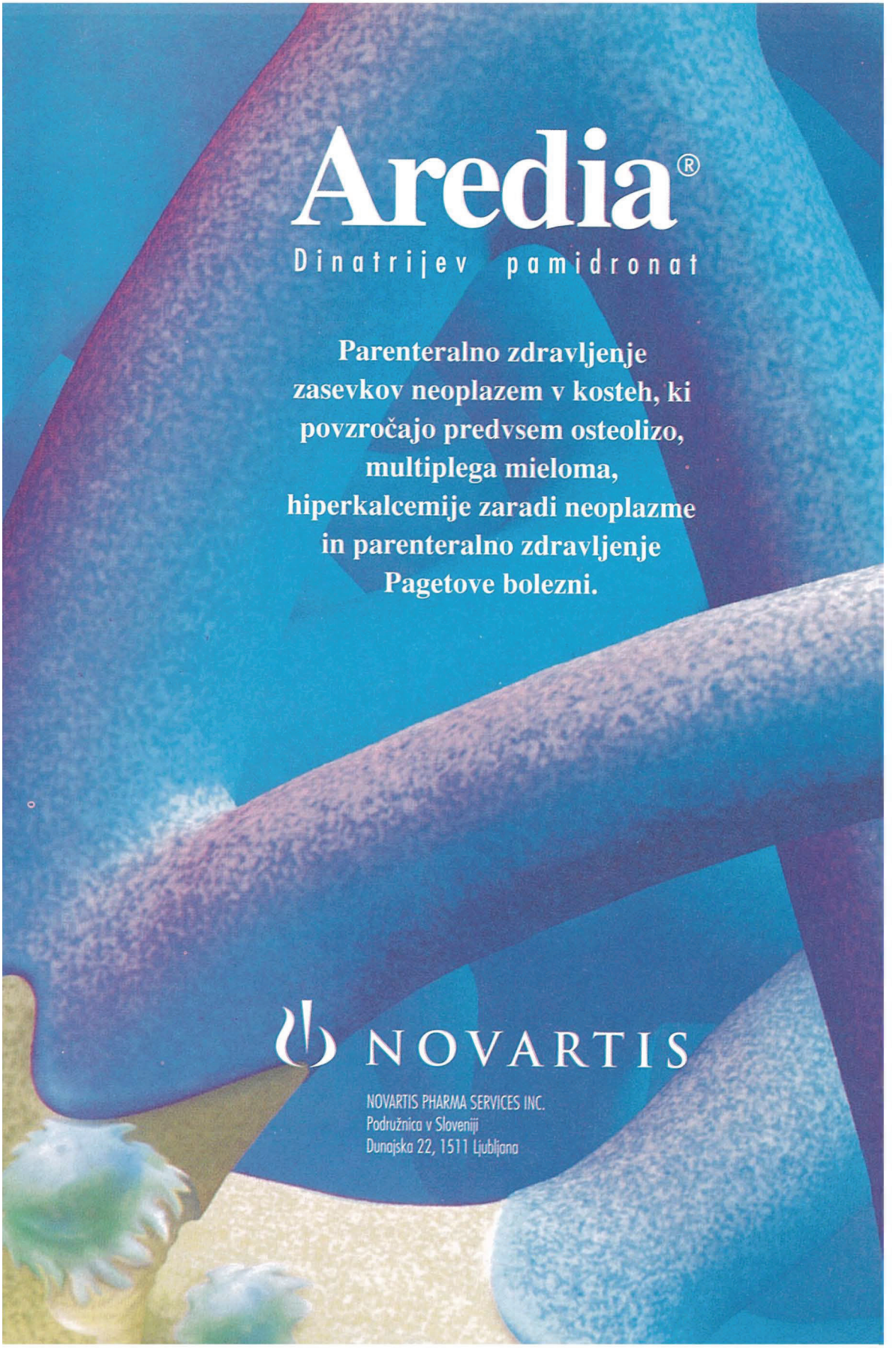
Aredia®
Dinatrijev pamidronat
Parenteralno zdravljenje zasevkov neoplazem v kosteh, ki povzročajo predvsem osteolizo, multiplega mieloma, hiperkalcemije zaradi neoplazme in parenteralno zdravljenje Pagetove bolezni.
NOVARTIS
NOVARTIS PHARMA SERVICES INC.
Podružnica v Sloveniji
Dunajska 22, 1511 Ljubljana

On ne gleda pustega pobočja.
On vidi zdravstveni kompleks prihodnosti.

V medicini ne moreš postati vodilni, če nimaš neke vizije in želje, da bi jo uresničil. V Philipsu delamo skupaj z vami, da spoznavamo vašo vizijo in tako ustvarjamo vrhunske rešitve za potrebe sodobnega zdravstva. Naša vizija je pomagati uresničevati vašo vizijo. Da bi izvedeli več, obiščite www.medical.philips.com.

PHILIPS

Let's make things better.

V družino Philips Medical Systems so odslej vključeni dosedanji ADAC Laboratories, Agilent Technologies Healthcare Solutions Group, ATL Ultrasound in Marconi Medical Systems.

Ziflazon®

kapsule

flukonazol

- *v svetu največ predpisovani sistemski antimikotik*
- *edini peroralni sistemski antimikotik za zdravljenje vaginalne kandidoze, ki ga je odobril FDA*

Skrajšano navodilo
Flukonazol je sistemski antimikotik iz skupine triazolov.

Odmerjanje pri različnih indikacijah:

vaginalna kandidoza	*150 mg v enkratnem odmerku*
mukozna kandidoza	*50 do 100 mg na dan*
dermatomikoze	*50 mg na dan ali 150 mg na teden*
sistemska kandidoza	*prvi dan 400 mg, nato od 200 do 400 mg na dan* *Največji dnevni odmerek je 800 mg.*
preprečevanje kandidoze	*50 do 400 mg na dan*
kriptokokni meningitis	*prvi dan 400 mg,* *nato od 200 do 400 mg na dan*
vzdrževalno zdravljenje	*200 mg na dan*

Kontraindikacije: Preobčutljivost za zdravilo ali sestavine zdravila. **Interakcije:** Pri enkratnem odmerku flukonazola za zdravljenje vaginalne kandidoze klinično pomembnih interakcij ni. Pri večkratnih in večjih odmerkih so možne interakcije s terfenadinom, cisapridom, astemizolom, varfarinom, derivati sulfonilureje, hidroklorotiazidom, fenitoinom, rifampicinom, ciklosporinom, teofilinom, indinavirom in midazolamom. **Nosečnost in dojenje:** Nosečnica lahko jemlje zdravilo le, če je korist zdravljenja za mater večja od tveganja za plod. Doječe matere naj med zdravljenjem s flukonazolom ne dojijo. **Stranski učinki:** Povezani so predvsem s prebavnim traktom: slabost, napenjanje, bolečine v trebuhu, driska, zelo redko se pojavijo preobčutljivostne kožne reakcije, anafilaksija in angioedem – v tem primeru takoj prenehamo jemati zdravilo. Pri bolnikih s hudimi glivičnimi obolenji lahko pride do levkopenije in trombocitopenije in do povečane aktivnosti jetrnih encimov. **Oprema in način izdajanja:** 7 kapsul po 50 mg, 28 kapsul po 100 mg, 1 kapsula po 150 mg. Na zdravniški recept. 1/99.
Podrobnejše informacije so na voljo pri proizvajalcu.

KRKA

Krka, d. d., Novo mesto
Šmarješka cesta 6
8501 Novo mesto

KEMOMED

PE: Stritarjeva 5, 4000 Kranj, Slovenija
tel.: (0)4/ 2015 050, fax: (0)4/ 2015 055
e-mail: kemomed@siol.net

Promega

MWG AG BIOTECH

TRP

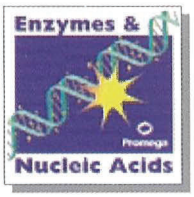

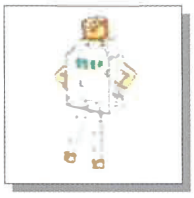

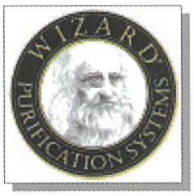

GENOMIKA - PROTEOMIKA

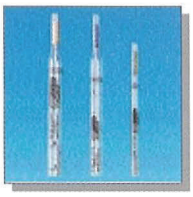

IZDELKI ZA MOLEKULARNO BIOLOGIJO

PLASTIKA ZA CELIČNE KULTURE

USF ELGA

Simply the right solution!

SANYO

LIFE TECHNOLOGIES™

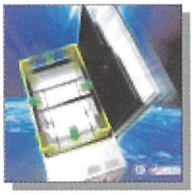

ČISTA VODA ZA LABORATORIJ

SKRINJE IN HLADILNIKI

CELIČNE KULTURE

BIOHIT

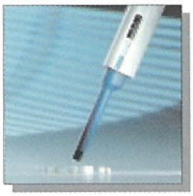

ELEKTRONSKE IN MEHANSKE AVTOMATSKE PIPETE

LABORMED

zastopa naslednja podjetja

Köttermann (Nemčija):
laboratorijsko pohištvo,
varnostne omare za kisline,
luge, topila, pline in strupe,
ventilacijska tehnika in digestorji

DAKO (Danska):
testi za aplikacijo v imunohistokemiji,
patologiji, mikrobiologiji, virologiji,
mono- in poliklonalna protitelesa

SVANOVA Biotech (Švedska):
Elisa testi za diagnostiko v veterini

NOVODIRECT BIOBLOCK (Francija):
kompletna oprema in pripomočki
za delo v laboratoriju

GFL (Nemčija):
laboratorijski aparati, omare in
skrinje za globoko zamrzovanje

ANGELANTONI SCIENTIFICA (Italija):
hladilna tehnika in aparati za laboratorije,
transfuzijo, patologijo in sodno medicino

EHRET (Nemčija):
laminar flow tehnika, inkubatorji,
sušilniki, suhi sterilizatorji in oprema
za laboratorijsko vzrejo živali - kletke

INTEGRA BIOSCIENCES (Švica):
laboratorijska oprema za mikrobiologijo,
biologijo celic, molekularno biologijo
in biotehnologijo

CORNING (ZDA):
specialna laboratorijska plastika
za aplikacijo v imunologiji, mikro-
biologiji-virologiji, ipd., mehanske eno-
in večkanalne pipete in nastavki

EVL (Nizozemska):
diagnostični testi za uporabo v
veterinarski medicini

HÜRNER (Nemčija):
ventilacijska tehnika

CSL - Biosciences:
diagnostični testi za uporabo
v veterinarski medicini

BIOMERICA (ZDA):
hitri testi za diagnostiko,
EIA /RIA testi

CHARLES ISCHI (Švica):
specialna oprema za testiranje izdelkov
v farmacevtski industriji;aparati za
procesno kontrolo in kontrolo kvalitete

ROSYS - ANTHOS (Avstrija):
fotometri, avtomatski pralni sistem za mikrotitrine plošče

LABORMED d.o.o.
Zg. Pirniče 96/c
SI - 1215 Medvode
Tel.: (0)1 362 14 14
Fax: (0)1 362 14 15

info@labormed.si

LABORMED, razstavni salon
Bežigrajski dvor
Peričeva 29, Ljubljana
Tel.: (0)1 436 49 01
Fax: (0)1 436 49 05

www.labormed.si

Instructions for authors

Editorial policy of the journal *Radiology and Oncology* is to publish original scientific papers, professional papers, review articles, case reports and varia (editorials, reviews, short communications, professional information, book reviews, letters, etc.) pertinent to diagnostic and interventional radiology, computerized tomography, magnetic resonance, ultrasound, nuclear medicine, radiotherapy, clinical and experimental oncology, radiobiology, radiophysics and radiation protection. The Editorial Board requires that the paper has not been published or submitted for publication elsewhere: the authors are responsible for all statements in their papers. Accepted articles become the property of the journal and therefore cannot be published elsewhere without written permission from the editorial board. Papers concerning the work on humans, must comply with the principles of the declaration of Helsinki (1964). The approval of the ethical committee must then be stated on the manuscript. Papers with questionable justification will be rejected.

Manuscript written in English should be submitted to the Editorial Office in triplicate (the original and two copies), including the illustrations: *Radiology and Oncology*, Institute of Oncology, Zaloška 2, SI-1000 Ljubljana, Slovenia; (Phone: +386 1 432 00 68, Tel./Fax: +386 1 433 74 10, E-mail: gsersa@onko-i.si). Authors are also asked to submit their manuscripts on a 3.5" 1.44 Mb formatted diskette. The type of computer and word-processing package should be specified (Word for Windows is preferred).

All articles are subjected to editorial review and review by independent referee selected by the editorial board. Manuscripts which do not comply with the technical requirements stated herein will be returned to the authors for correction before peer-review. Rejected manuscripts are generally returned to authors, however, the journal cannot be held responsible for their loss. The editorial board reserves the right to ask authors to make appropriate changes in the contents as well as grammatical and stylistic corrections when necessary. The expenses of additional editorial work and requests for reprints will be charged to the authors.

General instructions• Radiology and Oncology will consider manuscripts prepared according to the Vancouver Agreement (*N Engl J Med* 1991; **324:** 424-8, *BMJ* 1991; **302:** 6772; *JAMA* 1997; **277:** 927-34.). Type the manuscript double spaced on one side with a 4 cm margin at the top and left hand side of the sheet. Write the paper in grammatically and stylistically correct language. Avoid abbreviations unless previously explained. The technical data should conform to the SI system. The manuscript, including the references may not exceed 15 typewritten pages, and the number of figures and tables is limited to 4. If appropriate, organize the text so that it includes: Introduction, Material and methods, Results and Discussion. Exceptionally, the results and discussion can be combined in a single section. Start each section on a new page, and number each page consecutively with Arabic numerals.

Title page should include a concise and informative title, followed by the full name(s) of the author(s); the institutional affiliation of each author; the name and address of the corresponding author (including telephone, fax and e-mail), and an abbreviated title. This should be followed by the *abstract page*, summarising in less than 200 words the reasons

for the study, experimental approach, the major findings (with specific data if possible), and the principal conclusions, and providing 3-6 key words for indexing purposes. Structured abstracts are preferred. If possible, the authors are requested to submit also slovenian version of the title and abstract. The text of the report should then proceed as follows:

Introduction should state the purpose of the article and summarize the rationale for the study or observation, citing only the essential references and stating the aim of the study.

Material and methods should provide enough information to enable experiments to be repeated. New methods should be described in detail. Reports on human and animal subjects should include a statement that ethical approval of the study was obtained.

Results should be presented clearly and concisely without repeating the data in the tables and figures. Emphasis should be on clear and precise presentation of results and their significance in relation to the aim of the investigation.

Discussion should explain the results rather than simply repeating them and interpret their significance and draw conclusions. It should review the results of the study in the light of previously published work.

Illustrations and tables must be numbered and referred to in the text, with appropriate location indicated in the text margin. Illustrations must be labelled on the back with the author's name, figure number and orientation, and should be accompanied by a descriptive legend on a separate page. Line drawings should be supplied in a form suitable for high-quality reproduction. Photographs should be glossy prints of high quality with as much contrast as the subject allows. They should be cropped as close as possible to the area of interest. In photographs mask the identities of the patients. Tables should be typed double spaced, with descriptive title and, if appropriate, units of numerical measurements included in column heading.

References must be numbered in the order in which they appear in the text and their corresponding numbers quoted in the text. Authors are responsible for the accuracy of their references. References to the Abstracts and Letters to the Editor must be identified as such. Citation of papers in preparation, or submitted for publication, unpublished observations, and personal communications should not be included in the reference list. If essential, such material may be incorporated in the appropriate place in the text. References follow the style of Index Medicus. All authors should be listed when their number does not exceed six; when there are seven or more authors, the first six listed are followed by "et al.". The following are some examples of references from articles, books and book chapters:

Dent RAG, Cole P. *In vitro* maturation of monocytes in squamous carcinoma of the lung. *Br J Cancer* 1981; **43:** 486-95.

Chapman S, Nakielny R. *A guide to radiological procedures.* London: Bailliere Tindall; 1986.

Evans R, Alexander P. Mechanisms of extracellular killing of nucleated mammalian cells by macrophages. In: Nelson DS, editor. *Immunobiology of macrophage.* New York: Academic Press; 1976. p. 45-74.

Page proofs will be faxed to the corresponding author whenever possible. It is their responsibility to check the proofs carefully and fax a list of essential corrections to the editorial office within 48 hours of receipt. If corrections are not received by the stated deadline, proof-reading will be carried out by the editors.

Reprints: Fifty reprints are free of charge, for more contact editorial board.

For reprint information contact: International Reprint Corporation, 287 East "H" Street, Benicia, CA 94510, USA. Tel: (707) 746-8740; Fax: (707) 746-1643; E-mail: reprints@intlreprints.com

Durogesic®

TRANSDERMALNI FENTANIL

za 3 dni svobode

Nekaj cm² za 3 dni svobode

Nekaj cm² za 3 dni svobode

Nekaj cm² za 3 dni svobode

Dodatne informacije o zdravilu lahko dobite pri imetniku dovoljenja za promet:

JANSSEN-CILAG

JOHNSON & JOHNSON S. E., Podružnica Ljubljana, Šmartinska cesta 140, 1000 Ljubljana
E-mail: jac_slo@jnjsi.jnj.com

DUR-SLO-A-005-020801